HIGH TEMPERATURE MATERIALS FOR AEROSPACE APPLICATIONS

A Dissertation

by

ANDREA DIANE ADAMCZAK

Submitted to the Office of Graduate Studies of
Texas A&M University
in partial fulfillment of the requirements for the degree of

DOCTOR OF PHILOSOPHY

May 2010

Major Subject: Materials Science and Engineering

HIGH TEMPERATURE MATERIALS FOR AEROSPACE APPLICATIONS

A Dissertation

by

ANDREA DIANE ADAMCZAK

Submitted to the Office of Graduate Studies of
Texas A&M University
in partial fulfillment of the requirements for the degree of

DOCTOR OF PHILOSOPHY

Approved by:

Chair of Committee,	Jaime C. Grunlan
Committee Members,	Miladin Radovic
	Terry S. Creasy
	Daniel A. Singleton
Head of Department,	Ibrahim Karaman

May 2010

Major Subject: Materials Science and Engineering

ABSTRACT

High Temperature Materials for Aerospace Applications. (May 2010)

Andrea Diane Adamczak, B.S., Austin Peay State University; M.S., Texas A&M University

Chair of Advisory Committee: Dr. Jaime C. Grunlan

Further crosslinking of the fluorinated polyimide was examined to separate the cure reactions from degradation and to determine the optimum post curing conditions. Glass transition/melting temperatures were ascertained using DSC, while weight loss during curing and T_d were determined using TGA. Furthermore, the mechanical properties were measured using an Instron to relate to the thermal properties to find the optimum curing conditions. The polyimide resin exhibited the best post-curing conditions for further crosslinking for 8 hours at 410 °C based on T_g, thermal stability, and mechanical properties.

Blister temperatures, resulting from rapid heating, were obtained by monitoring changes in transverse thickness expansion using two different techniques. Both techniques employed showed similar blister temperatures in relation to the amount of absorbed moisture, regardless of sample size. The polyimide resin exhibited blister temperatures ranging from 225 – 362 °C, with 1.7 - 3.0 wt% absorbed moisture, and the polyimide composite had blister temperatures from 246 – 294 °C with 0.5 - 1.5 wt% moisture.

Weight loss of the fluorinated polyimide and its corresponding polyimide carbon fiber composite under elevated temperature was examined. Weight loss as a function of exposure temperature and time was measured using TGA and by pre- and post-weighing of specimens treated in an oven. Both techniques showed similar weight loss trends as a function of time and temperature, but TGA showed much greater weight loss due to greater surface area to volume (i.e., small sample size). The neat polyimide resin and carbon fiber composite exhibited negligible weight loss at temperatures below 430 °C for exposure times up to 20 minutes.

Transition-metal carbides were initially synthesized by carbothermal reduction of transition-metal halides and polymer precursor mixtures, at temperatures that range from 900 to 1500 °C in an argon atmosphere. TaC was synthesized from $TaBr_5$, as a model carbide for this process. Significant (> 40 vol%) amounts of TaC were formed at reaction temperatures as low as 900 °C for one hour, with greater times and temperatures leading to > 90 vol% yield. Universality of method was also proven by using other various transition-metal halide salts ($NbBr_5$, WCl_4, and WCl_6) with the polyimide.

TO MY FAMILY:

Dad and Peg, Mom and Dick

Peter, Brian, Michael, and Patrick

Lauren

Mindy

Thanks for all the love and support!

ACKNOWLEDGEMENTS

There are many people I would like to thank because without their help graduate school would not have been possible. I would like to start with my family because of their love and support I was able to reach this goal. To my parents: Mom, Dad, Dick, and Peg, thanks for all the guidance, encouragement, patience, and support you have given me through the years to achieve my goals I set for myself so many years ago. There is no way that I could repay you guys for everything except to make you proud of me through everything I do and strive to live a full life of happiness. To my brothers (Peter, Brian, Michael, and Patrick) whom I love dearly, thank you for being the best brothers to me and being there for me as I will always be here for you guys. To my dear stepdaughter Lauren, your help and support has been tremendous and you have grown up to be a smart and beautiful person. I will always be here for you and I love you so very much. To Mindy, words cannot express the thanks, love, and appreciation I have for you and your support, thank you so much and I love you.

I would like to thank my committee chair, Dr. Grunlan, and my committee members, Dr. Radovic, Dr. Creasy, and Dr. Singleton for their guidance and support throughout the course of this research. I greatly appreciate your support in this endeavor and the ability to finish my projects from Dr. Roger Morgan. Thanks also go to my colleagues and the department faculty and staff for making my time at Texas A&M University a great experience. I also want to extend my gratitude to the Air Force Office of Scientific Research and Dr.'s Charles Lee and Joycelynn Harrison, which provided

the support to work on an enjoyable project and continuing the funding after the passing of Dr. Morgan.

To my friends Charli Dvoracek and Marci Lizcano, you are the greatest and I appreciate all of your support and being there for me when I needed it the most. I hope to one day be able to repay you guys for the help you have given me. Adam Spriggs and Danielle Fitch, you two are the best undergrads and I know you guys will achieve anything you set your minds to. I greatly appreciate all of your hard work through the years and helping me through the good and bad times. To my friends from Austin Peay: John Hall and Amanda Deering, thank you so much for all of your love and support and being there for me always.

I would like to thank Dr. Morgan for taking me on as one of his final PhD students and giving me the opportunity to study composite materials of which I have thoroughly enjoyed. I appreciate him taking me on and seeing the potential within me to succeed. I extend my deepest thanks and appreciation to Dr. Jason Lincoln, Dr. Greg Schoeppner, Dr. Eugene E. Shin, Chris Burke, and everyone else at NASA Glenn Research Center for their guidance through my project. To Jason, I really appreciate all of your advice and help over the years as it was monumental in me accomplishing this goal, as well as supplying the materials needed for me to complete my projects.

Finally, I would like to thank all of my extended families for their love and support through this journey. It means the world to me to have your love and support and I greatly appreciate you all being behind me and there for me. To my Mom and

Dad, you mean the world to me and this achievement is just as much yours as it is mine, thank you so much for everything through the course of my life.

NOMENCLATURE

DSC	Differential Scanning Calorimeter
TGA	Thermogravimetric Analyzer
DMA	Dynamic Mechanical Analyzer
TMA	Thermomechanical Analyzer
UHTM	Ultra-High Temperature Material
SEM	Scanning Electron Microscope
EDS	Electron Dispersive Spectroscopy
FTIR	Fourier Transform Infrared Spectroscopy
ATR	Attenuated Total Reflectance
FPTI	Fluorinated Phenylethynyl Terminated Imide

TABLE OF CONTENTS

CHAPTER Page

CHAPTER Page

LIST OF FIGURES

FIGURE Page

FIGURE Page

FIGURE Page

FIGURE Page

LIST OF TABLES

CHAPTER I

INTRODUCTION

1.1 Background

High temperature polyimides are finding use in a variety of applications, from electronics to aerospace, due to their high thermal stability and excellent mechanical, chemical, and electrical properties.[1-2] Additionally, fiber-reinforced high temperature polymer matrix composites are particularly attractive for aerospace structures because of their low density,[2-3] high mechanical strength,[2,4-10] high modulus,[2,5,7-9] thermo-oxidative stability,[2,8-9,11-12] excellent electrical properties,[2,5,10,13] and superior chemical resistance.[2,4-5,9,14] A variety of polyimide-based composites have been studied for use in aerospace applications.[2,5,11,15] One in particular is a fluorinated phenylethynyl terminated imide (FPTI) polymer that is especially useful due to its environmental stability and high glass transition temperature (435 – 455 °C).[7] Due to this high dry T_g, the fluorinated polyimide is a good material to withstand the extreme service conditions experienced by military aircraft and reusable space vehicles.

The materials utilized in hypersonic vehicles will be exposed to severe mechanical, thermal and oxidative environments over short periods of time, and cause rapid, sequential overlapping degradation mechanisms. The primary structures for

---

This dissertation follows the style of *Chemistry of Materials*.

these vehicles need to be lightweight, strong and thermally durable. High temperature polyimides are the leading candidates for such applications.[16] An understanding of how these polyimide composites will react to the complex conditions of stress, temperature, and moisture is necessary to determine whether degradation of the polyimide matrix is accelerated or delayed. The performance of these composites is primarily dependent on the properties of the polymer matrix, but is also affected by the carbon fiber-matrix interface. Thus, knowing how the polyimide and its carbon fiber composite will behave under a range of thermal gradients and hygrothermal/thermo-oxidative environments is needed.

The structure-property relations of the FPTI polymer have previously been characterized in terms of oligomer synthesis, rheology, thermal properties, and cure reaction kinetics.[4,7,15,17] The polyimide and corresponding carbon fiber composite, discussed in this prior work, is currently being evaluated for leading edge primary structures and engine components. Despite its promise, there are still significant knowledge gaps in understanding the polyimide's structure-property-performance relationship for future aerospace applications. In particular, the trade-off between attainable full cure and the overlap with the onset of thermal degradation. Filling in some of these knowledge gaps is the focus of Chapters III-V.

High temperature ablation resistant materials with low brittleness are required to achieve higher hypersonic speeds, especially on the leading edges, which are exposed to extreme thermal environments (e.g. >3000 °C). Polyimide composites alone are not able to withstand these environments, necessitating a new class of materials. The addition of

transition-metal carbides to the current polyimide composite is one approach to this requirement. Transition-metal carbides are refractory materials with the highest known melting points, that in many cases exceed 2600 °C.[18-19] Besides high temperature stability, these materials exhibit outstanding hardness,[18,20] good wear resistance,[21] chemical inertness,[18,22-24] high elastic moduli,[25-26] and strength.[26-27] Tantalum carbide exhibits one of the highest melting points (3880 °C) of any known material. TaC has also been formed by *in-situ* decomposition of $TaCl_5$ or $TaBr_5$ in the presence of thermal dissociating poly(cyanogen) in inert atmospheres up to 1800 °C.[28] However, the TaC formation was not efficient as a protective coating due to its inhibition of further carbonization of the inner liquid tantalum core with the carbon from the thermal dissociation of the polymer matrix. It is now clear that the tantalum must be distributed within the polymer matrix on the molecular level for this thermally induced TaC *in-situ* thermal protective coating mechanism to be effective. In Chapter VI a successful protocol for the low temperature formation of transition-metal carbides is described.

1.2 Research Goals and Dissertation Outline

The overall goal of this dissertation is two-fold. Ascertaining the multiple mechanical, thermal, chemical, and physical degradation mechanisms for FPTI polyimide and its carbon fiber composites for lightweight structural applications for hypersonic vehicles is the first objective. The second objective is to characterize and develop a transition-metal carbide thermal protective coating upon exposure to rapid heating from a mixture of polymer and transition-metal halides.

This dissertation will address four key topics:

1. Characterization of time-temperature-mechanical properties (TTMP) of FPTI polyimide resins from 400-500 °C in inert atmospheres to separate cure reactions from oxidative induced degradation (Chapter III).
2. Determination of blister formation thresholds for the FPTI polyimide resin and its carbon fiber composite as a function of inherent moisture content (Chapter IV).
3. Understand the thermal degradation of FPTI polyimide resin and its carbon fiber composite by studying weight loss measurements as a function of temperature-time exposures (Chapter V).
4. Development of low temperature method for transition-metal carbide formation through intimate molecular distribution of transition-metal halide salts within FPTI polyimide (Chapter VI).

The overall structure of this work, to understand FPTI polyimide and its carbon fiber composite and carbide formation for thermal protection, is shown in Figure 1.1.

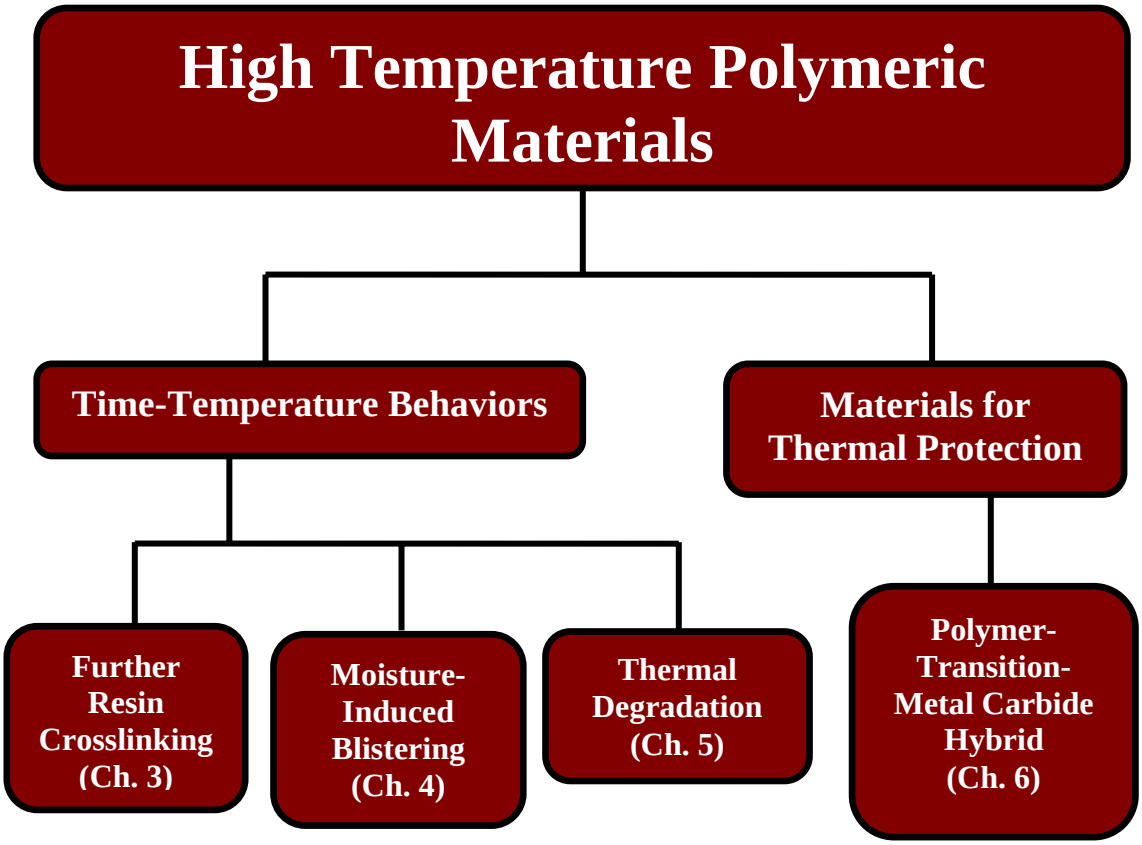

Figure 1.1. Overview of the high temperature materials research performed for this dissertation.

CHAPTER II

LITERATURE REVIEW

2.1 Requirements for High Temperature Materials

The need for better high temperature materials in the aircraft industry has been growing due to the renewed interest in space exploration and the desire to travel faster at low altitudes. Advanced composites are a type of high temperature materials that are composed of long, high-performance reinforcements and resins with excellent thermal and mechanical properties. Typical reinforcement fibers include carbon and graphite, aramid, silicon carbide and other types of ceramic fibers. Epoxies, bismaleimides (BMI), cyanate esters, high performance thermoplastics, and polyimides comprise the key materials used as the matrix, and are for the most part thermosetting materials.[29-30] Composite materials properties are controlled by their fiber, matrix, and fiber-matrix interface properties.[31]

Advanced composites are generally designed for high strength, high stiffness, low weight, and the ability to withstand high temperatures.[30,32] The fiber reinforcements are normally considered strong, high modulus fibers that are 10-100 μm in diameter.[33-34] These fibers can be oriented in several arrangements such as unidirectional, transverse, and weave, that each have advantages and disadvantages. An example of carbon fibers woven together to make a fabric sheet is shown in Figure 2.1. These fibers can then be embedded into a matrix resin with a maximum loading of 60-70%.[29] The addition of fiber reinforcements is intended to enhance the mechanical or physical properties of the

matrix material, such as strength, stiffness, coefficient of thermal expansion, conductivity, resistance to oxidation, and thermal transport.[29-30,33-35]

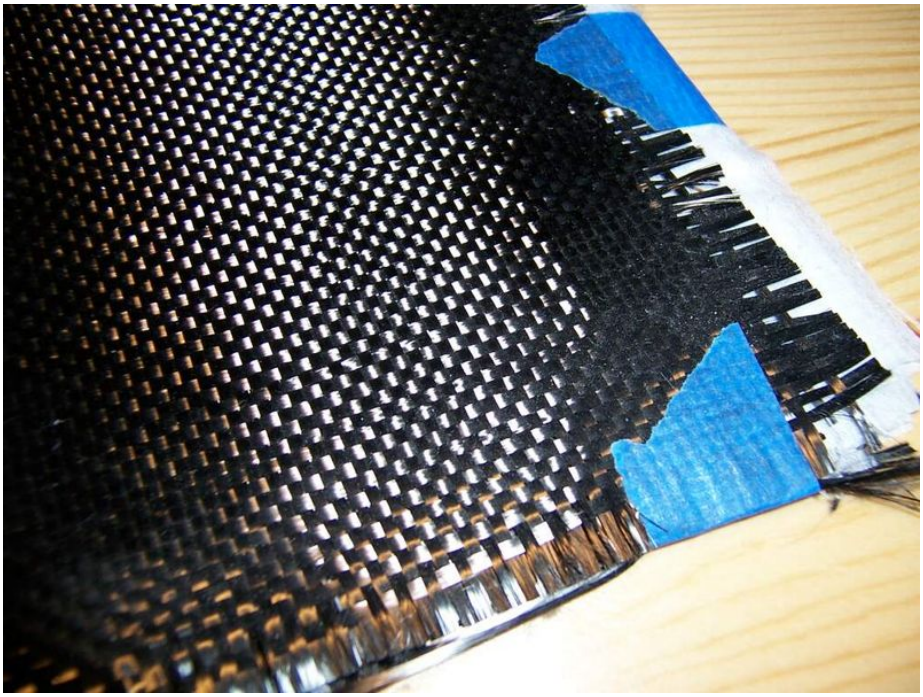

Figure 2.1. Carbon fiber fabric made of carbon fiber ropes woven together.[36]

The matrix material within a composite is the continuous phase that gives shape to the structure,[29-30] so any type of material that can be easily molded and sustain the mold shape can be used. Over 90% of modern composites are composed of some type of polymeric material.[29] The matrix material provides a number of functions that it gives to the composite much like that of the fiber reinforcements. Some of these functions include stabilizing and transferring stress to the fibers, acting as a glue to hold the fibers together, allowing fiber properties to be spread throughout composite, providing

interlaminar strength, and protecting fibers from mechanical and environmental degradation.[29-31,33] Unfortunately, the matrix material is also the weak link of the composite, preventing the fiber from providing its full benefit.[31] While there are a few thermoplastic composites being used for advanced applications, the majority of composites are composed of thermosets since the 1970's.[37] Thermoset resins are used because they can be processed (shaped) at low temperatures and upon curing of resin they form highly crosslinked amorphous solids.[29] Once a thermoset has been cured, it cannot be converted back to a liquid and maintains its shape. In general, thermosets have high glass transition temperatures (T_g), which is crucial when considering a matrix material for high temperature applications.

The performance of composites is not only dependent on the fiber reinforcement and matrix, but also relies on a strong interface between the two materials.[29,35] The mechanical and physical properties of the composite are strongly influenced by this interaction. For high modulus, strong, and tough composites, adhesion between the fiber reinforcement and matrix must be maximized and withstand degradation.[35,38-39] When selecting materials for composites, it is important to consider the level bonding that will occur between the fiber reinforcement and matrix material to optimize the necessary properties.

2.1.1 Fiber Reinforcements

Several types of fiber reinforcements exist for use in high temperature composites and their selection is determined by considering the fiber properties before

being added with the matrix.[31] Some of the most commonly used reinforcements are silicon carbide, aramid, and carbon fibers. Silicon carbide fibers exhibit high modulus (480 GPa), high strength (2.1 GPa), high stiffness, and good thermal stability, but their use is more common in metal and ceramic composites.[29,40-41]

Aramid fiber reinforcements are the most common organic fibers used in high performance composites. The fiber is made by processing the polyamide (Fig. 2.2) and then spinning it into fibers. Aramid fibers have been used commercially since 1971 and have found a wide variety of uses, from rubber-related goods to ballistic protection.[29-30,41] These fibers exhibit high strength (4.5 GPa), good modulus (120 GPa), low density, high toughness, and are chemically inert.[30] While aramid fibers are high melting (500 °C), they perform best at moderate temperatures (~250 °C). Downfalls to the use of aramid fibers are that they are affected by light and high moisture absorption.[29-30,40-41]

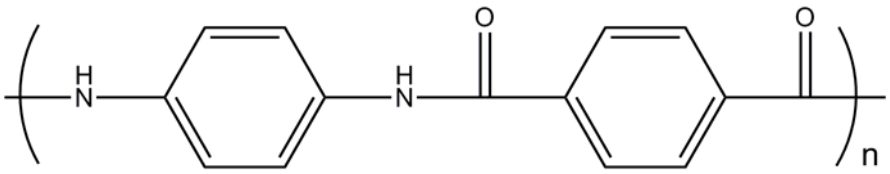

Figure 2.2. Chemistry of aramid fiber.

Carbon fiber reinforcements exhibit the highest strength (~4 GPa), high modulus (~300 GPa), high thermal conductivity, good electrical conductivity, low density, resistance to creep, and chemical inertness.[30,40] Carbon fibers are also lightweight and have excellent thermal stability. These properties combined are attractive for use in high

temperature materials. Thomas Edison first used carbon fibers in 1878 to make the light bulb, but it was not until the 1950's and 60's when carbon fibers were developed and produced for their excellent mechanical properties.[29,41] Brittleness, low impact resistance and elongation, and susceptibility to oxidation are a few negative aspects to carbon fiber reinforcements.[29] Nevertheless, the beneficial properties outweigh these negative aspects and are thus the fiber reinforcement of choice for the present work.

2.1.2 Matrix Materials

Thermoset resins are the most ideal candidate for high temperature composites due to their ability to withstand high temperatures relative to most thermoplastic resins.[29,40] Other advantages to using thermosets include relatively low processing temperature, good fiber wetting, ability to form complex shapes, and resistance to creep.[42] Typical thermosetting materials include epoxies, bismaleimides, cyanate esters, and polyimides. Figure 2.3 shows the chemical structures for each of these resin types.

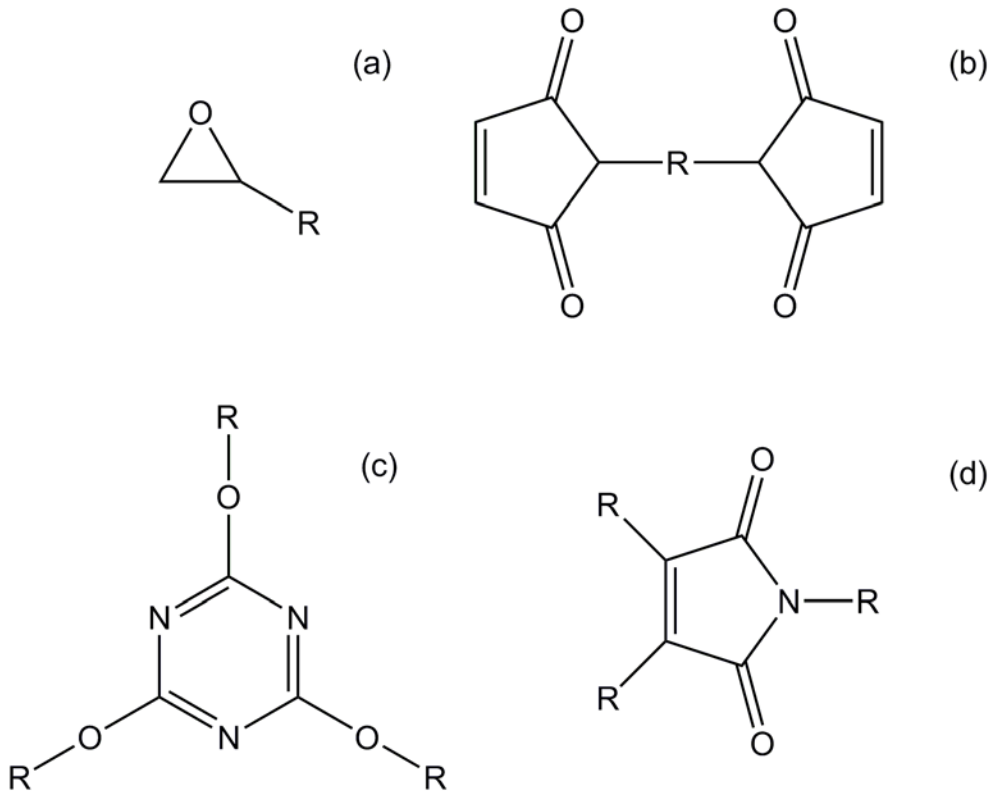

Figure 2.3. Basic monomer structures for epoxy (a), bismaleimide (b), cyanate ester (c), and imide (d).

Since their introduction in 1947, epoxy resins have been the most developed and most commonly used of the thermoset materials, largely because of their excellent mechanical properties and processing characteristics.[29-30,40,43-44] Epoxy composites are used in a variety of applications including aerospace, sporting goods, and medical devices. Epoxies have very good mechanical properties, adhesion (provide a good interface), moderate creep resistance, and good electrical resistance.[29-30,40] A few pitfalls associated with epoxy resins are moderate creep resistance, poor toughness, poor UV resistance, and limited high temperature performance.[29,40,42] These resins are typically

limited to usage temperatures below 125 °C, despite having T_g's up to 180 °C (Fig. 2.4).[29,42] Epoxies are used as a standard for the development of new classes of resin materials due to their common usage.[44]

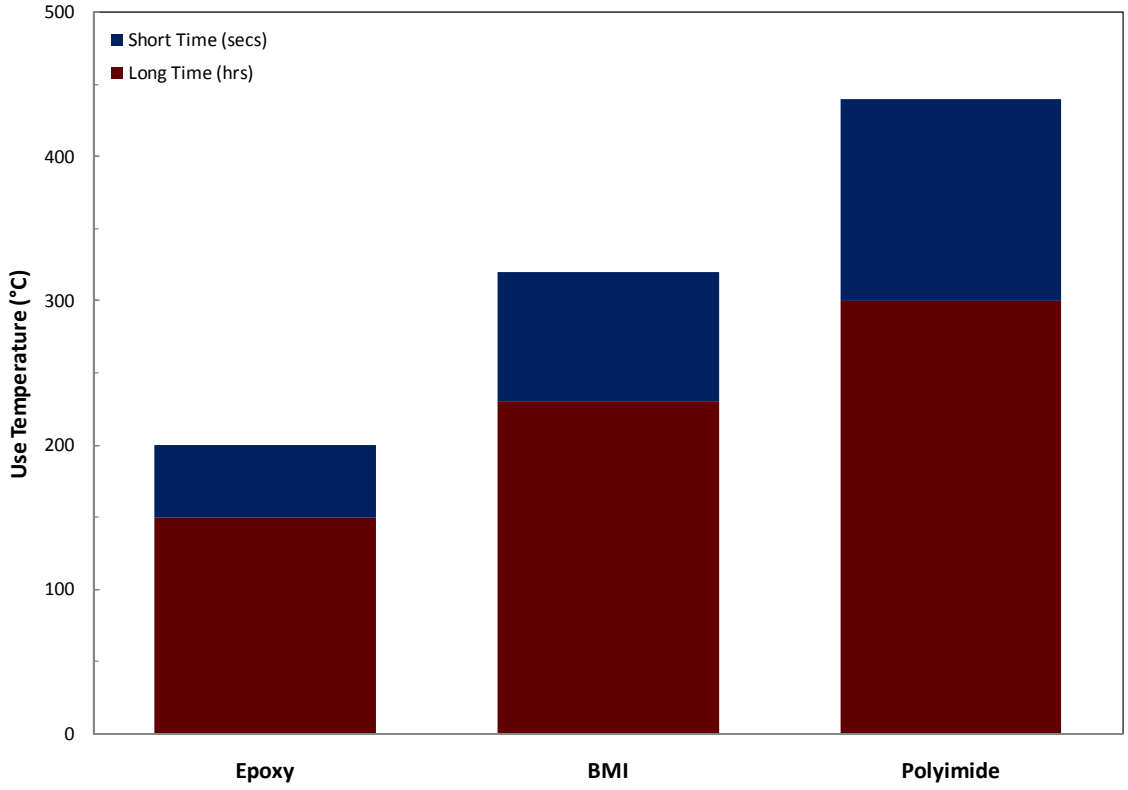

Figure 2.4. Use temperatures for common resin matrix composite materials.[30,43]

Bismaleimide (BMI) resins became attractive for high temperature composites due to better thermo-oxidative and hot/wet properties compared to epoxies.[29] BMIs are similar to polyimides in structure, as shown in Figures 2.3b and d. BMI resins exhibit T_g's near 300 °C, which in turn leads to good performance properties below this

temperature.[5,29,45] Major disadvantages of using BMIs is the concern of long-term health and safety issues with the monomer and final product, despite having higher usage temperatures compared to epoxies (Figure 2.4).[30,42] Cyanate esters are another class of materials that exhibit better thermal and strength properties in relation to epoxy resins, but they are not as good as BMIs.[30,44] The major advantages of cyanate esters include low dielectric loss and low moisture absorption.[29-30,42,44] The basic cyanate ester structure is shown in Figure 2.3c. The major concern with cyanate esters lies with long-term thermal stability in moist conditions due to moisture reacting with any unreacted monomer units present.[30,42]

Polyimide resins are the most promising of the matrix materials due to their resistance to extremely high temperatures, with T_g's greater than 300 °C.[5,29-30,42,45] Besides their excellent thermal stability, polyimides also exhibit good thermo-oxidative stability, excellent toughness, and good mechanical properties.[29,45] The basic structural unit of polyimides is shown in Figure 2.3d, and many variations can be made to the structural unit of the backbone and endcaps. The high glass transition temperatures and high thermo-oxidative stability are due to the combination of the imide and aromatic structures.[44] Some challenges associated with polyimides, over the other matrix materials mentioned, are the higher processing temperatures, long cycles, and higher pressures.[30] These issues will be explored in more detail in Section 2.3. Based on the excellent properties and higher usage temperatures (Fig. 2.4) that polyimides exhibit, this was the matrix material chosen for the present work.

2.2 High Temperature Polyimides

Throughout the 1950's and 60's a great amount of research was being done in an effort to develop thermally stable polymers for longer exposure times and higher temperatures.[44,46] Polyimides were the ones that stood out (after their introduction in 1964) due to their processability, properties, heat resistance, usefulness, and inexpensive starting materials.[43-44] There is a wide array of polyimides that have been developed, studied, and used for many applications. The best examples of these materials are reviewed in detail here as a basis of comparison for the matrix used in the present work.

2.2.1 PMR-15

The PMR-15 polyimide was first discovered in 1970, but received little interest due to processing problems.[45,47] In 1972, the PMR (polymerization of monomeric reactants) approach was improved at NASA Lewis Research Center.[45,48-49] The 15 refers to the molecular weight (1500 g/mol) of the imidized polymer. Figure 2.5 is the imide structure of PMR-15 before crosslinking into a thermoset at 343 °C.[45] PMR-15 has a T_g of 345 °C, which was considered a highly thermally stable polymer at the time, especially when compared to that of epoxy materials.[50] The T_g and properties of PMR-15 are not of the neat resin, but of the carbon fiber composite due to processing conditions. The flexural strength and modulus of PMR-15 at room temperature is 845 MPa and 66 GPa, respectively.[51] The retention of mechanical properties and minimal weight loss are obtained up to 230 °C for long exposure times, and for shorter times up

to 316 °C.[2] The strength decreases to 562 MPa at 288 °C, while the modulus only decreases to 59 GPa.[51]

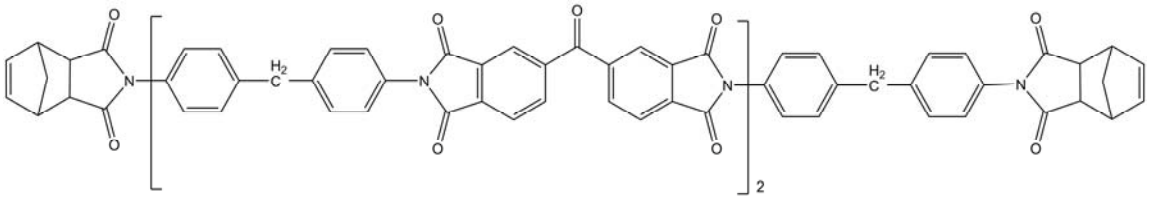

Figure 2.5. PMR-15 chemistry before crosslinking.

PMR-15 has been widely used for a variety of applications. The first component to use the PMR-15 composite was the F404 engine and other components include nozzle flaps, fan blades, and the space shuttle aft body flap.[45] Despite PMR-15's good thermal and mechanical properties, there are limitations to the material's further use. Quality control, variability from batch-to-batch, and high fabrication costs are two of the problems on the manufacturing level.[2,45] Other issues such as microcracking, high processing temperatures, resin flow control, and long term thermo-oxidative stability are common not only with PMR-15 but other composite materials as well.[45] Despite the limitations mentioned above, health concerns (mutagenic) over the dianiline (monomer) used in PMR-15 is the major reason it has not been widely used in the last 20 years, and has led to the development of other polyimide systems.[2,30,45]

2.2.2 6FDA Based Polyimides

A series of polyimides were developed to remedy the issues with PMR-15. Avimid-N, PMR-II-50, and AFR-700B are polyimides that contain an aromatic diamine and either the acid-ester or dianhydride form of 2,2'-bis(3,4-dicarboxyphenyl) hexafluoropropane. The dianhydride form is commonly referred to as 6FDA, and for simplicity all three forms will be discussed using this abbreviation. The combination of these monomers allows for a more thermally and thermo-oxidatively stable polyimide with a higher resistance to microcracking compared to PMR-15.[45] The use of 6FDA allows for enhanced processability of the polyimide and also provides greater moisture resistance and fracture toughness, while maintaining excellent thermo-oxidative stability due to the presence of the fluorine substituents.[8,44] Other improvements to polyimide processability with the addition of fluorine substituents include: solvent solubility, melt characteristics, low dielectric constant, low moisture adsorptivity, and optical transparency.[8,44]

Avimid-N

DuPont discovered Avimid-N in 1971 (also known as NR-150), which is the neat polyimide resin.[52] Avimid-N was withdrawn from the market in the early 1980's due to low interest, but was reintroduced in the 1990's.[45] The T_g for this polyimide is 355 °C and it retains its properties after 100 hours of exposure to temperatures just above the T_g.[2,45] The structure for Avimid-N is shown in Figure 2.6. The initial endcaps for this polyimide were phthalic anhydride; however, the endcaps for DuPont's production of

Avimid-N are unclear.[52] The flexural strength and modulus of Avimid-N carbon fiber composites at room temperature are 1207 MPa and 104 GPa, respectively.[53] After exposure to 316 °C, the strength decreases to 510 MPa, while the modulus decreases to 79 GPa.[53] While the room temperature properties are much higher than PMR-15, the loss of strength and modulus is greater after exposure to temperatures close to the T_g.[45]

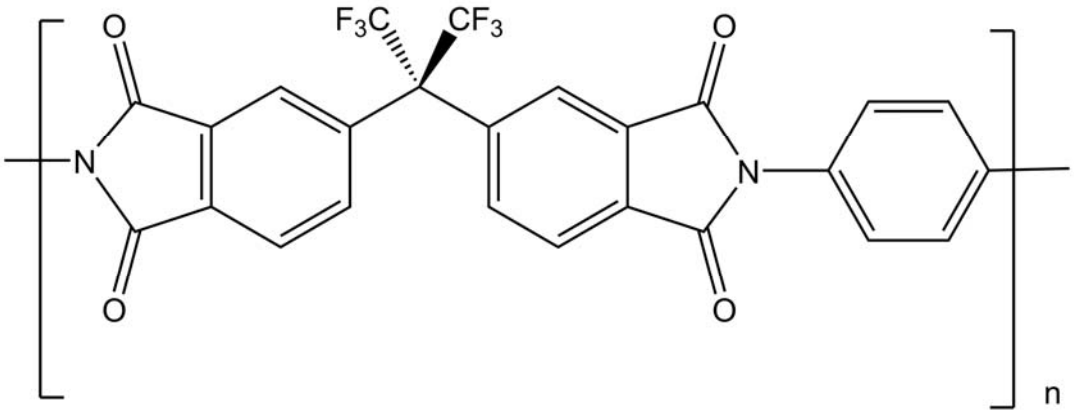

Figure 2.6. Avimid-N polymer structure.

The applications of Avimid-N are not readily available, but it was suitable for jet engine parts due to high T_g, high toughness, and excellent thermo-oxidative stability.[45] Overall use of this polyimide was minimal, despite the excellent properties, due to processing issues and inability to meet certain temperature requirements for aerospace applications.[54] During the synthesis, water by-products are produced, and this formation hinders the formation of the polyimide.[2] Other problems include little flow of the material during crosslinking and solvent removal.[2,45] The starting materials are a good starting point if the processing issues could be overcome.

PMR-II-50

PMR-II-50 was developed in the late 1980's (following PMR-15) in order to find a more thermally stable material. The 50 refers to the molecular weight of 5000 g/mol, much like that of PMR-15. The key differences between Avimid-N and PMR-II-50 are the endcaps used and starting with the acid-ester form of 6FDA instead of the dianhydride. The endcaps used are the same as that of PMR-15, a norbornyl structure, as shown in Figure 2.7. Initial work with this material showed that changing the monomers and increasing the molecular weight of the pre-polymer created an improvement in thermal stability. PMR-II-50 carbon fiber composite flexural strength is very high at 1840 MPa, which reduces to 593 MPa after exposure to 343 °C, and has a T_g of 370 °C.[55]

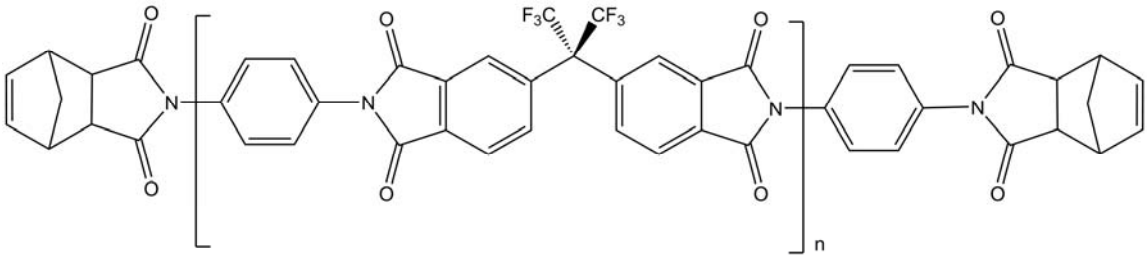

Figure 2.7. PMR-II-50 chemical structure before crosslinking.

Currently, the PMR-II-50 composite is not widely being used due to processing issues, although an easier method has been developed using an autoclave to produce high quality composite laminates.[55] Other processing issues include volatile byproducts, high viscosities, limited high temperature processing materials and expensive tooling.[56]

Another issue with PMR-II-50 is the resin's inability to meet certain temperature requirements for some aerospace applications.[54] PMR-II-50 exhibit excellent thermal and mechanical properties, except for the occurrence of microcracking due to the material's brittleness from its high crosslink densities.[56] The CF_3's present in the backbone of PMR-II-50 give the polyimide excellent thermo-oxidative stability up to 400 °C.

AFR-700B

AFR-700B was developed by Tito Serafine at TRW under Northrop's Structural Composite Material program that was funded by the Air Force Materials Laboratory and DARPA.[54,57] The structure of AFR-700B is shown in Figure 2.8 and the repeating unit has a degree of polymerization (n) of 8.[54] The major difference, besides the n value, between PMR-II-50 and AFR-700B is in the way they are processed. AFR-700B has a T_g around 400 °C and excellent thermo-oxidative stability.[15]

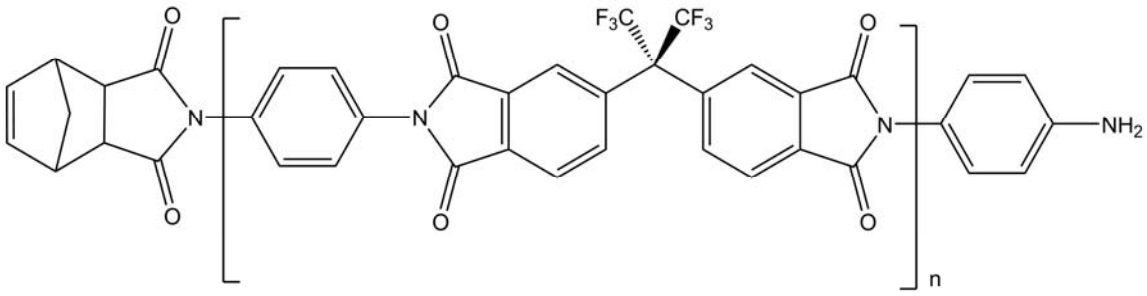

Figure 2.8. AFR-700B chemical structure before crosslinking.

AFR-700B has been used on the fuselage trailing edges of the F-117A Stealth Fighter. However, the material does not withstand hygrothermal exposure due to the weak norbornene crosslinks, which significantly decreases the strength and T_g of the material.[5,15] The nadic endcaps are hydrolyzable in the presence of moisture or oxidative environments, and replacing the endcaps with phenylethynyl results in a very stable polyimide, which is further discussed in the next section.

2.2.3 Acetylene Terminated Polyimides

There has been a lot of research on polyimides using acetylene terminated endcaps. This chemistry was chosen due to the drawbacks to norbornyl endcapped polyimides, such as poor thermo-oxidative stability from the norbornene ring and weakening of crosslinking unit, and processing issues due to the formation of side products during crosslinking.[8,58-59] Landis and coworkers conducted most of the early research using acetylene terminated polyimides in 1974.[60-61] The use of acetylene terminated endgroups results in resins that have good solvent and moisture resistance, and excellent physical and mechanical properties.[8,44] The polyimide resins described in this section, Thermid 600, PETI-5 and others, and AFR-PE-4, all use an acetylene terminated endcap.

Thermid 600

Thermid 600 was developed by Gulf Chemical Division Company in 1975, and later acquired by National Starch.[45] Thermid 600 has seen limited use commercially

because of processing difficulties, such as poor flow characteristics and the lack of solubility in common solvents.[44] The difficulties are likely from the ethynyl groups reacting that inhibit flow before a complete melt or soft state can form.[45] The imidization temperature and the temperature at which the ethynyl groups polymerize (195 °C) are also too close to allow for complete removal of the byproducts.[2] The T_g for Thermid 600 is 370 °C and the polyimide resin also has good thermo-oxidative stability up to 316 °C.[45,62] The structure for Thermid 600 is shown in Figure 2.9. The room temperature tensile strength and modulus of Thermid 600 resin is 96.5 MPa and 3.79 GPa, respectively, and the flexural strength and modulus is 124 MPa and 4.48 GPa.[63] Thermid 600 composite has a room temperature flexural strength of 1.28 GPa that decreases to 1.04 GPa after exposure to 316 °C.[64] The flexural modulus of the composite sees a similar drop from 104 GPa to 83 GPa after being exposed to 316 °C.

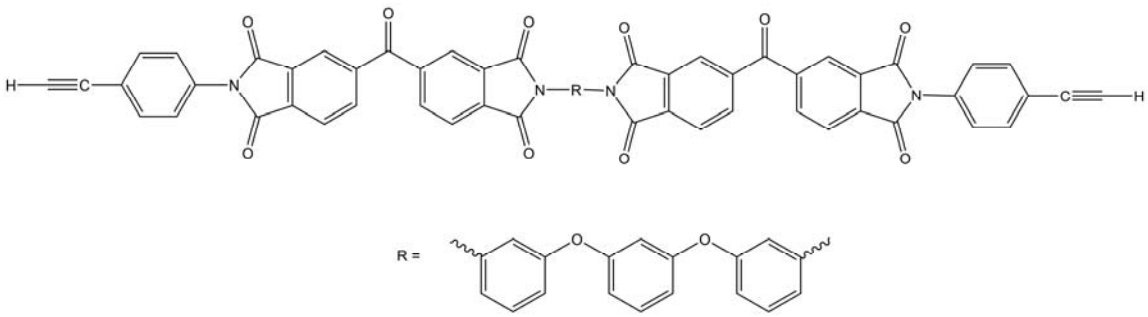

Figure 2.9. Thermid 600 chemical structure before crosslinking.

PETI-5

PETI-5 was developed in 1996 at NASA Langley Research Center in an effort to find a material for the High Speed Civil Transport (HSCT) vehicle for the new High Speed Research (HSR) Program.[30,65] The T_g for PETI-5 varies between 250 and 270 °C due to variances of molecular weights of 1250, 2500, and 5000 g/mol.[2,66-67] The molecular weights were adjusted in an attempt to improve processability of the resin, with 5000 g/mol being the starting point during initial development.[67] The structure of PETI-5 is shown in Figure 2.10. PETI-5 has the optimum combination of properties (when compared to other phenylethynyl terminated polyimides), such as high toughness, mechanical, physical, and chemical properties.[13] The room temperature tensile strength and modulus of PETI-5 resin is 129.6 MPa and 3.1 GPa, respectively. After exposure to 177 °C, the resin tensile strength drops to 84.1 MPa and the tensile modulus decreases to 2.3 GPa.[66] The flexural strength and modulus of the PETI-5 composite are 1083 MPa and 55 GPa, respectively, and after exposure to 177 °C they decrease to 787 MPa and 54 GPa, respectively.

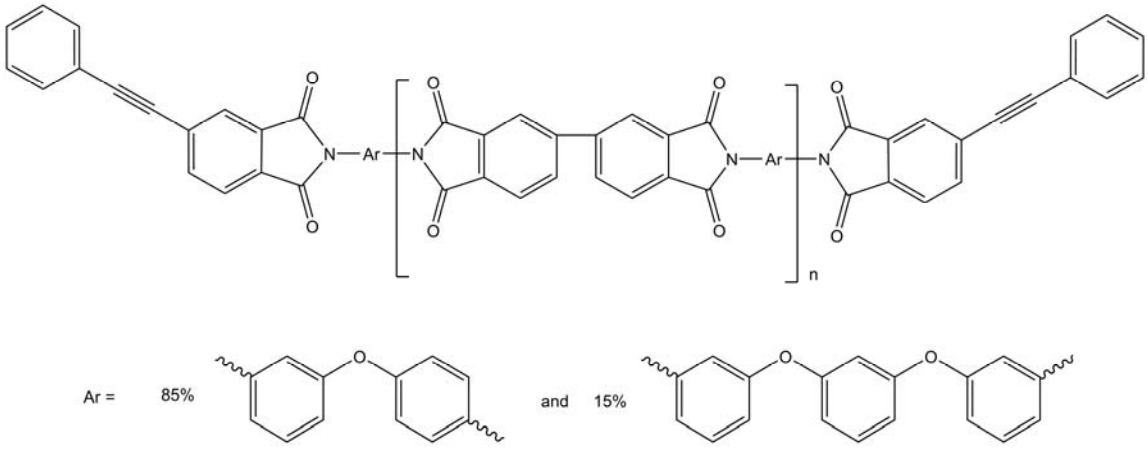

Figure 2.10. PETI-5 chemical structure before crosslinking.

The HSCT program ended in 1998 after the Boeing announcement of delaying the launch by 10 years due to the program not being economically viable.[68] While PETI-5 has excellent properties up to 177 °C, its T_g is too low and there are slight processing issues.[4,69] More recently, there has been an increasing demand for a material that has properties similar to PETI-5's, but with a higher T_g and thermal stability.

AFR-PE-4

Based on the properties of AFR-700B and PETI-5, it was postulated that using the endcaps from PETI-5 (phenylethynyl groups) and the fluorinated backbone from AFR-700B (6FDA) would produce a polyimide with the hydrolytic stability (PETI-5) and thermal stability (AFR-700B) properties needed for future applications.[70] AFR-PE-4 (also referred to as FPTI) was first reported in the literature in 1994.[71-73] FPTI exhibits extremely high T_g's (435-455 °C) and significant mechanical property improvements at higher temperatures (compared to previously mentioned polyimides).[74] Simpler

processing methods, high ductility, and better thermo-oxidative stability of FPTI are other attributes of this newer polyimide.[74] The structure of the FPTI oligomer is shown in Figure 2.11. This is the polyimide used in the present study to further understand its characteristics for use in future aerospace vehicles.

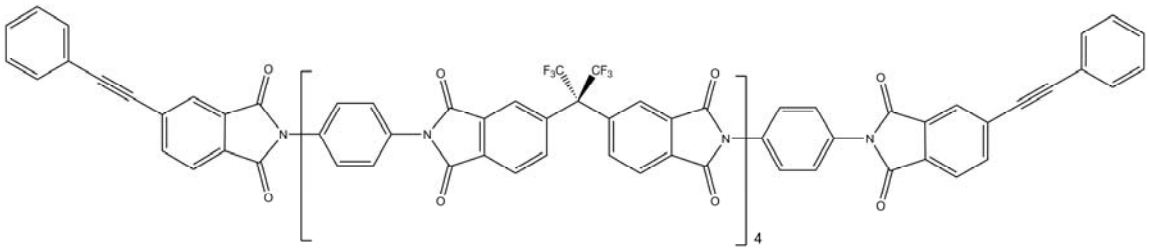

Figure 2.11. FPTI oligomer chemical structure before crosslinking.

2.3 Present/Future Aerospace Applications

Polymer fiber composites have been used in aircraft since the first flight of the Wright Brothers Flyer 1 in 1903.[31] Since then they have been widely used for a plethora of aviation and aerospace needs. In general, polymer fiber composites can be found in airframes, engines, high-speed military aircraft, and the space shuttle (Figure 2.12).[5] In the last 25 years, the National Aeronautics Space Administration (NASA) and Air Force have been pursuing the development of high temperature materials to further advance their aircraft.

Figure 2.12. This Space Shuttle tile is composed primarily of a silicon-based material[75] that is exposed to 1260 °C during reentry.[76]

Fiber reinforcements have been used in a wide variety of applications over the years and will continue to be used. Silicon carbide has been mass produced since the early 1900's; however, silicon carbide fibers are a more recent development within the last 30 years. Silicon carbide is not as widely used as aramid or carbon fibers. Silicon carbide fibers can be found in aircraft wing structural elements and missile body casings.[29] Aramid fibers were developed in 1971 and are not as widely used today due to moisture penetration.[42] These fibers have been used on the leading edges of aircraft wings, fairings, radomes, skins or face sheets for honeycomb panels, and other structures where impact damage is expected.[29,42] Aramid fibers were used on the leading edges of the Voyager aircraft that flew nonstop around the world.[29] The structural and nonstructural components on helicopters are also made using aramid fibers to provide protection against small arms fire and one-third of the MBB BK117 helicopter is composed of aramid fibers.[40,42] Today, aramid fibers are mainly being used as high

energy impact containments, such as high performance pressure vessels, due to their high strength and resistance to penetration damage.[29,42] These fibers are also used in filament wound vessels and containment rings in engines.[42]

Carbon fibers were patented in 1961 and are the most widely used fibers today for reinforcement.[29] They can be found in a wide array of applications from airframes to engines.[16,42] Carbon fibers are chosen for their stiffness, strength, low weight, and thermal properties. On aircraft, carbon fibers are used on control surfaces, fuselages, doors and landing gear assemblies, as well as helicopter rotor blades.[29] They are also used on rockets and missiles, aerospace antennas, and many space structures (e.g. satellites and telescope mounts).[29,40] Carbon fibers are also used in the Hubble Space Telescope and space shuttle for their superior heat resistance.[29]

Polymer matrix materials are found in many aviation and aerospace applications, such as rocket motor cases, tail fins, and wings.[40] Epoxies are also being used to modify older aircraft wings. Epoxy carbon fiber composites are being used on the space shuttle payload bay doors and the remote manipulator arm.[77] Two-thirds of the MBB BK117 helicopter are composed of these composites.[40] Bismaleimide resins have found use where higher temperatures are needed for protection where epoxies cannot be used.[42] The RB162 engine made by Rolls-Royce was one of the first aerospace applications to use bismaleimides.[45] The F16XL aircraft used bismaleimides on the wing skins and ribs in the best known application. The F-22 Raptor fighter jet is largely composed of bismaleimides (e.g. wings, empennage, fuselage, and understructure).[29] This resin is also used on the aft flap hinge fairing of the C-17, and tailboom of Bell helicopters.[29]

Cyanate ester resins are the least used of the polymer resins discussed earlier. They are most commonly found on advanced stealth composites, radomes, antennae skins, and space structures.[29] Polyimide resins, on the other hand, are being used more often due to their high thermal stability. High speed military aircraft are using large structural composite parts that include polyimides in the advanced aircraft systems, engine components, and casings.[40,42] Polyimide resins are also being used as firewalls in recently built fighter aircraft, and for skins on high-speed developmental aircraft for thermal stability.[29] They can also be found on the booster tail and fins of the space shuttle.[40] In some cases, much higher temperature materials are needed, which are more ceramic in nature. This is especially true for aircraft that will exceed Mach 14, making the skin temperature 5700 °C due to aerodynamic friction.

2.4 Ultra-High Temperature Materials

High temperature materials are becoming of greater importance as the desire to produce hypersonic vehicles increases. Figure 2.13 illustrates current operating temperatures for various applications along with selected materials melting temperatures.[78] There is a need to find materials that are capable of operating at temperatures greater than 3000 °C. Ultra-high temperature materials (UHTMs) are a class of materials that are chemically and physically stable at temperatures above 2400 °C.[22] UHTMs are potential candidates for applications associated with extreme environments (e.g. hypersonic flight, rocket propulsion, atmospheric re-entry) because they are high melting, hard, retain their strength at high temperatures and have mild

thermal expansion.[22,79-80] In general, the ultra-high temperature classification is generally considered to begin at 1600 °C with no upper temperature limit.[22]

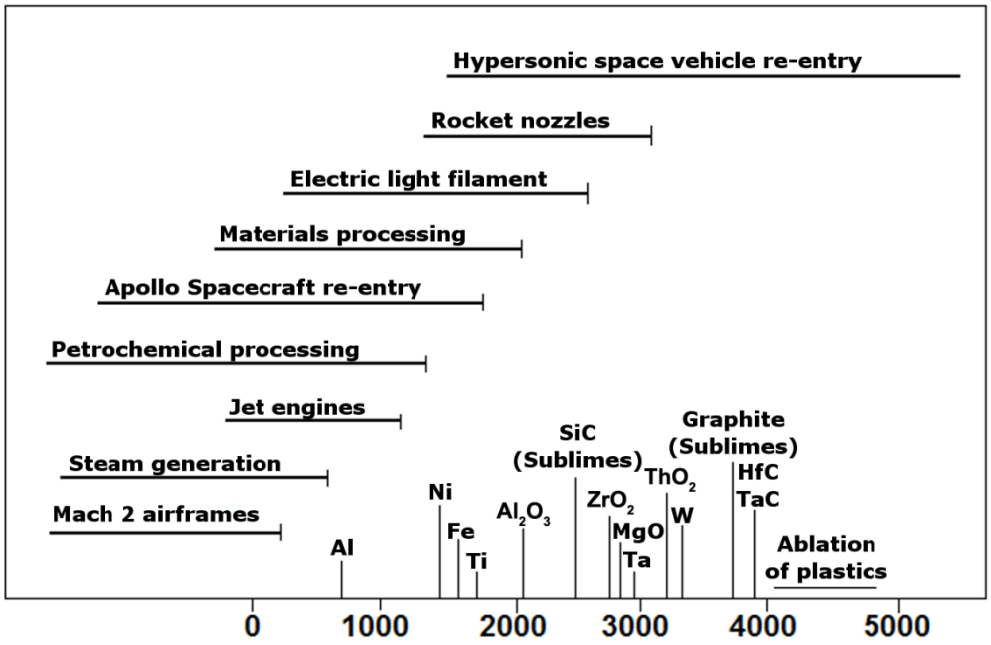

Figure 2.13. Typical operating temperatures in high-temperature environments. Melting temperatures of various materials are shown at the bottom of this chart.[78]

Materials that are being investigated for extreme environments are refractory materials with melting temperatures above 3000 °C, which consist of early transition-metals and borides, carbides, or nitrides.[22] These refractory materials provide strength, durability, hardness, optical, electrical, and magnetic properties in addition to withstanding high temperatures.[19] Over thirty years ago, zirconium- and hafnium-borides and silicon carbide were considered the most promising materials identified by the Air Force.[79,81] In the early 1990's, NASA began to work with these materials and in

1997 tested their applicability in thermal structures for ballistic probes.[81] The nose tip was first composed of HfB_2 and 20% SiC, while three years later three different materials were tested for the leading edge (HfB_2-SiC, ZrB_2-SiC, and ZrB_2-SiC-C).[81]

2.4.1 Transition-Metal Carbides

Transition-metal carbides are stable at high temperature (melting temperatures greater than 3000 °C), have outstanding hardness,[18,20] good wear resistance,[21] chemical inertness,[18,22-23,82] high elastic moduli,[25-26] and strength.[26-27] Such an unusual combination of properties extends the potential use of transition-metal carbides beyond high-temperature applications to electronic components, cutting tools, or catalysts for chemical conversions.[83] Tantalum carbide is one of the refractory carbides to receive the most attention due to its extremely high melting point of 3880 °C and a boiling point of 5500 °C under atmospheric conditions. While other transition-metal carbides were explored in the present work, tantalum carbide was the primary focus due to these excellent properties.

Over the past ten years there has been significant research on production methods for transition-metal carbides. Originally, transition-metal carbides were prepared via a powder metallurgical technique that involved elemental transition-metals (or oxides) with solid carbon or carbonaceous gases by carbothermal reduction.[18,23,84-86] This technique requires temperatures above 1700 °C and long exposure times to produce the transition-metal carbides due to a lack of heat transfer.[87-88] Other methods for producing transition-metal carbides have been reported to include carbothermal reduction of

transition-metal rapid metathesis reactions,[89-90] solid state reactions,[85,91] gas-solid reactions,[92-95] gas-phase reactions,[96-97] carbothermal reaction assisted by microwaves,[84] electrochemical and solution state methods,[98-99] and high-frequency plasma.[100] Like that of conventional techniques, these methods involve high-temperature, high-energy, and time consuming processes with relatively low yields and residual impurities (such as free carbon, oxides, and sub-carbides).[84-85]

There have been many recent efforts to synthesize transition-metal carbide powders or bulk components at lower processing temperatures. One approach that has been gaining attention is the use of polymer precursors to produce transition-metal carbides at lower temperatures (below 1700 °C) via carbothermal reduction.[101-104] The idea is to also simultaneously produce final products in the form of thin films, coatings, fibers, or composites.[105] Preiss et al showed that polymeric precursors, such as niobium and tantalum alkoxides and molybdenum ethylene glycolate, could be used for processing TaC, NbC and Mo_2C thin films and fibers at temperatures as low as 1400 °C.[105]

In an attempt to further lower the processing temperature and formation of tantalum carbide, binary hydrogels, consisting of saccharose (or carbonaceous gel) and alkoxides (or peroxo acids) of Nb and Ta, were used as the organic gel constituent and starting materials for the transition-metal component, respectively.[103] The TaC and NbC powders were produced at 1400-1500 °C based on the conclusion that the gels transform into carbide precursors under pyrolysis at low temperatures (600-700 °C) thus allowing the reactive carbon and finely dispersed oxide particles to be intimately mixed. The

precursor thus formed is of higher reactivity, showing lower reduction temperatures (by 250-300 °C) than physical mixtures of oxides and carbon black.

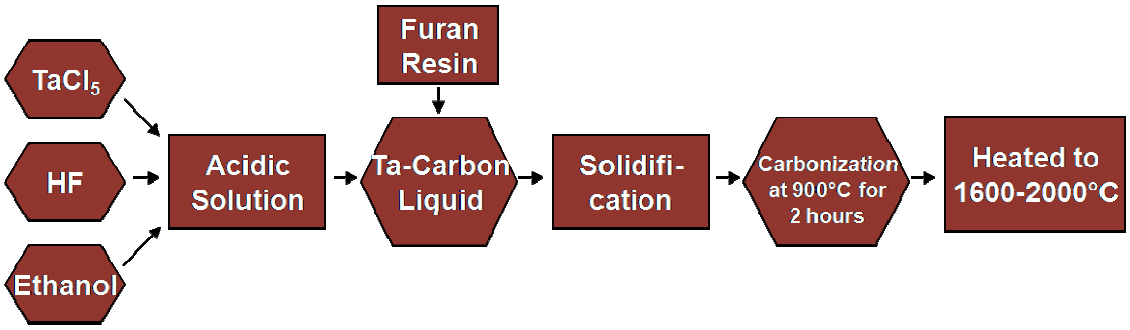

Figure 2.14. Flowchart showing the complex experimental procedure for production of tantalum carbide using the liquid polymer precursor method.[101]

Apart from transition-metal containing organic precursors, transition-metal carbides were also successfully synthesized from mixtures of transition-metal compounds and liquid organic/polymeric precursors.[101-102] Xiang et al report the formation of tantalum carbide using a liquid precursor route after forming pure tantalum oxide at 900 °C from a complex mixture of tantalum chloride in hydrofluoric acid and oxygen-containing furan resin precursor (shown in Figure 2.14).[101] The results shown here clearly demonstrate that intimate mixing of transition-metal halides on the molecular level with a polymer precursor was successful, despite the very acidic nature of the starting materials and production of carbide at temperatures greater than 1600 °C. Lei et al report on the preparation of transition-metal carbide nanoparticles using various transition-metal oxides and melamine as the precursor, as shown in Figure 2.15.[102] The

formation temperature of 1100 °C for these carbides, with rather small sizes, was reported and is much lower than conventional methods.

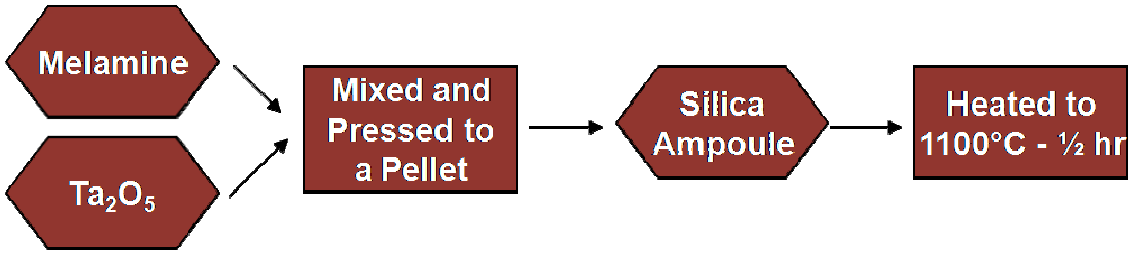

Figure 2.15. Flowchart showing the experimental procedure for the production of tantalum carbide at low temperature.[102]

It seems that if the transition-metal salt could be dispersed on the molecular level within the polymer before thermal exposure that transition-metal carbide formation would occur throughout material rather than just as a coating. In Chapter VI, we demonstrate the ability to produce tantalum and other transition-metal carbides using this approach. Tantalum bromide was the initial focus due to its high boiling point (349 °C) and the subsequent tantalum carbide exhibits one of the highest known melting points (3880 °C). The carbon source material chosen was the FPTI polyimide studied in earlier parts of this work due its high thermal resistance. The *in-situ* mixing of these two materials leads to the highest thermal resistance ceramic (tantalum carbide) using the highest thermal resistance polyimide (FPTI). Additionally, the carbide is formed at temperatures below 1200 °C.

CHAPTER III

FURTHER POLYIMIDE RESIN CROSSLINKING

3.1 Introduction

Initial studies with the neat fluorinated polyimide (Figure 2.11) showed excellent thermal cure and stability, with reaction conversion less than 80% and a decomposition temperature of 524 °C that resulted in 5 wt-% loss.[4,7] The added fluorinated polyimide stability comes from the combination of the perfluoromethyl substituents in the backbone of the oligomer (from AFR700B) and the phenylethynyl endcaps (from PETI-5).[15] In the present work, further crosslinking of the fluorinated polyimide is examined to separate the cure reactions from degradation and to determine the optimum post curing conditions. Glass transition and melting temperatures were ascertained using DSC, while weight loss during curing and decomposition were determined using TGA. Furthermore, the mechanical properties (i.e. tensile strength and elastic modulus) were measured and related to the thermal properties to find the optimum curing conditions. The polyimide resin exhibited the best post curing conditions at 410 °C for 8 hours based on T_g, thermal stability, and mechanical properties.

3.2 Experimental

3.2.1 Materials

Fluorinated phenylethynyl-terminated imide oligomer was obtained from Performance Polymer Solutions Inc. (Centerville, OH) and used as received.

3.2.2 Sample Preparation

Fluorinated polyimide neat resin panels (2mm thick) were prepared at NASA Glenn Research Center in a 10.2 x 10.2 cm steel compression mold. Resin pieces were cut into 3 mm squares and 10 x 25 mm strips using a diamond blade saw cutter for TGA and DMA testing, respectively. Resin panels were cut into 10.1 x 1.9 cm samples for mechanical property testing with an Instron. All resin pieces were then placed in a vacuum oven at 70 °C for a minimum of 24 hours to dry prior to testing.

3.2.3 Characterization

Differential scanning calorimetry (DSC) of the polyimide was performed with a DSC Q20 (TA Instruments, New Castle, DE). Samples (3 mm squares) were heated to targeted temperatures, from 410 – 500 °C, in increments of 30 °C and held for 0.5, 1, 2, 4, and 8 hours under a nitrogen atmosphere. After cooling to room temperature, samples were then heated to 650 °C. Glass transition temperatures (T_g) and melting temperatures (T_m) were determined using Universal Analysis software (TA Instruments, New Castle, DE). Thermogravimetric analysis (TGA) of the polyimide was performed with a TGA Q50 (TA Instruments, New Castle, DE). Samples (3 mm squares) were heated to

targeted temperatures, from 410 – 500 °C, in increments of 30 °C and held for 0.5, 1, 2, 4, and 8 hours under a nitrogen atmosphere. After cooling to room temperature, samples were then heated to 750 °C. Weight loss was measured during further curing conditions, and the decomposition temperature (T_d) was taken to be the point of 5% weight lost during the run. Char yields were obtained from the end of the run and include weight lost during cure. Tensile strength and elastic modulus were obtained using an Instron 5900 Series Dual Column Tabletop Instrument (Norwood, MA). Samples were further cured using a Barnstead Thermolyne 48000 Furnace (Dubuque, IA). The furnace was heated to a targeted temperature, from 410 – 500 °C, in increments of 30 °C under a nitrogen atmosphere. Samples (10.1 x 1.9 cm) were individually placed in the oven for 0.5, 1, 2, 4, and 8 hours. Testing was then performed at room temperature using pneumatic side action grips. The further cured polyimide samples were imaged using a Zeiss Axio Imager.M2m (Thornwood, NY) optical microscope. Images were collected using the z-stacking method and combined using instrument software. The degree of curing was obtained using a Bruker (Billerica, MA) Alpha-P ATR infrared spectrometer with Opus 6.5 software.

3.3 Results and Discussion

3.3.1 Thermal Properties

Figure 3.1(a) shows the glass transition temperatures as a function of cure time in relation to the cure temperatures for the polyimide resin. The 410 °C temperature run showed the best linear trend as cure time was increased, with 8 hours resulting in the

highest T_g (458 °C). While the 440 and 470 °C cure temperatures gave high T_g's for 0.5 and 1 hour cure times, the T_g's became increasingly higher with some of the cure times resulting in an undeterminable T_g from the data. The 2 and 4 hour cure times resulted in T_g's around 500 °C for the 440 °C cure temperature. Beyond 2 hours for the 470 °C cure condition, the T_g's were indistinguishable and samples visually showed signs that degradation had started to occur. Despite the high T_g (530 °C) for the 500 °C 30 minute curing, the sample visually appeared to be degraded on the exterior. This data suggests that the cure conditions need to be any cure time at 410 °C or less than two hours for cure temperatures below 470 °C. The melting temperatures as a function of cure time in relation to the cure temperatures are shown in Figure 3.1(b). There was not as much variability in T_m as there was for the T_g, but the T_m's decreased slightly as the cure time was increased regardless of curing condition. This increase in T_g is a result of restriction of chain mobility caused by a greater crosslinked structure. Based on the results obtained in Figure 3.1, the four hour at 440 °C cure resulted in the best combination of glass transition and melting temperature.

Weight loss during cure, decomposition temperature (T_d), and char yield were also obtained for the further cured resin. Figure 3.2(a) shows the weight loss during cure as a function of cure time with respect to the cure temperature. The TGA was used to first cure the samples and then heated further to obtain the T_d's. The 410 °C curing temperature showed little weight loss (< 2.4%), even with 8hr curing time.

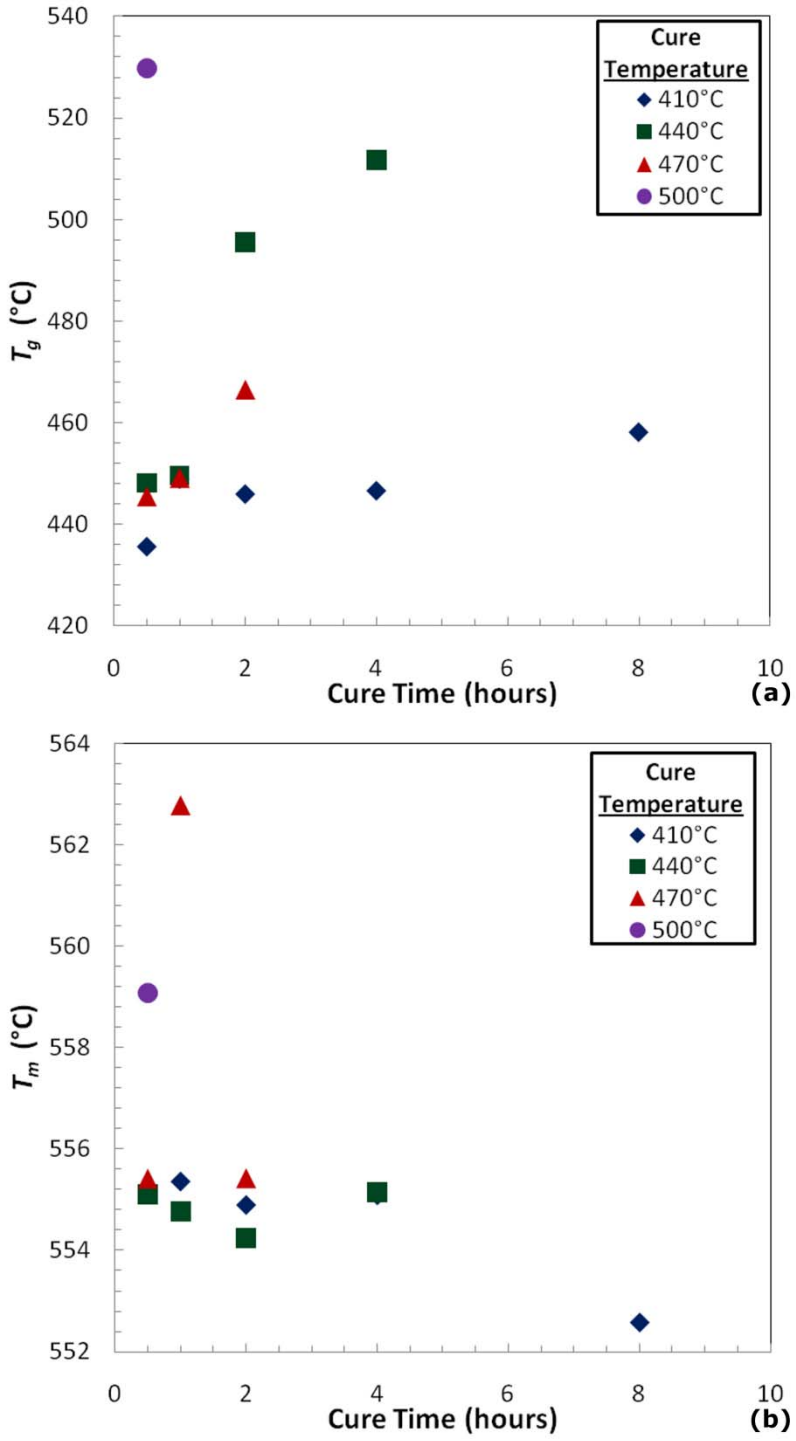

Figure 3.1. Polyimide resin T_g (a) and T_m (b) as a function of further curing time at varying cure temperatures.

Both the 410 and 440 °C curing temperatures showed linear weight loss trends as the curing time was increased, while the 470 and 500 °C curing temperatures exhibited a logarithmic trend with significant weight loss (> 10%) for cure times > 2 hours for 470 °C and all cure times for 500 °C. These trends are expected, in particular with the higher cure temperatures, due to the eventual overlap of continued crosslinking and degradation. The decomposition temperature trends are similar to the weight loss during cure except that the 470 °C cure temperature exhibits a linear trend, as shown in Figure 3.2(b). The difference in T_d's for each cure temperature from 30 minutes to 8 hours nearly doubled with each 30 °C cure temperature increment. While having a high T_d is beneficial, the amount of weight loss during cure for those samples with higher T_d's is too great for using those cure temperatures/times for post curing conditions.

3.3.2 Mechanical Properties

The elastic modulus (Fig. 3.3(a)) and tensile strength (Fig. 3.3(b)) were measured for each of the polyimide resin cure times/temperatures. The 410 °C cure temperature, regardless of cure time, maintained the best elastic modulus and tensile strength properties. Cure times less than four hours at 440 °C maintained moderate elastic modulus and tensile strength despite being lower than the 410 °C cure temperature/times. Curing at 470 °C for 8 hr and > 30 minutes at 500 °C resulted in samples that were too brittle or degraded to be tested. Based on these results, curing 8 hours at 410 °C produces the best mechanical properties (E ~ 2.1 GPa and TS ~ 45 MPa).

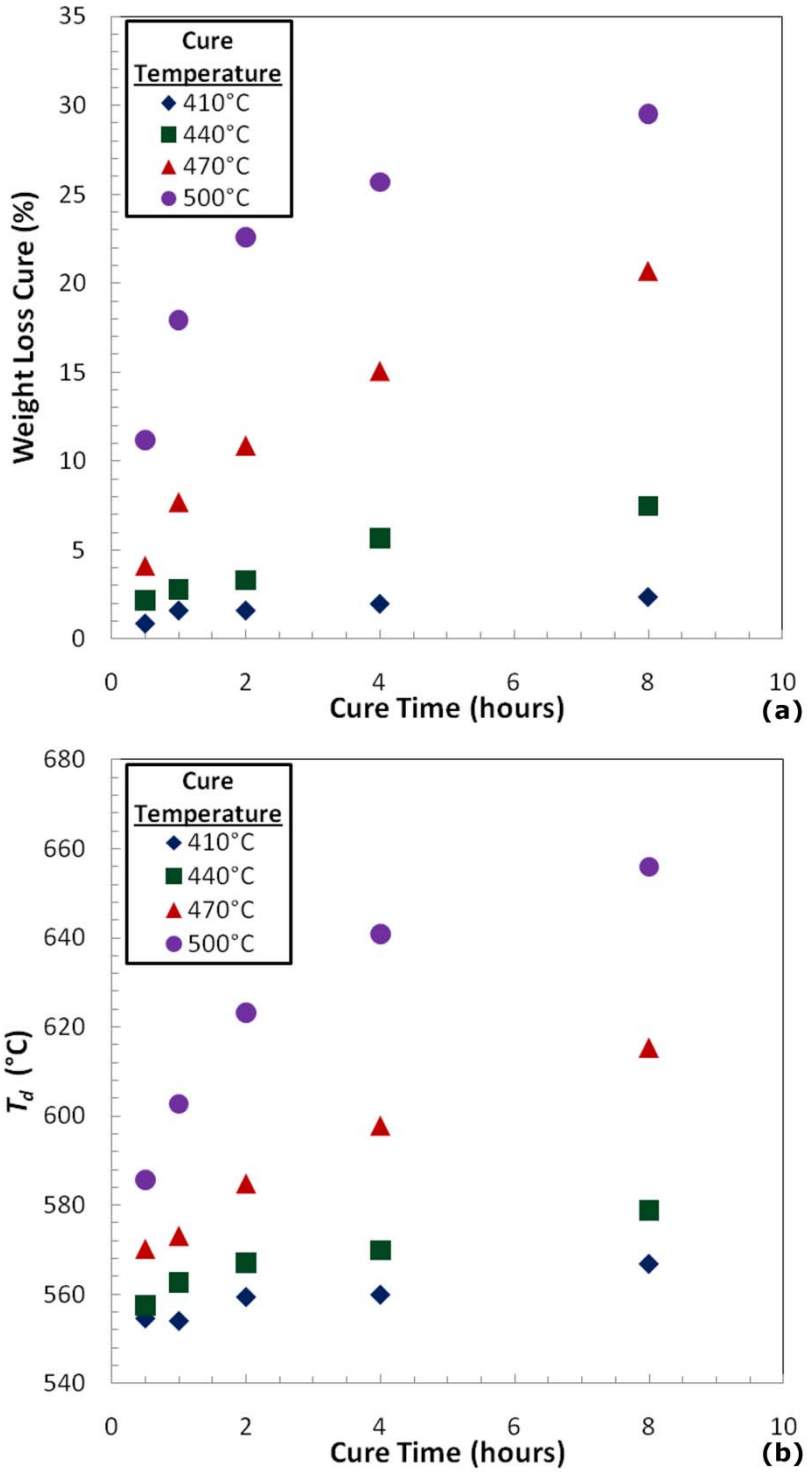

Figure 3.2. Polyimide resin weight lost during cure (a) and degradation temperature (b) as a function of further curing time at varying cure temperatures.

3.3.3 Optical Microscopy

Optical microscope images for five selected further cured samples are shown in Figure 3.4 based on the thermal and mechanical properties results. Two samples, cured at 410 °C for 30 minutes (Fig. 3.4(a)) and 8 hours (Fig. 3.4(b)), suggest that there are still regions of uncrosslinked material due to the brighter brown areas. The sample cured one hour at 440 °C (Fig. 3.4(c)) was selected in order to determine if sample maintained structural integrity on the micro scale. This cure time/temperature condition shows remaining uncrosslinked material, but also indicates no significant degradation occurred. Figure 3.4(d) and (e) are the 30 minute cure time at 470 and 500 °C curing temperatures, respectively. These samples not only showed major degradation from the optical images, but also appeared to be degraded to the naked eye. All of the optical images in Figure 3.4 verify that the lower curing temperatures are better for obtaining a further cured sample that maintains structural integrity.

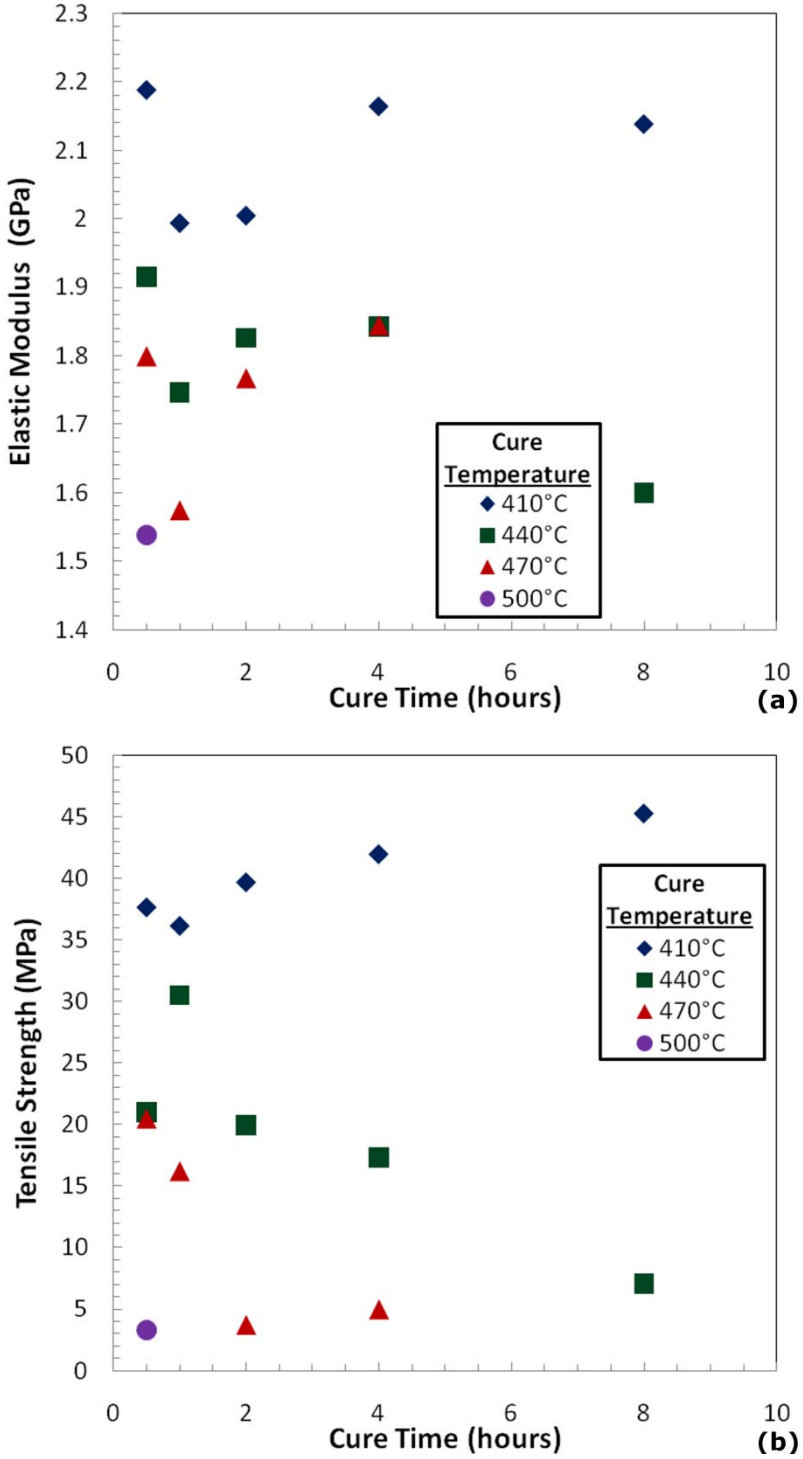

Figure 3.3. Polyimide resin elastic modulus (a) and tensile strength (b) as a function of further curing time at varying cure temperatures.

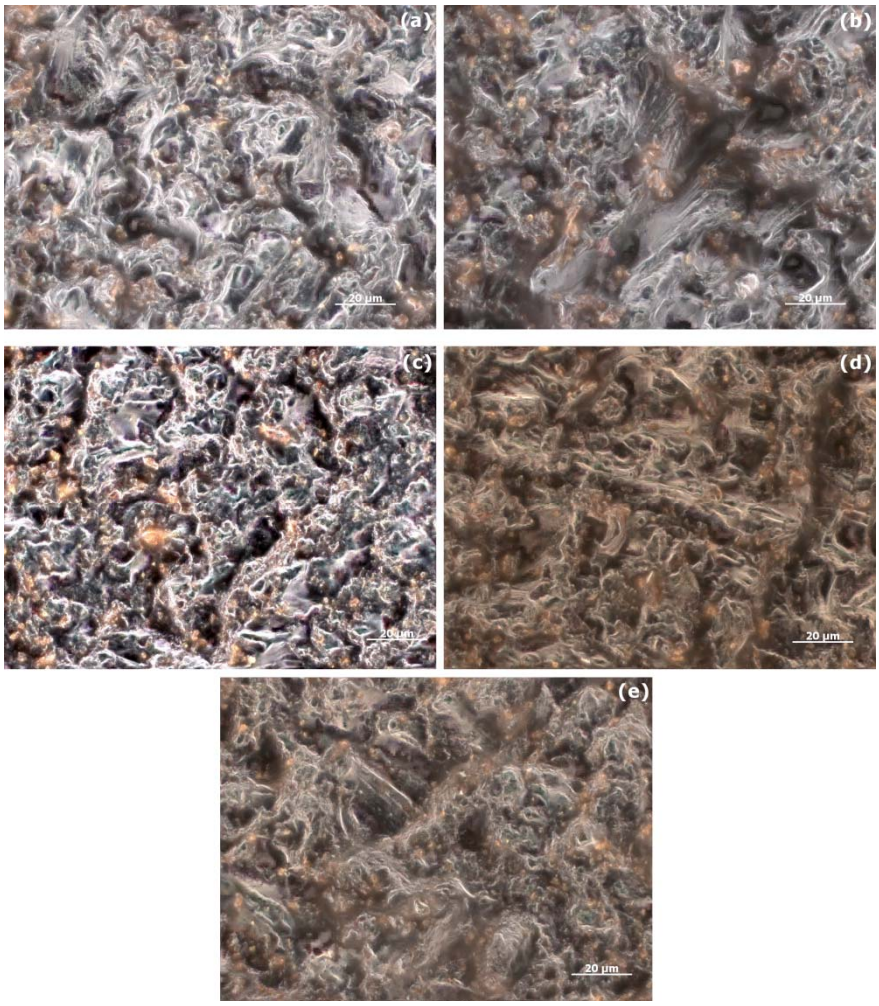

Figure 3.4. Polyimide resin cured for 30 min at 410 °C (a), 8 hours at 410 °C (b), 1 hour at 440 °C (c), 30 min at 470 °C (d), and 30 min at 500 °C (e).

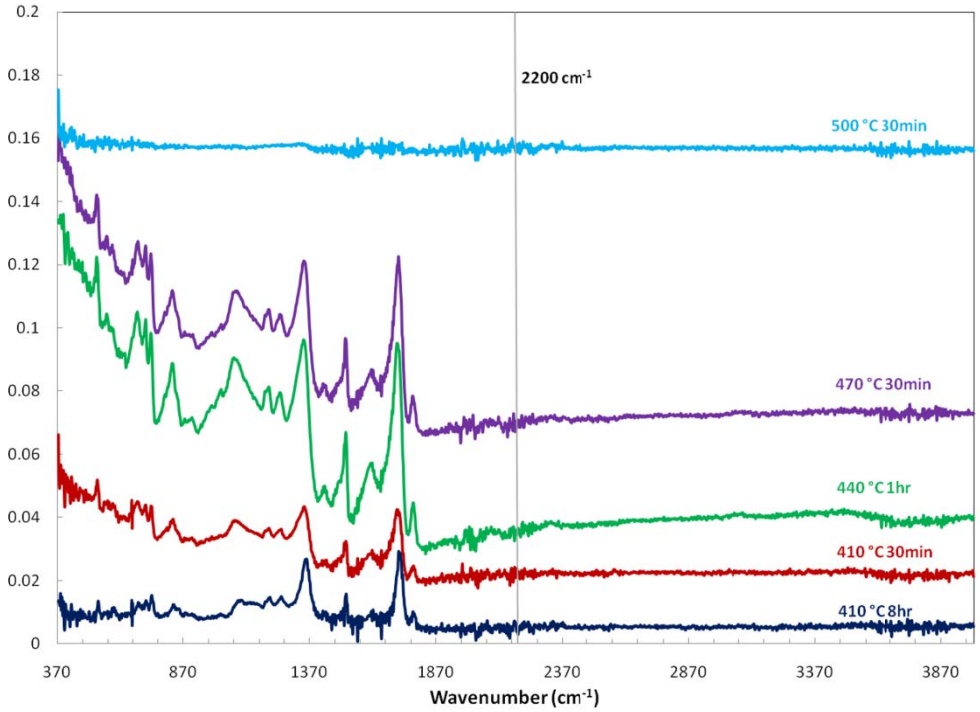

Figure 3.5. ATR FTIR results of further cured polyimide resin for selected cure times/temperatures.

3.3.4 Degree of Crosslinking

Figure 3.5 shows the results obtained from ATR FTIR for the same samples used for the optical images. With increasing cure time/temperature, the intensity of carbon double (1640-1680 cm^{-1}) and single bonds (800-1300 cm^{-1}) increases, indicating further crosslinking of the triple bonds (2100-2260 cm^{-1}). As the cure temperature is raised to 470 °C, these bond intensities begin to drop due to degradation, which is expected based on the thermal and mechanical property data. There is a small presence of triple bonds still remaining for both of the 410 °C samples, which is also suggested by the lower intensity of the carbon double and single bonds. The 500 °C sample lacks the

appearance of major chemical bond shifts due to the severity of degradation that occurred.

3.4 Conclusions

Increased glass transition temperatures were observed for the fluorinated polyimide with any increase in curing time or temperature. Based on the results obtained from DSC, curing for 4 hr at 440 °C results in the best glass transition and melting temperatures. The TGA results indicate that curing below 440 °C, regardless of time, generally improves the polyimide in terms of thermal stability. Tensile testing also proved to be a useful indicator of the optimum post cure conditions, suggesting the best strength and modulus at 410 °C for 8 hours. Despite these results, infrared spectroscopy indicated that the 410 °C cure temperature, regardless of cure time, does not result in full cure. A greater understanding of the extent of crosslinking for the polyimide resin is essential in order to maximize the thermal stability for aerospace applications.

CHAPTER IV

MEASUREMENT OF BLISTER FORMATION IN FLUORINATED POLYIMIDE AND ITS CARBON FIBER COMPOSITE

4.1 Introduction

Despite their promise, an area of concern for composites to be used in severe environments is their ability to withstand hygrothermal degradation.[3,106-109] Moisture that is absorbed and then trapped can cause microcracking, blistering, or steam delamination upon rapid heating.[3] This trapped moisture can lead to a reduction in strength and strain at failure due to blistering and micro-cavitation.[106,110] Blistering, in particular, occurs when there is enough moisture pressure to exceed the strength of the material, which happens when the temperature and water content is high.[5,107] In general, polyimides are very thermally stable due to their high T_g's and decomposition temperatures,[15] but their uptake of moisture needs further study, especially for the fluorinated polyimide, due to initial findings with similar polyimides (PMR-II-50, AFR700B, and PETI-5).[3,106-109] Adding reinforcements to the neat polyimide resin, such as carbon fiber, has been shown to improve the hygrothermal degradation of the composite material.[109,111] Polyimide carbon fiber composites can absorb up to 1.5 wt% moisture in the matrix, trapped inside voids or pre-existing flaws.[109] In moist composites, blisters can form in the resin or at the fiber-resin interface upon exposure to a rapid thermal spike. Thermal expansion and swelling is not an issue for carbon fibers

in the presence of moisture, so blistering occurs only in the resin material and at the resin-carbon fiber interface due to increasing temperature and moisture.[112]

Here a blistering study was performed on the same fluorinated polyimide and carbon fiber composite examined in Chapter III. Blister temperatures, resulting from rapid heating, were obtained by monitoring changes in transverse thickness expansion using two different techniques. In one case, a transverse extensometer was used to measure the thickness changes, while quartz UV lamps provided a means to control rapid heating of the material (known as the QUV method). Thermomechanical analysis (TMA) was used as a secondary method to determine whether sample size influences the temperature at which the resin and composite will blister. Both techniques showed similar blister temperatures in relation to the amount of absorbed moisture, regardless of sample size. The polyimide resin exhibited blister temperatures ranging from 225 – 362 °C, with 1.7 - 3.0 wt% absorbed moisture, and the polyimide composite had blister temperatures from 246 – 294 °C with 0.5 - 1.5 wt% moisture. In general, increasing moisture content in the polyimide will reduce blister temperature, but there is no clear relationship between these values and modulus reduction. The blister testing methodologies developed here will help to determine the ability of any high temperature polymer and its carbon fiber composite to withstand hygrothermal degradation for future use in military and aerospace applications.

4.2 Experimental

4.2.1 Materials

Fluorinated phenylethynyl-terminated imide oligomer and polyimide carbon fiber composite with 55 wt% carbon fiber, T650-35/8HS/AFRPE-4 10 ply (4 mm thick), were purchased from Performance Polymer Solutions Inc. (Centerville, OH) and used as received.

4.2.2 Sample Preparation

Fluorinated polyimide neat resin panels (2 mm thick) were prepared at NASA Glenn Research Center in a 10.2 x 10.2 cm steel compression mold. Resin pieces were cut into 1 mm and 1 inch squares using a micromatic precision slicing machine for testing using the TMA and QUV method, respectively. Composite pieces were cut into 1 mm squares and 1 inch circles using a diamond blade saw for TMA and QUV testing, respectively. The various testing specimen parameters differed for the techniques used, resulting in the different specimen sizes. Both resin and composite pieces were placed in a vacuum oven at 70 °C for a minimum of 24 hours to dry prior to testing. The samples were then placed into a humidity controlled oven at 100 °C and 95% RH to introduce moisture.

4.2.3 Blister Testing

Thickness expansion was measured using an LSM 6200 laser scan micrometer and LSM-506S laser measuring system (Mitutoyo, Aurora, IL) (i.e., transverse extensometer) equipped with quartz lamps as a heating source, as shown in Figure

4.1(a). A schematic of this apparatus is shown in Figure 4.1(b). The samples were placed on two alumina rods supported at the ends by metal stands and positioned in the center of the quartz lamps and heated to 500 °C with a 50 °C/min heating rate. The laser extensometers, with a resolution of 0.5 μm, were positioned so that the only obstruction was the sample. To maintain structural integrity of the test specimens, a temperature calibration was performed on a small test block of resin and composite (to remain in place during testing for each material) and a dry sample of resin and composite to verify any temperature differences that may arise between the different specimens. Calibration curves verified there was little difference between specimens for the resin and composite as shown in Figure 4.2. This calibration confirms that the temperature of the sample specimen is the same as the control block for the entire test. The alumina rods were placed sufficiently far away from the testing area and therefore showed no effect on the data as demonstrated in the calibration. Thermomechanical analysis of the polyimide resin and polyimide-carbon fiber composites was performed with a TMA 2940 Thermal Analyzer (TA Instruments, New Castle, DE). Samples were heated to 500 °C under an air atmosphere using a 50 °C/min heating rate. Blister temperatures for both techniques were taken as the onset of rapid dimensional change as a function of temperature.

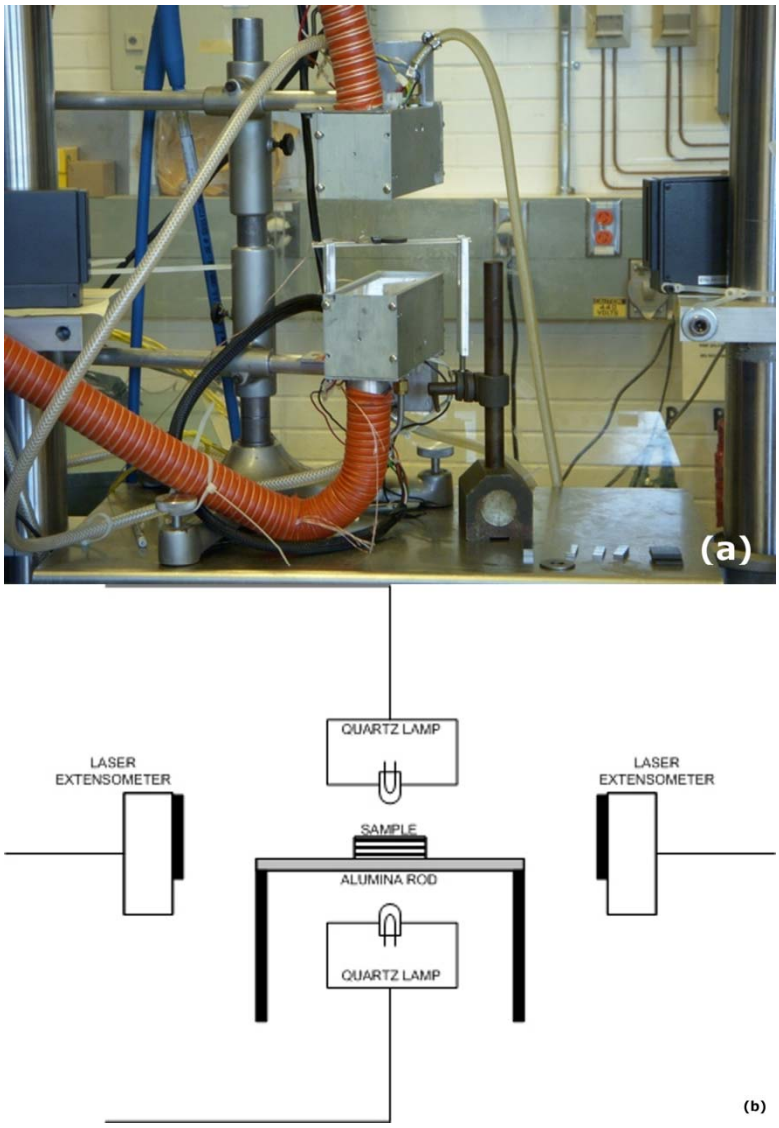

Figure 4.1. QUV transverse extensometer apparatus (a) for measuring dimensional changes as a function of temperature. The schematic (b) shows the key components of this device.

4.2.4 Characterization

Dynamic mechanical analysis (DMA) was conducted on post-blistered samples to determine how the storage modulus is influenced by blistering. Samples were tested at room temperature using a single cantilever, multi-frequency-strain sweep method.

Optical microscopy was performed with a Hirox 3-D Microscope (River Edge, NJ) using 200x magnification. Scanning electron microscopy of the composite was performed with an FEI Quanta 600 FE-SEM (Hillsboro, OR) at 100x, 200x, and 500x magnification. Images for both techniques were taken of the cross-sections from the center of the composite.

4.3 Results and Discussion

4.3.1 Transverse extensometer testing of polyimide resin and polyimide carbon fiber composite

Figure 4.3 shows how the temperature marking the onset of blister formation is determined using the QUV method. The load cell voltages do not need to be converted to actual displacement given that the temperature at the onset of blistering is the only data of interest. Two linear lines are fit to the data on either side of the inflection point in this voltage as a function of temperature curve. The point at which the two fit lines meet is taken as the temperature at which blistering begins. Figure 4.4(a) shows blister temperature as a function of percent moisture in the neat polyimide resin. Blister expansion was observed for non-moisture induced samples, which has also been found by others.[5,107]

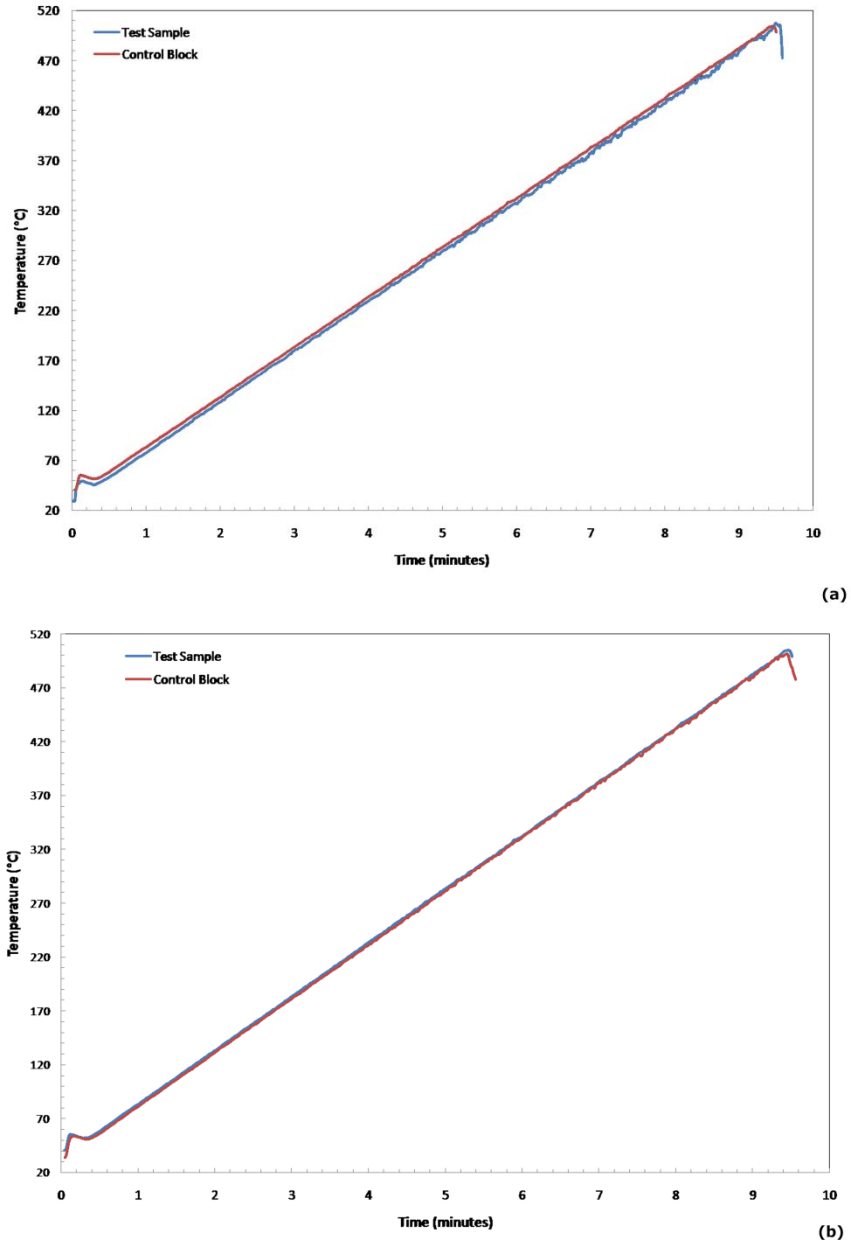

Figure 4.2. Temperature calibration for polyimide resin (a) and composite (b).

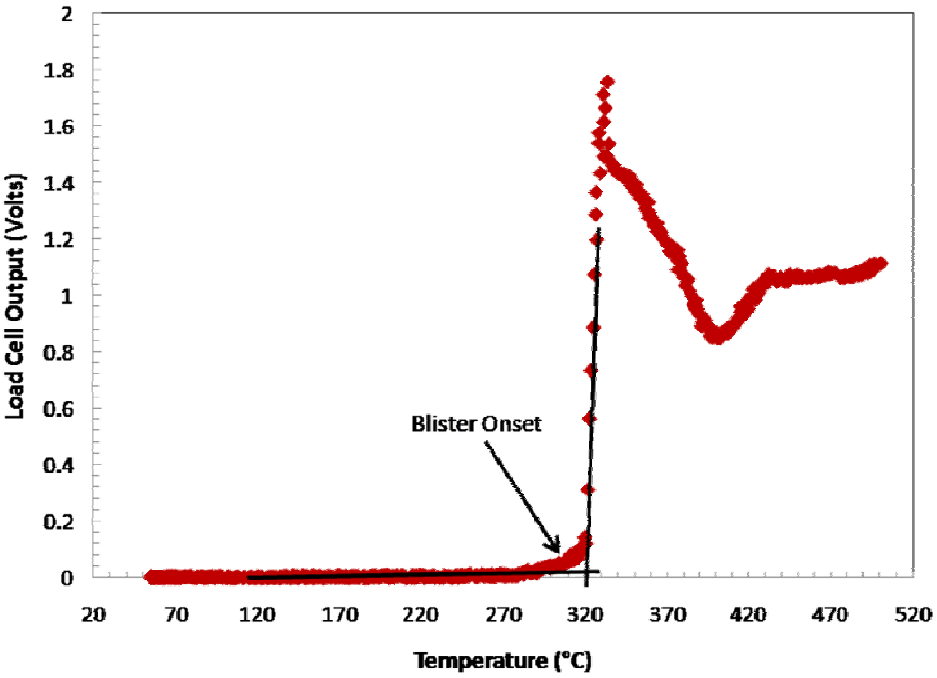

Figure 4.3. Load cell voltage as a function of sample temperature obtained using the QUV method. The temperature marking the onset of blistering, for both polyimide and polyimide carbon fiber composite, is taken as the intersection of fit lines. The data shown here is from a test with the neat polyimide resin.

The resin samples absorbed 1.7 - 3.1 wt% moisture that resulted in blister onset temperatures ranging from 225 – 379 °C. The data shows that there is little correlation between the amount of moisture in the resin and onset of blister formation. Samples with the same, or very similar, absorbed moisture had blister temperatures vary more than 100 °C. This large variation is most likely due to the structural integrity of the resin (i.e., voids generated in the matrix during processing). Upon rapid heating of samples with the same moisture content, the samples with more defects are more likely to blister at lower temperatures compared to those with few defects. This is due to more moisture being confined in one localized spot within the material, which readily produces a blister

compared to a sample with the moisture more uniformly distributed throughout the sample.

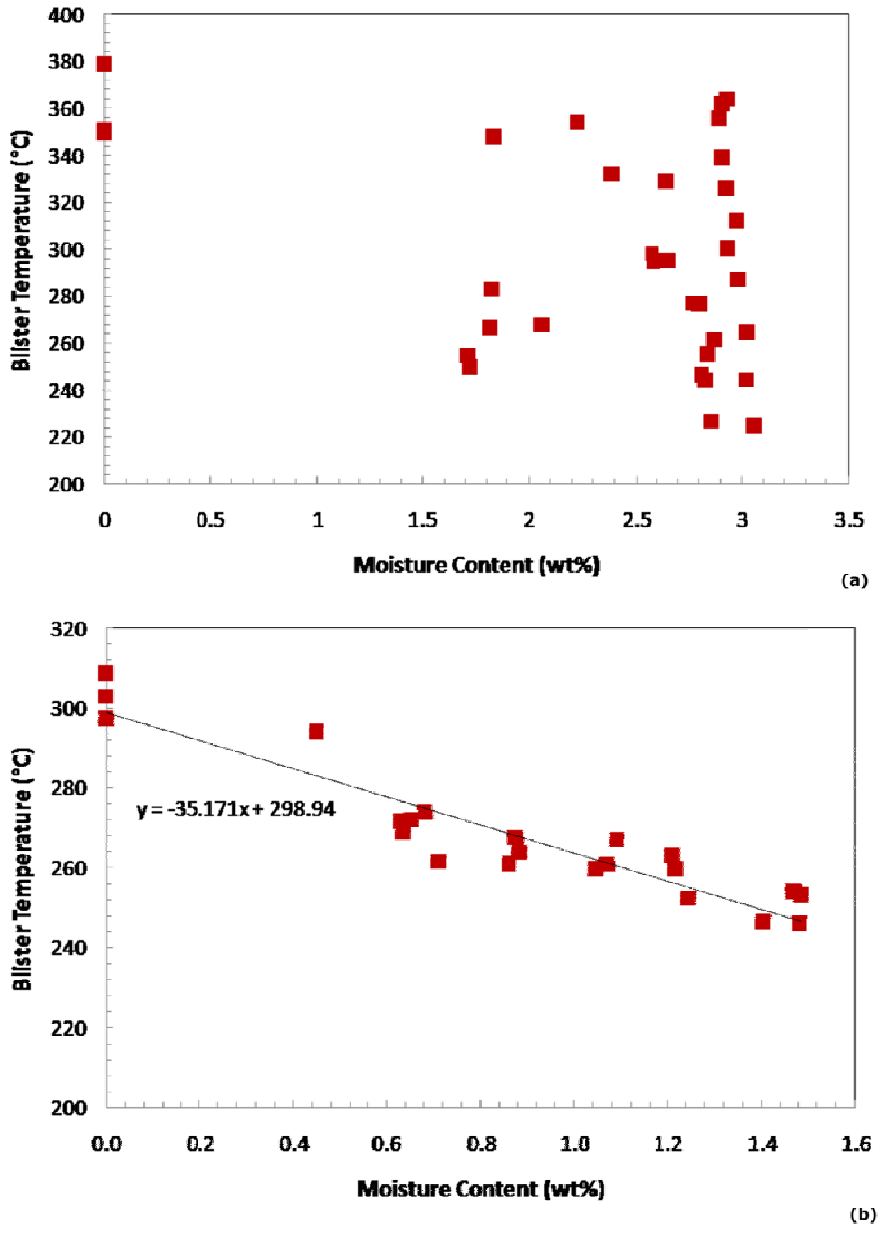

Figure 4.4. Temperature marking onset of blister formation as a function of moisture content in neat polyimide resin (a) and carbon fiber composite (b). The trendline shown in (b) has an R^2 value of 0.88.

Figure 4.4(b) shows the relatively linear inverse relationship between blister onset temperature and moisture content for the polyimide carbon fiber composite samples. The amount of moisture absorbed for the composites is much lower than the resin samples. Moisture contents of 0.4 - 1.5 wt% resulted in blister onset temperatures of 246 – 294 °C. These low onset temperatures are not surprising because composites typically have more voids and pre-existing flaws, in particular due to a weak interface between the resin and carbon fiber, that lead to lower amounts of moisture causing blistering relative to the neat resin. The composite does not absorb as much moisture as the neat resin due to the large concentration (55 wt%) of non-moisture absorbing carbon fiber.[29] Table 4.1 shows the amount of moisture uptake, thickness change, blister temperature, and storage modulus for the composites. While the blister temperature is affected in relation to the amount of moisture present, there is no clear relationship between the thickness change or storage modulus of the composite with respect to moisture amounts or blister temperature. The sample not subjected to moisture nor blistering conditions exhibited a storage modulus of 8333 MPa. However, the non-moisture induced/blistered sample and moisture induced/nonblistered sample resulted in storage moduli of 1442 and 2600 MPa, respectively. Therefore, a reduction in storage modulus is a result of both moisture and blistering conditions. Optical microscope and SEM images support this assertion. The dry composite does not show any voids or flaws in the optical microscope image (Figure 4.5(a)); however, the SEM images clearly indicate voids within the resin and at the resin-carbon fiber interface (Figures 4.6(a) and (b)). In the optical micrographs (Figure 4.5) the light areas are the carbon fiber, while

the darker areas are the resin. The areas with alignment and orientation are the carbon fiber in the SEM images (Figure 4.6). Both types of imaging clearly illustrate the degradation that occurs in the resin and at the interface between resin and fiber due to blistering. It is interesting to note that blistering also splits the carbon fiber itself in these images. This could occur as a result of resin material flowing into gaps in the carbon fiber weave during processing. Figure 4.5(c) is an OM image taken from the edge of a blistered sample, which reveals that the composite undergoes oxidation on the surface during heating. This is apparent due to the inability to distinguish the layers of polyimide resin and carbon fiber.

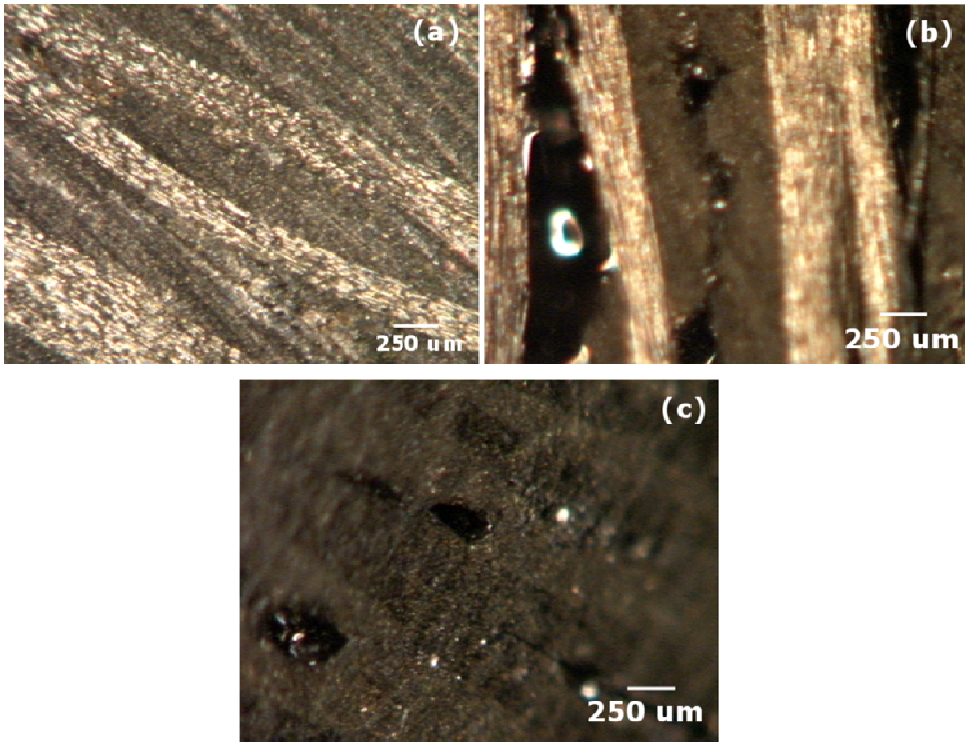

Figure 4.5. Optical microscope images of the polyimide carbon fiber composite before exposure (a) and after being subjected to blister conditions (b) from inside the sample. An image taken from the edge of the composite is also shown (c).

Table 4.1. Polyimide composite parameters after heating to 500 °C.

Weight % Moisture	Change in Thickness (%)	Blister Temperature (°C)	Storage Modulus (MPa)
0	-	-	8333
0	10.4	303	1442
0.16	-	-	2600
0.45	9.9	294	999
0.63	12.5	272	1885
0.68	10.5	274	1674
0.87	8.4	268	1768
0.88	10.4	264	1964
1.04	10.2	260	2423
1.07	8.8	261	1585
1.09	14.4	267	1486
1.21	10.8	263	1307
1.48	16.6	246	966

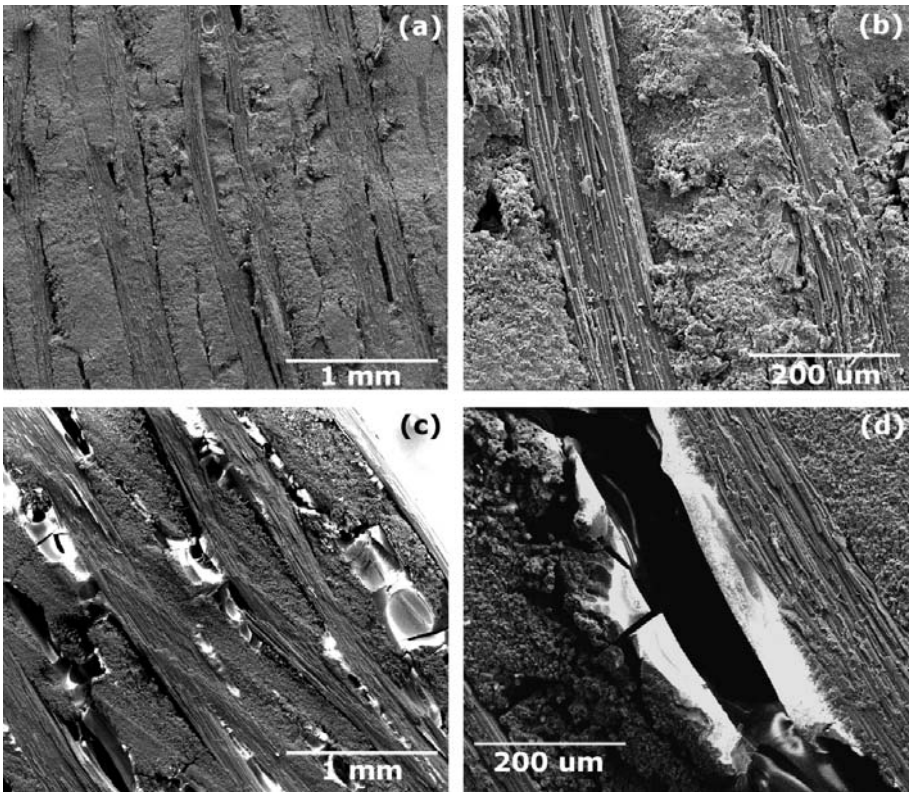

Figure 4.6. SEM images of polyimide carbon fiber composite before exposure ((a) and (b)) and after being subjected to blister conditions ((c) and (d)).

4.3.2 Thermomechanical analysis of polyimide resin and polyimide carbon fiber composite

Thermomechanical analysis is an alternate technique that can be used to measure the onset of blistering in the polyimide resin and its carbon fiber composite. The TMA method is similar to the QUV technique, but the blister temperature is determined by evaluating the derivative of dimension change as a function of temperature, rather than the absolute dimension change, due to greater accuracy in obtaining fit lines to the data. Figure 4.7 shows an example of dimension change as a function of temperature. The blister temperatures obtained for the polyimide resin range from 277 – 377 °C for samples that absorbed 2.0 - 2.6 wt% moisture, as shown in Figure 4.8(a). When compared with Figure 4.3(a), the same trend observed for the QUV method is seen with the TMA method. The larger samples used for the QUV method were able to absorb slightly more moisture, but samples with the same amount of moisture resulted in similar blister temperatures for both methods. These results confirm the validity and accuracy of both techniques and suggest that smaller samples do not release moisture from the sides, but rather keep it trapped inside and expand the resin in the same manner as the larger samples.

Blister temperatures as a function of absorbed moisture for the polyimide composite are shown in Figure 4.8(b). The same linear trend as that found using the QUV method is observed. The smaller composite samples absorbed similar percentages of moisture as the larger samples, ranging from 0.1 - 1.4 wt%, and blister onset temperatures (247 – 266 °C) were also similar.

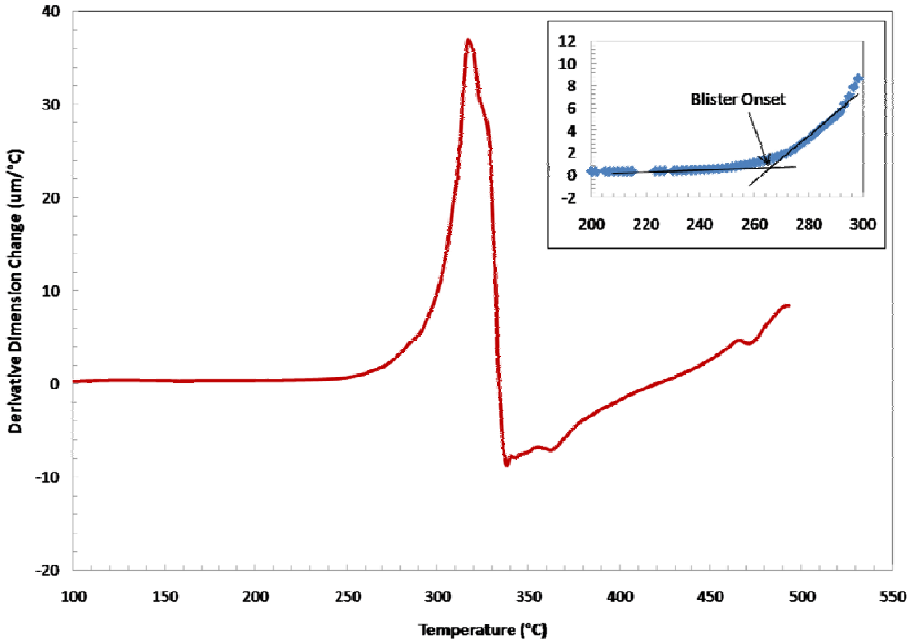

Figure 4.7. First derivative of dimension change as a function of temperature for polyimide measured with TMA. The inset is a magnified view of the inflection of the curve that highlights how the blister onset is determined.

Although not truly quantitative, the agreement between the TMA and QUV methods suggests sample size is not a significant issue for blister measurements. The QUV method exhibits a more linear relationship, as indicated by a larger R^2 value, and may be considered more precise than TMA. If small samples with smaller amounts of absorbed moisture had been available, there would likely be less of a disparity between these two techniques. The advantage of thermomechanical analyzers is that they are commercially available, relatively inexpensive, and require less material (i.e., smaller sample size).

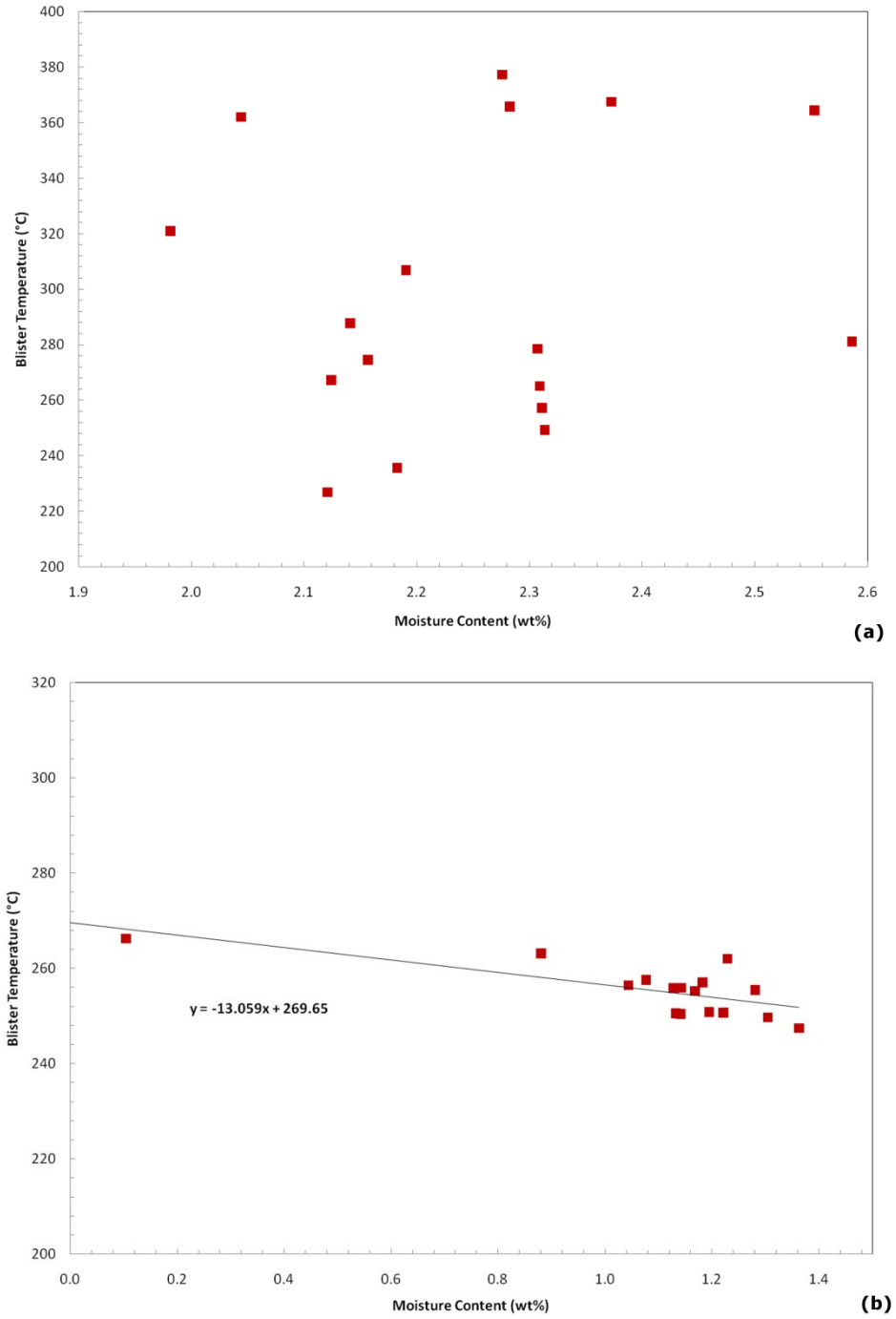

Figure 4.8. Polyimide resin (a) and carbon fiber composite (b) blister temperature as a function of moisture uptake measured with TMA. The trendline shown in (b) has an R^2 value of 0.51.

4.4 Conclusions

Absorbed moisture produces irreversible damage to the fluorinated polyimide and its carbon fiber composite at temperatures as low as 246 °C, due to blister formation. The neat polyimide resin exhibits greater hygrothermal stability than the carbon fiber composite, in part due to fewer flaws within the resin. The polyimide composite shows a linear decrease in blister temperature as a function of moisture present. Both of the testing methods employed in this work (QUV and TMA) were successful in evaluating the onset of blistering. Each technique measured similar trends and blister temperatures, although the QUV method (with larger sample size) appeared to be more precise. Future work with the fluorinated polyimide will include further crosslinking and strength testing of both the resin and composite at elevated temperatures and exposure times. Greater crosslinking is expected to reduce moisture uptake by the resin due to a decrease in voids, which will increase the temperature associated with the onset of blister formation. It is also expected that this absorbed moisture and the resulting blister temperature results will be used to produce a model to predict the effects of moisture in the composites at higher temperatures than those explored here. With a better understanding of hygrothermal induced composite damage, improvements can be made to these high temperature materials, which are of great need for aerospace applications.

CHAPTER V

THERMAL DEGRADATION OF HIGH TEMPERATURE FLUORINATED POLYIMIDE AND ITS CARBON FIBER COMPOSITE*

5.1 Introduction

Adding reinforcements, such as carbon fiber to neat polyimide resin, results in lower weight loss due to a smaller amount of resin in the composite being subjected to degradation.[35,111] This added stability is a result of the polyimide resin matrix only being able to oxidize, or undergo other forms of degradation, from the surface of the material. This allows the composite to withstand higher temperatures than the neat polyimide resin due to less neat resin material at the surface.[12] In this chapter, weight loss of the fluorinated polyimide and its corresponding polyimide carbon fiber composite under elevated temperature is examined. Weight loss as a function of exposure temperature and time was measured using thermogravimetric analysis (TGA) and by pre- and post-weighing of specimens treated in an oven. Both techniques showed similar weight loss trends as a function of time and temperature, but TGA showed much greater weight loss due to greater surface area to volume (i.e., small sample size).

---

*Reprinted with permission from "Thermal Degradation of High Temperature Fluorinated Polyimide and its Carbon Fiber Composite" by A. D. Adamczak *et al*., 2010. *Journal of Applied Polymer Science*, 115, 2254-2261, © 2010 by Wiley Periodicals, Inc.

The neat polyimide resin and carbon fiber composite exhibited negligible weight loss at temperatures below 430 °C, for exposure times up to 20 minutes. This study serves to highlight the thermal stability, and clarify the thermal degradation mechanism, of this fluorinated polyimide and its carbon fiber composite for future use in high temperature applications.

5.2 Experimental

5.2.1 Materials

Fluorinated phenylethynyl-terminated imide oligomer and polyimide carbon fiber composite with 55 wt-% carbon fiber concentration, T650-35/8HS/AFRPE-4 10 ply (4 mm thick), were obtained from Performance Polymer Solutions Inc. (Centerville, OH) and used as received.

5.2.2 Sample Preparation

Fluorinated polyimide neat resin panels were prepared at NASA Glenn Research Center in a 10.2x10.2 cm steel compression mold to produce 2 mm thick panels. Resin pieces were cut into 3 and 6 mm squares using a micromatic precision slicing machine. Composite pieces for testing were cut into 3 and 6 mm squares using a band saw. Resin and composite pieces were then placed in a vacuum oven at 70 °C for a minimum of 24 hours to dry prior to testing.

5.2.3 Weight Loss Testing

Oven aging of specimens was accomplished using a Barnstead Thermolyne 48000 Furnace (Dubuque, IA). The furnace was heated to a targeted temperature, from

250 – 510 °C, in increments of 20 °C under an air atmosphere. Samples (6 mm squares) were individually placed in the oven for 2 - 20 minute time intervals in increments of 2 minutes, and a new sample was used for each time interval and temperature increment (140 total samples were tested). Weight loss measurements for all resin and composite samples were recorded and percent weight loss was calculated. Percent weight loss was calculated using Equation 5.1:

$$\%\ \text{Weight loss} = \frac{\text{sample initial weight-sample final weight}}{\text{sample initial weight}} * 100 \qquad (5.1)$$

Thermogravimetric analysis of polyimide resin and polyimide-carbon fiber composites was performed with a TGA Q50 Thermal Analyzer (TA Instruments, New Castle, DE). Samples (3 mm squares) were heated to targeted temperatures, from 250 – 510 °C, in increments of 20 °C and held for 20 minutes under an air atmosphere, unless otherwise noted, using the equilibrate method. Weight loss was determined as a function of time at increments of 2 minutes, from 2 - 20 minutes, to compare with results obtained from oven testing.

5.2.4 Characterization

Optical microscopy of the resin and composite was performed with a Hirox 3-D Microscope (River Edge, NJ) using 200x magnification. Images of the cross-sections of each material were obtained after being exposed to 250 °C, 370 °C, 490 °C and 510 °C for 20 minutes, along with an unaged control specimen. Scanning electron microscopy of the composite was conducted using an FEI Quanta 600 FE-SEM (Hillsboro, OR) at 500x and 2000x magnification. Degradation of the polyimide resin was investigated

using a Netzsch Thermogravimetric Analysis 209 F1 Iris (Burlington, MA) instrument that was coupled with a QMS Aeolos mass spectrometer (Selb, Germany) and a Bruker Tensor 27 FTIR (Madison, WI). Analysis was performed under air with a 20 mL/min flow rate, 20 mg sample size and a 10 °C/min heating rate (used to heat the sample to 800 °C). The coupling system between the TGA, FTIR and MS was heated up to 200 °C to prevent condensation of evolved gases.

5.3 Results and Discussion

5.3.1 Oven weight loss

The weight loss of the polyimide resin, and its carbon fiber composite, provides insight into the stability of these materials at various time and temperature exposures. Figure 5.1(a) shows the percent weight loss as a function of temperature for the neat polyimide resin. At temperatures below 430 °C, the weight loss is less than 1% for exposure times up to 20 minutes. This polyimide is able to withstand higher temperature environments (without degrading) than most other polymers due to its highly aromatic chemical structure and highly crosslinked network (Figure 2.11).[2] When exposure temperatures are above 450 °C, the weight loss exceeds 1% after 14 minutes, especially at 490 °C with exposure times greater than 10 minutes and 510 °C with exposure times greater than 6 minutes. The decomposition temperature (T_d) for the polyimide resin, as shown in Figure 5.1(a), is 522 °C in air and 524 °C in nitrogen. Furthermore, the resin has lost 5% of its weight at 529 °C in air, while this same level of degradation does not occur until 538 °C in nitrogen. The lower degradation temperature observed with an air

atmosphere indicates a modest level of oxidation.[113] This fluorinated polyimide can withstand up to ten minutes at 510 °C, just below its T_d, with only a 4.5% weight loss in air. A broader set of raw time and temperature data is shown in Table 5.1.

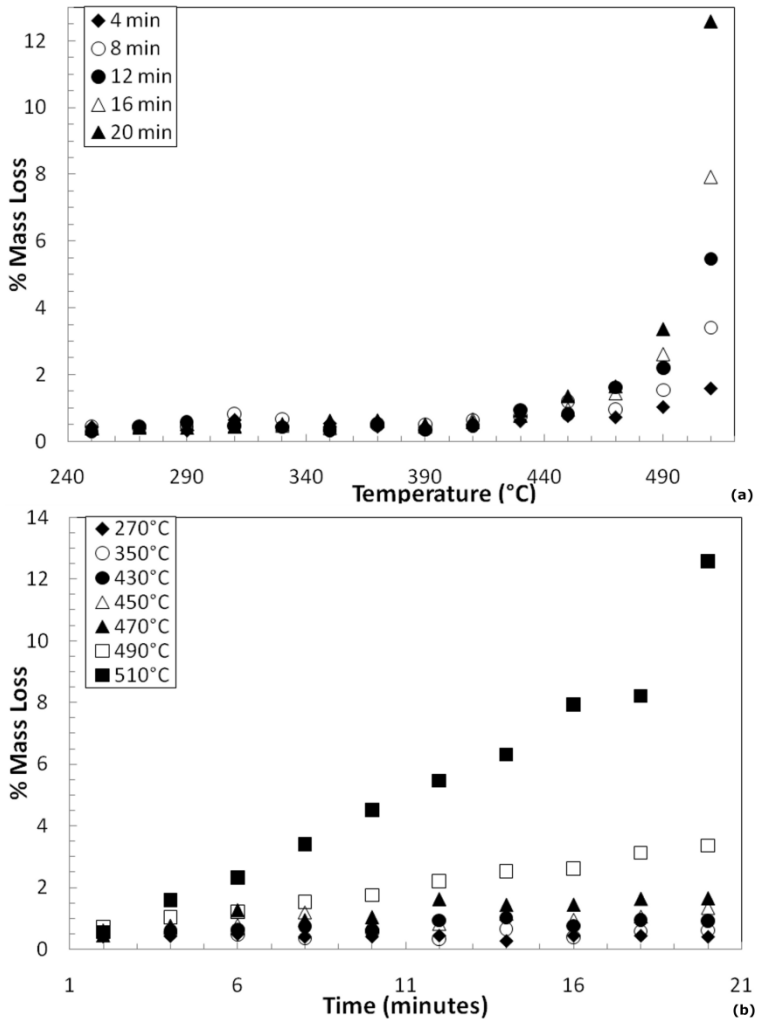

Figure 5.1. Polyimide resin weight loss in oven as a function of exposure temperature (a) and time (b).

Table 5.1. Polyimide resin weight loss in oven. Values in table are loss percentage.

Temp (°C)	Time (min)									
	2	**4**	**6**	**8**	**10**	**12**	**14**	**16**	**18**	**20**
250	0.39	0.43	0.47	0.45	0.43	0.29	0.65	0.38	0.45	0.42
270	0.41	0.43	0.50	0.41	0.42	0.45	0.27	0.45	0.45	0.41
290	0.16	0.33	0.42	0.43	0.57	0.57	0.40	0.52	0.65	0.41
310	0.40	0.65	0.47	0.82	0.35	0.47	0.74	0.45	0.64	0.44
330	0.42	0.45	0.59	0.67	0.47	0.42	0.61	0.47	0.34	0.52
350	0.46	0.54	0.49	0.35	0.57	0.34	0.66	0.40	0.59	0.62
370	0.51	0.44	0.42	0.48	0.52	0.52	0.68	0.61	0.46	0.63
390	0.38	0.42	0.60	0.50	0.24	0.35	0.56	0.44	0.59	0.50
410	0.66	0.51	0.63	0.64	0.76	0.46	0.57	0.66	0.69	0.58
430	0.55	0.61	0.64	0.75	0.61	0.94	1.02	0.76	0.95	0.92
450	0.61	0.76	0.79	1.20	0.85	0.82	1.16	0.96	1.06	1.35
470	0.46	0.72	1.26	0.95	1.04	1.62	1.43	1.44	1.63	1.65
490	0.72	1.04	1.22	1.54	1.76	2.21	2.53	2.61	3.13	3.36
510	0.56	1.59	2.33	3.41	4.51	5.46	6.31	7.92	8.21	12.57

Oven-based weight loss shows an exponential trend up to 510 °C (Figure 5.1(a)) and this is expected to continue to higher temperatures. It is not until 430 °C that any significant degradation is observed (Figure 5.1(b)), which is expected when the temperature is below the polyimide's decomposition temperature of 522 °C. A similar observation can be made when considering weight loss as a function of time at varying temperatures, as shown in Figure 5.1(b). At lower temperatures, regardless of time exposure (up to 20 minutes), there is minimal weight loss until 470 °C. This data demonstrates the fluorinated polyimide's ability to withstand lower temperatures for longer durations with little or no weight loss. Furthermore, this polyimide is able to withstand higher temperatures than PETI-5 (Figure 2.10) due to its low T_g (270 °C) and a low decomposition temperature of 510 °C.[15]

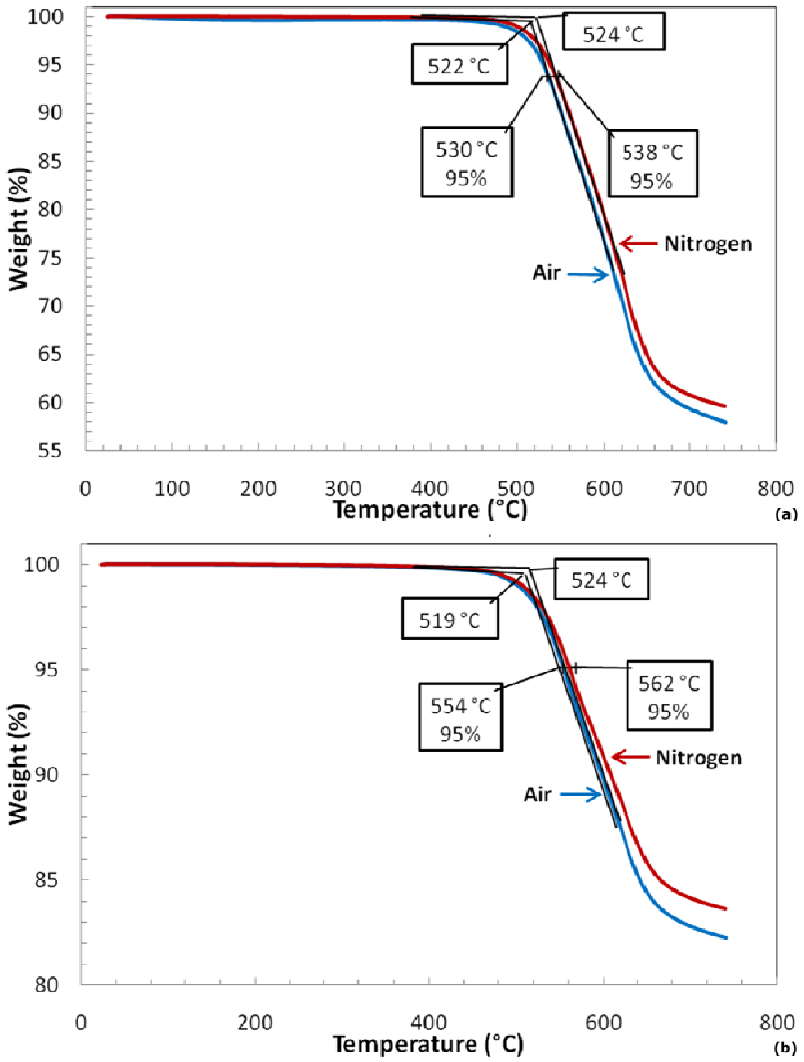

Figure 5.2. Weight loss as a function of temperature measured with a heating rate of 20 °C per minute. Decomposition temperature of polyimide resin (a) and polyimide composite (b) in air and nitrogen is shown at onset and 5% weight loss.

The lower stability in PETI-5 is due to differences in the backbone structure of the polyimide, such as the lack of CF_3 groups and the addition of ether linkages, which create other pathways for degradation to occur at high temperatures. AFR700B (Figure 2.8) has a similar structure to that of the fluorinated polyimide used here, except that

AFR700B uses a nadic end-cap as the crosslinker. Both PETI-5 and AFR700B have high T_g's, but AFR700B is not as thermally stable due to hydrolytic scission of its norbornene crosslinks.[7] The superior thermal stability of the fluorinated polyimide (highest T_g and T_d) is due to its combination of the best features of PETI-5 (endcaps) and AFR700B (perfluoromethylsubstituents).

Adding carbon fiber to the fluorinated polyimide further enhances its thermal stability. The decomposition temperature of the polyimide containing 55 wt-% carbon fiber, defined as the point at which 5% weight loss occurs, is 554 °C in air and 562 °C in nitrogen, as shown in Figure 5.2(b). This high degradation temperature allows the composite to withstand 510 °C for up to 20 minutes and maintain weight loss below 5%. At temperatures below 470 °C, weight loss is less than 1% regardless of the amount of exposure time. This enhanced thermal stability, relative to the neat polyimide, is a result of a strong fiber-matrix interface.[40] An elevated T_g (491 °C) is evidence of this strong interaction. The adsorption of the polyimide to the carbon fiber surface delays decomposition due to prevention of air from permeating the interface.[2,5,40,114-115] Figure 5.3 shows that this strong interaction remains after exposure to 510 °C for 20 minutes. These cross-sectional images of polyimide composite, exposed to 510 °C for 20 minutes, show the carbon fiber tightly interfaced with the matrix. Cracks in the polyimide are very apparent at both low (Figure 5.3(a)) and high (Figure 5.3(b)) magnification, but no significant gaps are observed where polymer meets fiber. When exposure temperatures are greater than 490 °C the composite begins to show signs of weight loss greater than 1% at all studied exposure times, as shown in Figure 5.4.

This result is not surprising because the temperature is nearing the decomposition temperature. A broader set of time and temperature weight loss data for the composite is shown in Table 5.2.

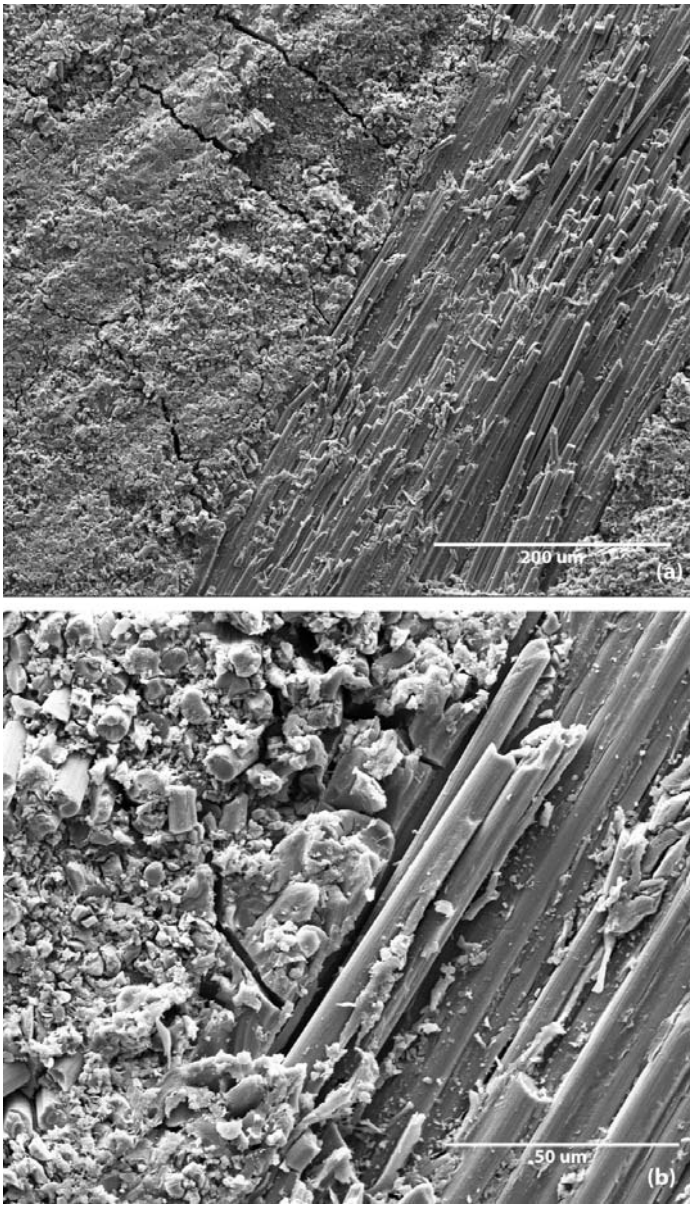

Figure 5.3. Scanning electron microscope images of polyimide composite cross-sections, after aging at 510 °C for 20 minutes, at 500x (a) and 2000x magnification (b).

Table 5.2. Polyimide composite weight loss in oven. Values in table are loss percentage.

Temp (°C)	Time (min)									
	2	**4**	**6**	**8**	**10**	**12**	**14**	**16**	**18**	**20**
250	0.27	0.25	0.36	0.25	0.35	0.19	0.29	0.31	0.29	0.43
270	0.29	0.57	0.32	0.19	0.42	0.20	0.39	0.26	0.37	0.41
290	0.26	0.22	0.17	0.23	0.24	0.47	0.29	0.32	0.23	0.29
310	0.27	0.38	0.21	0.31	0.43	0.23	0.49	0.50	0.40	0.42
330	0.27	0.42	0.41	0.54	0.72	0.38	0.31	0.38	0.35	0.47
350	0.47	0.40	0.27	0.39	0.53	0.55	0.30	0.46	0.41	0.38
370	0.22	0.61	0.35	0.28	0.43	0.39	0.40	0.33	0.55	0.34
390	0.19	0.38	0.25	0.31	0.68	0.47	0.61	0.47	0.52	0.45
410	0.38	0.42	0.25	0.70	0.57	0.51	0.54	0.54	0.56	0.60
430	0.46	0.62	0.49	0.73	0.73	0.35	0.58	0.53	0.47	0.58
450	0.58	0.92	1.02	0.98	0.60	0.43	0.79	1.10	0.63	0.71
470	0.68	1.05	1.16	0.89	1.06	0.89	0.96	0.92	0.90	0.97
490	0.99	1.06	1.48	1.65	0.98	1.89	1.74	2.02	2.22	2.20
510	1.37	1.98	2.44	2.61	3.88	2.84	3.67	4.19	4.97	5.33

The composite not only exhibits lower weight loss with the addition of carbon fiber, it enhances other properties.[111] Carbon fiber acts as a protective barrier for the resin in the composite to prevent exposure to destabilizing elements. This protection allows the resin to withstand higher temperatures while also increasing the strength, thermal oxidative stability, and higher strength to weight ratio than their metal counterparts.[113] The barrier from the carbon fiber also delays the decomposition of the polyimide resin within the composite. This is supported by the optical micrographs shown in Figures 5.5 and 5.6. There is no change in the neat resin or composite at the lower temperatures as seen in Figures 5.5(b), 5.5(c), 5.6(b) and 5.6(c). The light areas in the composite are the carbon fiber, while the darker areas are the resin. At 510 °C, the neat resin (Figure 5.5(e)) has qualitatively degraded more than the resin within the

carbon fiber composite (Figure 5.6(e)). Also of note, is the delayed degradation at the interface between the carbon fiber and resin in the composite. This observation further reinforces the idea that the composite material has a strong fiber-matrix interface, thus resulting in good thermal stability up to 20 minutes. The carbon fiber in the composite also prevents structural defects from occurring at higher temperatures, as seen from the images taken at 490 °C (compare Figures 5.5(d) and 5.6(d)).

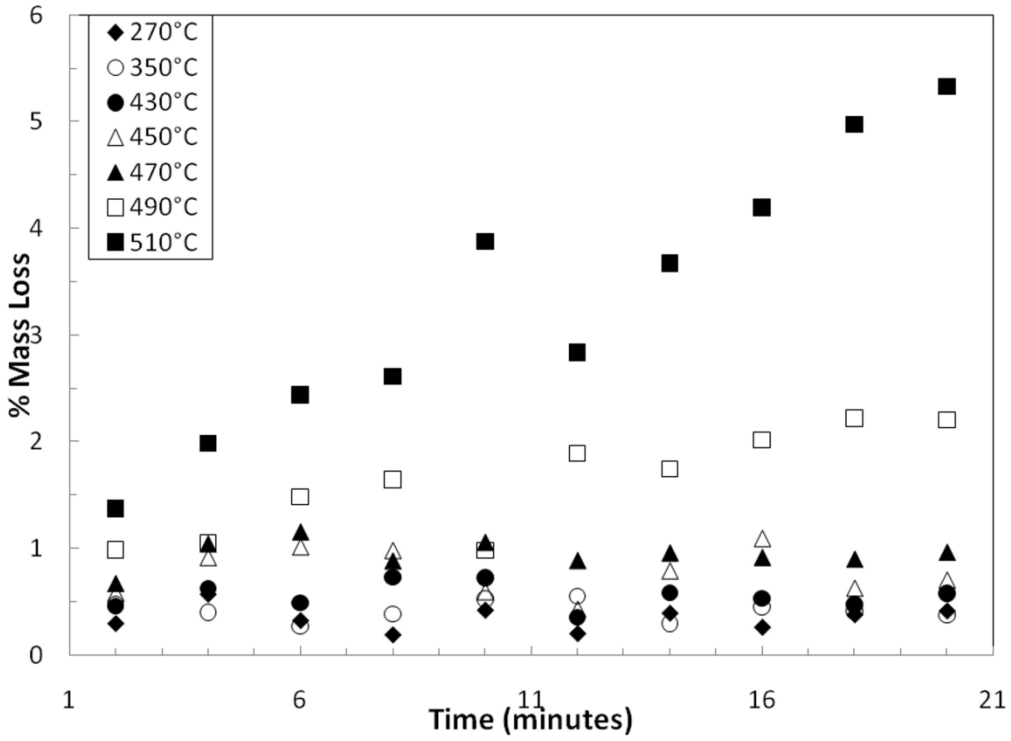

Figure 5.4. Polyimide composite weight loss in oven as a function of exposure time to various temperatures.

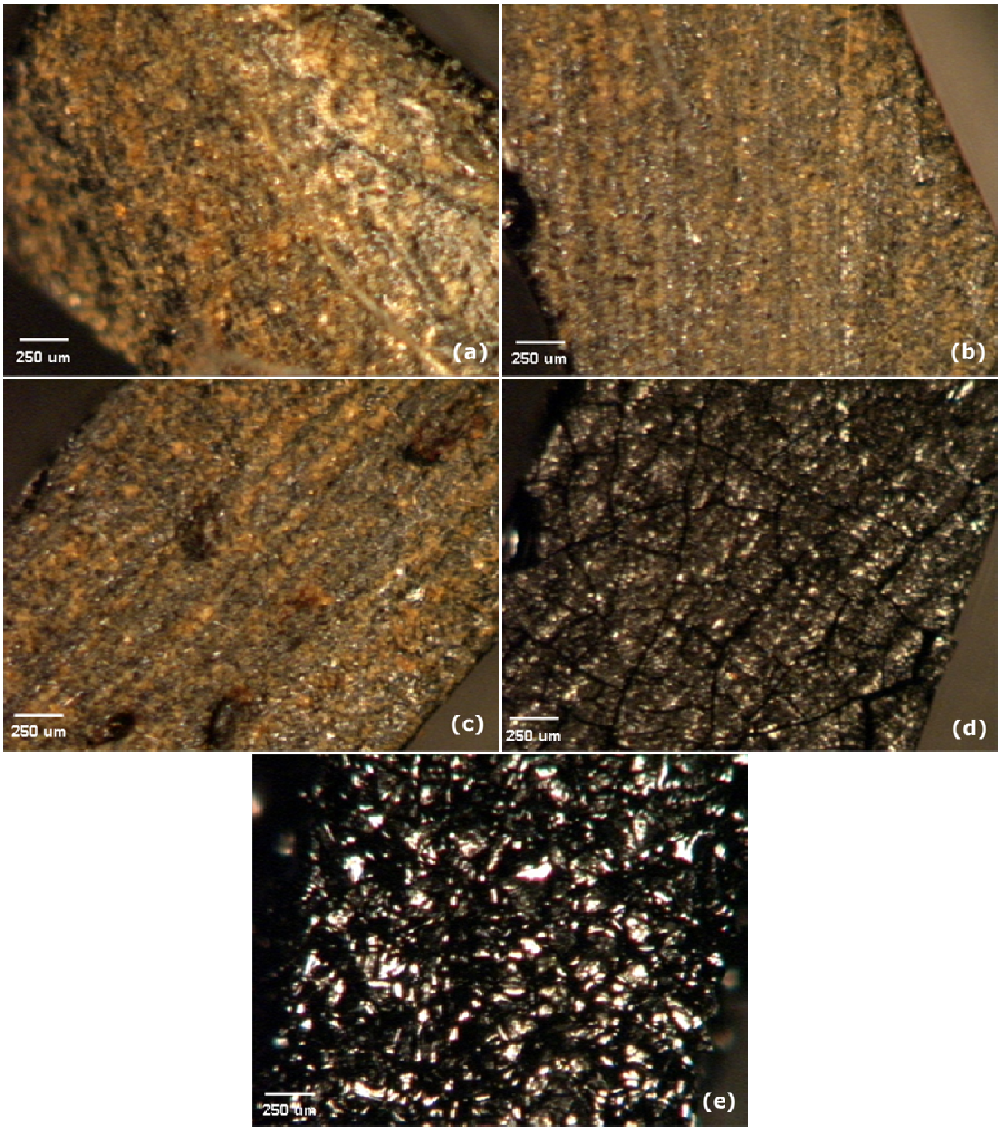

Figure 5.5. Optical microscope images for neat polyimide resin prior to aging (a) and aged at 250 °C (b), 370 °C (c), 490 °C (d), and 510 °C (e) for 20 minutes.

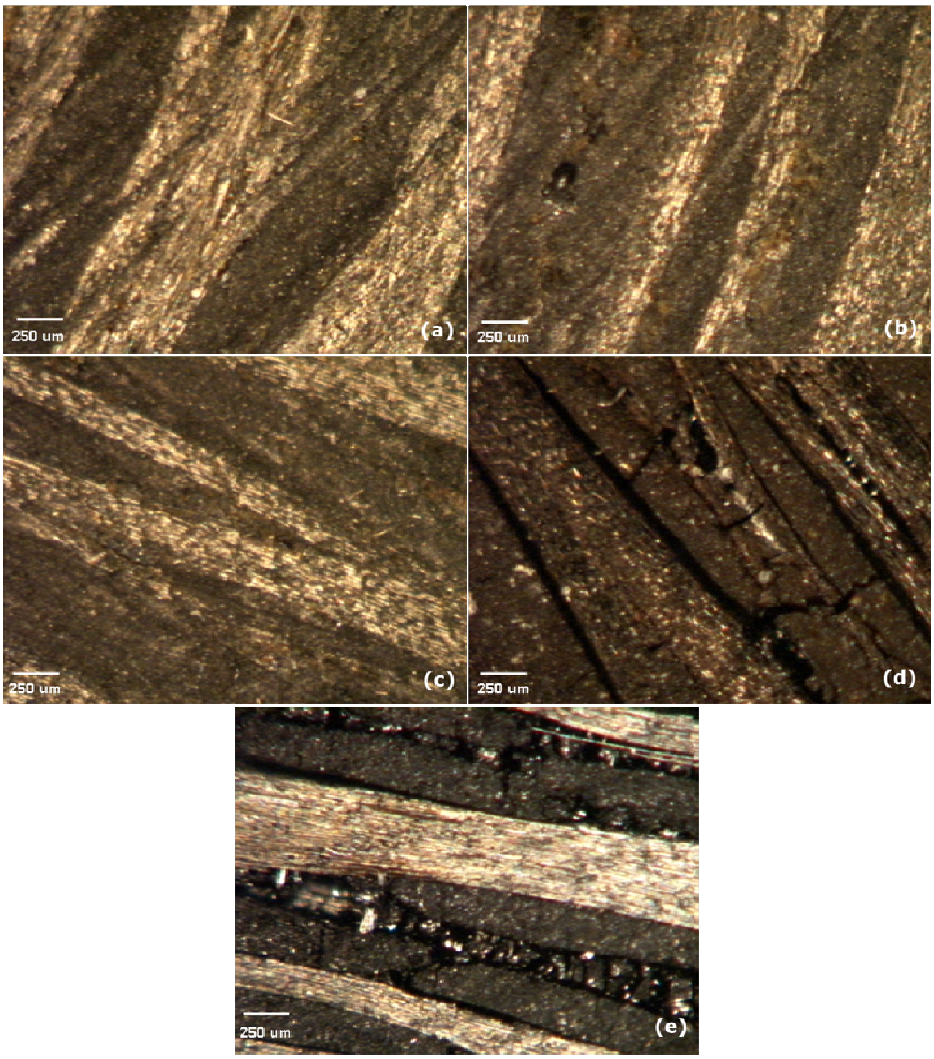

Figure 5.6. Optical microscope images for polyimide composite prior to aging (a) and aged at 250 °C (b), 370 °C (c), 490 °C (d), and 510 °C (e) for 20 minutes.

5.3.2 Mechanism of polyimide degradation

Previous studies have focused on how similar PMR (polymerization of monomer reactants) type polyimides degrade at high temperatures in an attempt to predict the long-term, high-temperature performance.[8,113] There are two different pathways that degradation occurs for these polyimides. One degradation route is through the cleavage

of the C-N imide bonds that leads to a direct loss of CO, CO_2, and low levels of ArNCO. The second degradation pathway is from the loss of CF_3 and F from the two CF_3 linkages in the backbone of the polyimide, which is independent of the loss of CO and CO_2. Figure 5.7 shows the loss of the CF_3 and NCO bonds using a combination of TGA and infrared spectroscopy for the fluorinated polyimide resin exposed to temperatures from 530 – 700 °C in air. At lower temperatures, the major degradation pathway appears to be a loss of CF_3 linkages (CHF_3 has characteristic peak at 1150cm^{-1}) from the backbone of the polyimide, whereas there is minimal loss of CO and CO_2. The higher temperatures primarily show loss of the NCO chemical bonds (isocyanate stretching is at 2340 cm^{-1}) with the CF_3 intensity decreasing as exposure temperature increases. These results suggest that both degradation pathways are independent of each other, but it is interesting to note that the breakdown of the backbone via NCO bonds occurs at much higher temperatures than the decomposition temperature of the polyimide resin material.

5.3.3 Thermogravimetric analysis

Weight loss measured using thermogravimetric analysis, of the fluorinated polyimide resin and composite, was performed as an alternative to oven aging. Figure 5.8 shows weight loss of the neat polyimide resin for temperatures ranging from 250 – 510 °C and 2 - 20 minute hold times once each temperature was reached. When compared with Figure 5.1(b), it is clear that the TGA gives a much higher weight loss, relative to oven aging, for temperature exposures over 450 °C.

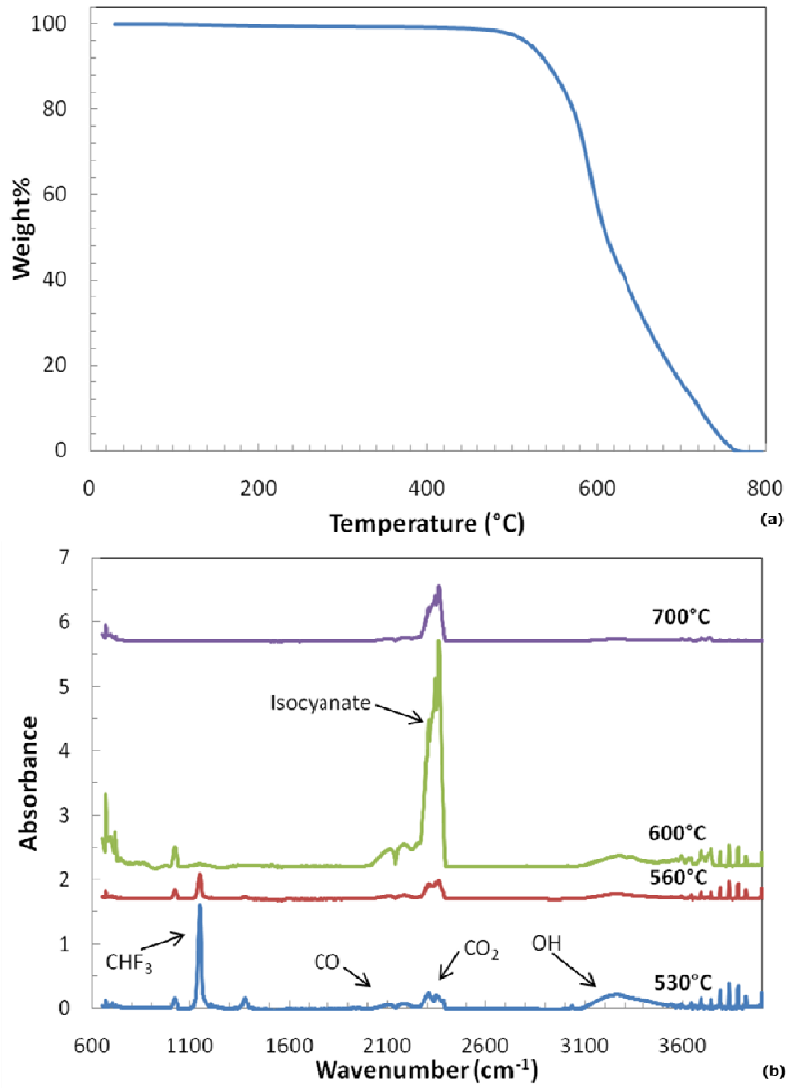

Figure 5.7. Polyimide weight loss as a function of temperature in air measured with a TGA-IR system (a). FTIR spectra of degradation products collected during heating (b).

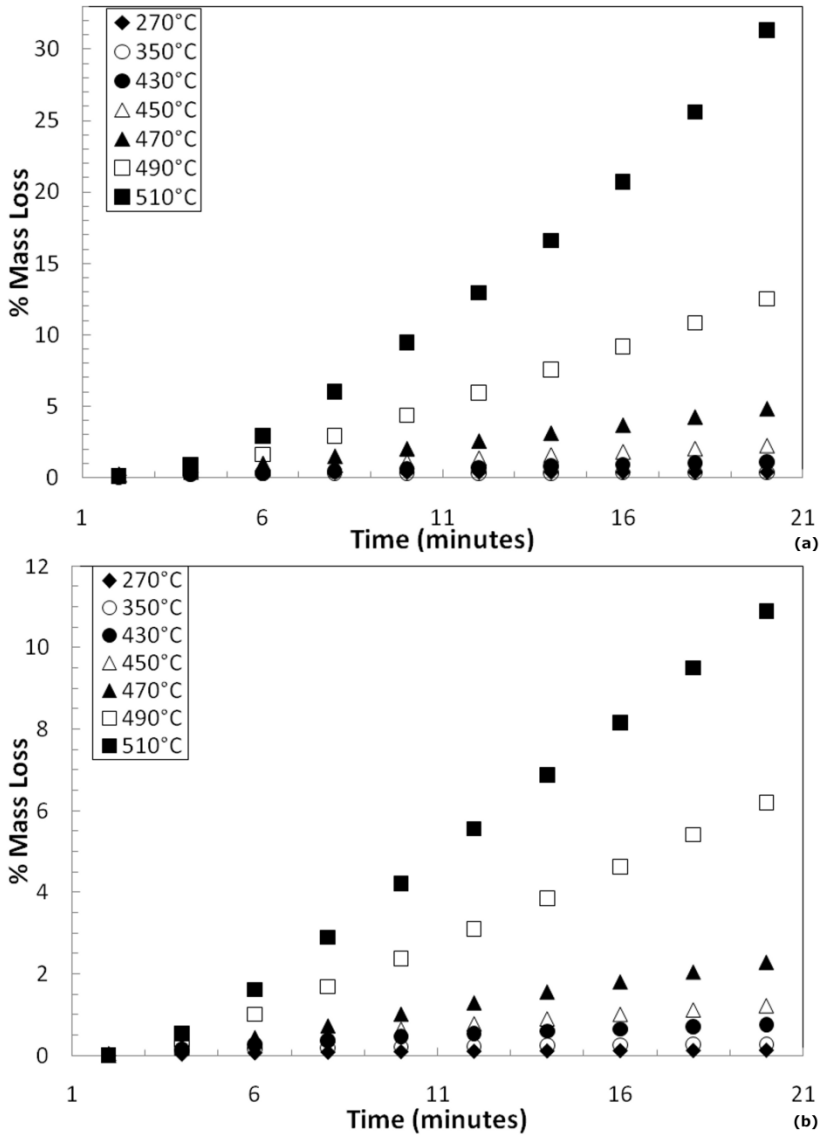

Figure 5.8. Polyimide resin (a) and carbon fiber composite (b) weight loss, measured with TGA, as a function of exposure time to various temperatures.

This discrepancy between oven and TGA is likely due to several factors, of which sample size is one of the most significant. TGA requires a much smaller sample, which results in better heat transfer compared to the oven due to greater surface area to volume ratio.[114] Another issue with the oven is that opening, to place a sample inside, lowers the actual temperature and therefore less time is spent at the exposure temperature. The air flow over the sample in the TGA may also be enhancing weight loss. The oven technique is more reliable for small exposure times (2 - 10 minutes) because the TGA takes 6 - 8 minutes to reach the required test temperature and therefore gives a distorted weight loss. These factors cause the carbon fiber composite to show enhanced weight loss with TGA as well, as shown in Figure 5.8(b).

An examination of weight loss as a function of temperature for the polyimide resin (Figure 5.8(a)) shows little loss prior to 450 °C. It should be noted that both TGA and oven testing produce the same general weight loss trends as a function of time and temperature. At lower temperatures, regardless of exposure time, there is no visible difference in weight loss prior to 450 °C. At higher temperatures, the TGA gives a clearer separation between test conditions relative to the oven. Much like neat polyimide, the composite shows little weight loss below 450 °C (Figure 5.8(b)), where the amount of exposure time begins to yield appreciable degradation. These trends are the same as those found with oven aging (Figure 5.4), except for the higher weight loss at 510 °C. Weight loss for a broader set of times and temperatures, measured with TGA, are shown in Tables 5.3 and 5.4 for neat polyimide and its composite, respectively.

Table 5.3. Polyimide resin weight loss using TGA. Values in table are loss percentage.

Temp	Time (min)									
(°C)	2	4	6	8	10	12	14	16	18	20
250	0.11	0.32	0.35	0.36	0.36	0.37	0.37	0.37	0.37	0.37
270	0.14	0.33	0.35	0.36	0.36	0.36	0.37	0.37	0.37	0.37
290	0.02	0.16	0.18	0.18	0.19	0.19	0.19	0.19	0.19	0.19
310	0.08	0.25	0.26	0.27	0.27	0.27	0.27	0.27	0.27	0.27
330	0.06	0.23	0.24	0.25	0.25	0.26	0.26	0.26	0.26	0.26
350	0.10	0.29	0.30	0.31	0.32	0.32	0.33	0.34	0.35	0.36
370	0.04	0.21	0.22	0.24	0.26	0.29	0.31	0.33	0.35	0.37
390	0.15	0.34	0.36	0.41	0.46	0.51	0.55	0.59	0.62	0.66
410	0.22	0.38	0.44	0.54	0.62	0.70	0.76	0.82	0.88	0.92
430	0.05	0.22	0.34	0.47	0.60	0.72	0.82	0.92	1.01	1.10
450	0.15	0.39	0.61	0.87	1.12	1.36	1.59	1.82	2.03	2.25
470	0.26	0.58	1.01	1.52	2.04	2.57	3.11	3.67	4.24	4.82
490	0.12	0.63	1.61	2.90	4.37	5.96	7.57	9.19	10.84	12.51
510	0.15	0.88	2.92	6.03	9.47	12.95	16.61	20.73	25.61	31.33

Table 5.4. Polyimide composite weight loss using TGA. Values in table are loss percentage.

Temp	Time (min)									
(°C)	2	4	6	8	10	12	14	16	18	20
250	0.00	0.07	0.09	0.10	0.11	0.12	0.12	0.13	0.13	0.13
270	0.00	0.03	0.06	0.08	0.09	0.10	0.11	0.12	0.12	0.13
290	0.01	0.16	0.22	0.26	0.28	0.30	0.31	0.32	0.33	0.33
310	0.00	0.09	0.11	0.13	0.14	0.15	0.15	0.16	0.16	0.17
330	0.00	0.08	0.14	0.17	0.19	0.20	0.21	0.22	0.23	0.24
350	0.00	0.12	0.16	0.19	0.21	0.23	0.24	0.26	0.27	0.28
370	0.00	0.13	0.20	0.24	0.27	0.30	0.32	0.34	0.35	0.37
390	0.00	0.09	0.16	0.21	0.26	0.29	0.32	0.35	0.37	0.39
410	0.00	0.14	0.25	0.33	0.39	0.44	0.49	0.52	0.56	0.59
430	0.00	0.15	0.27	0.37	0.46	0.53	0.59	0.65	0.70	0.75
450	0.05	0.24	0.36	0.50	0.65	0.78	0.90	1.02	1.12	1.23
470	0.00	0.18	0.44	0.72	1.01	1.29	1.55	1.80	2.04	2.28
490	0.01	0.39	1.01	1.68	2.37	3.10	3.85	4.62	5.41	6.21
510	0.02	0.54	1.61	2.90	4.22	5.56	6.87	8.16	9.50	10.89

5.4 Conclusions

Very little degradation (< 1% weight loss) was observed for a fluorinated polyimide and its carbon fiber composite, when exposed to temperatures below 430 °C. Beyond 470 °C, both neat resin and carbon fiber-filled composite displayed relatively linear weight loss as a function of time, but this linear slope grew exponentially with temperature. Thermogravimetric analysis of the polyimide, done in air and nitrogen, suggests that oxidation is a relatively minor factor in the degradation process. Infrared spectroscopy performed during degradation confirmed that fluorinated species are the first to leave, followed by isocyanate groups at much higher temperature (~600 °C). The polyimide composite shows a higher thermal stability compared to the neat polyimide resin for the exposure times studied here. When exposed to 510 °C for 20 minutes, the composite had a maximum weight loss of 10.9% using TGA and 5.3% using an oven, while the neat polyimide had a maximum weight loss of 31.3% and 12.6% for TGA and oven, respectively. The TGA method gives a more accurate weight loss for exposure times greater than 10 minutes, whereas the oven technique appears more useful when exposure times are less than 10 minutes. We found that for exposure times up to 20 minutes the composite shows better thermal stability; however, long term aging at lower temperatures of similar composites frequently showed the opposite effect.[35] Both polyimide resin and composite were found to undergo thermolysis and modest oxidation during degradation. Future work for the fluorinated polyimide will include improved crosslinking and protection of thermally sensitive side groups (e.g., -CF_3). With a better understanding of degradation conditions and mechanism, improvements can be made to

these high temperature materials. There will be a continual need for composites with ever higher thermal stability, especially as aircraft travel at ever increasing speeds.

CHAPTER VI

LOW TEMPERATURE FORMATION OF ULTRA HIGH TEMPERATURE TRANSITION-METAL CARBIDES FROM SALT-POLYMER PRECURSORS*

6.1 Introduction

Transition-metal carbides were initially synthesized by carbothermal reduction of transition-metal halides and polymer precursor mixtures, at temperatures that range from 900 to 1500 °C in an argon atmosphere. TaC was synthesized from $TaBr_5$, as a model carbide for this process, because it has one of the highest known melting points of 3883 °C.[18] A high temperature polyimide, with a glass transition temperature of 440 °C, was used as the polymer matrix to prevent significant loss of carbon at high reaction temperatures. Significant (> 40 vol%) amounts of TaC were formed at reaction temperatures as low as 900 °C for one hour, with greater times and temperatures leading to > 90 vol% yield. Polystyrene and polyvinyl acetate were also used to successfully produce TaC with high yield (> 90 vol%), which demonstrates the universality of this method. Universality of method was also proven by using other various transition-metal halide salts ($NbBr_5$, WCl_4, and WCl_6) with the polyimide. Using a series of interrupted studies, it is shown that tantalum carbide must first go through tantalum oxide during this low temperature process.

---

*Part of this chapter is reprinted with permission from "Low Temperature Formation of Ultra High Temperature Transition Metal Carbides from Salt-Polymer Precursors" by A. D. Adamczak *et al*., 2010. *Journal of the American Ceramic Society*, in press, © 2010 by Wiley Periodicals, Inc.

Finally, the atomic ratio of tantalum to carbon was varied in an attempt to generate robust films/coatings that could act as thermal protection layers for high speed aircraft.

6.2 Experimental

6.2.1 Materials and Methods

The fluorinated phenylethynyl-terminated imide (FPTI) oligomer (Performance Polymers Solutions Inc., Centerville, OH) (0.76 mmol, 2.0 g) was dissolved as received in 150 mL of *N*-methyl pyrrolidinone (Alfa Aesar, Ward Hill, MA) and heated to 100 °C. The solution was then left to stir for at least 24 hours to ensure complete homogeneous mixture. Polyvinyl acetate (PVAc) with a molecular weight of 90,000 g/mol (Polysciences, Inc., Warrington, PA) and polystyrene (PS) with a molecular weight of 305,000 g/mol (Ineos Styrenics, Channahon, IL) were prepared, separately, in the same manner as the FPTI. The tantalum bromide salt [$TaBr_5$] (Alfa Aesar, Ward Hill, MA) (3.5 mmol, 2.0 g) was measured and dissolved in 100 mL absolute ethanol (Acros, West Chester, PA) in a dry box under an inert atmosphere. The $TaBr_5$ solution was stirred under an inert atmosphere for approximately 1 hour before adding to the FPTI/NMP solution in a reaction vessel. The resulting combined mixture was heated to 210 °C slowly under an argon atmosphere to remove all solvent. The intimately mixed solids were then placed in a furnace (Barnstead Thermolyne 48000, Dubuque, IA) and heated to 340 °C under an argon atmosphere for 4 hours to cure the oligomer (this step was not performed for PS and PVAc). The niobium bromide salt [$NbBr_5$] (Alfa Aesar, Ward Hill, MA) was measured and dissolved in 100 mL absolute ethanol (Acros, West

Chester, PA) in a dry box under an inert atmosphere. The $NbBr_5$ solution was stirred under an inert atmosphere for approximately 1 hour before adding to FPTI/NMP solution in a reaction vessel. The resulting mixture was heated to 210 °C slowly under an argon atmosphere to remove all solvent. The intimately mixed solids were then placed in a furnace (Barnstead Thermolyne 48000, Dubuque, IA) and heated to 340 °C under an argon atmosphere for 4 hours to cure the oligomer. The tungsten chlorides, WCl_4 and WCl_6, (Alfa Aesar, Ward Hill, MA) were measured and dissolved separately in 100 mL methanol (Acros, West Chester, PA) in a dry box under an inert atmosphere. The WCl_4 and WCl_6 solutions were stirred under an inert atmosphere for approximately 1 hour before adding to FPTI/NMP solution in a reaction vessel. The resulting mixture was heated to 210 °C slowly under an argon atmosphere to remove all solvent. The ratio study used 0.5 g (0.86 mmol) tantalum bromide with varying amount of imide oligomer to achieve the appropriate Ta:C ratio (1:2, 1:3, 1:5, or 1:10) then following the procedure detailed above.

6.2.2 Carbide Formation

The FPTI polyimide/$TaBr_5$ mixture was put in an alumina crucible and placed in a tube furnace (MHI H18-40HT, Cincinnati, OH) using an alumina tube. The ends were sealed and tube was evacuated and flushed with argon for five cycles at two minutes each. The furnace was programmed according to testing time and temperatures ranging from one hour to eight hours and 350 – 1500 °C. The PS/$TaBr_5$ and PVAc/$TaBr_5$ intimate mixtures were put in an alumina crucible separately and placed in the tube

furnace, and programmed according to the desired testing time and temperatures. The other FPTI polyimide/transition-metal salt ($NbBr_5$, WCl_4, and WCl_6) mixtures were also put in an alumina crucible and placed in the tube furnace, and programmed according to the desired testing time and temperatures. The interrupted mechanism study involved heating to a desired temperature (350 - 600 °C) and holding for one hour. After one hour, the samples were removed immediately from the tube furnace to flash cool the sample.

6.2.3 Characterization

Samples were analyzed using a Bruker-AXS D8 Advanced Bragg-Brentano X-ray Powder Diffractometer (Madison, WI). The samples were crushed into a very fine powder, and analyzed using a quartz ground disk (GM Associates, Inc., Oakland, CA). Scanning was performed with a 0.0148 step size, 0.2 step time, and a 2Θ range of 20-100°. TaC peaks were confirmed by comparison to card No. 01-077-0205, while card No. 01-079-1375 was used to verify Ta_2O_5 peaks. Tantalum bromide ($TaBr_5$) peaks were verified using card No. 00-018-1295. Spectra containing niobium were confirmed using card No. 01-074-1222 for NbC and Nb_2O_5 was verified by card No. 01-071-0336. WC peaks were verified using card No. 00-035-0776 and WO_2 was confirmed by comparing to card No. 00-032-1393. The amount of carbide and oxide formation for all materials was calculated by quantitative analysis using the Rietveld Method and Topas version 4 software. Scanning electron microscopy (SEM) and energy-dispersive spectroscopy (EDS) were performed using an FEI Quanta 600 FE-SEM (Hillsboro, OR)

equipped with a conventional Everhart-Thornley detector, back-scattered electron detector, IR-CCD chamber camera, Oxford EDS system (equipped with X-ray mapping and digital imaging) and cathodoluminescence detector. The microstructure and dispersion of transition-metal halide/carbide was observed with SEM and EDS.

6.3 Results and Discussion

The approach reported here is unique because transition-metal halide salts were used that are soluble in the same organic solvents as the polymeric precursor (see Table 6.1) and have sublimation/boiling temperatures lower than or close to the decomposition temperatures of the polymer. Direct solubility of transition-metal halides and polymer precursors in soluble organic solvents allows for more intimate mixing on the molecular level. In addition, transition-metal halides have been shown to react with organic compounds in solution and form complex compounds[83] that possibly lower the transition-metal carbide's processing temperature.[116] This, together with low sublimation/boiling points of those transition-metal salts, and solubility in the same organic solvents as polymeric precursors, yields lower processing temperatures.

Fluorinated phenylethynyl-terminated imide oligomer was selected as the polymer precursor because of its high thermal stability, low density and excellent mechanical properties,[117-118] which makes it a good candidate material for high-temperature aerospace composites. Commodity polymers, such as polyvinyl acetate and polystyrene, were also used as polymeric precursors to successfully synthesize these transition-metal carbides. FPTI and $TaBr_5$ precursor mixtures (Figure 6.1) were used to

synthesize TaC *in-situ* using 900-1500 °C temperatures in an argon atmosphere, as shown in Figure 6.2. X-ray diffraction (Fig. 6.2(a)) shows that the major reaction products are TaC and Ta_2O_5, the proportion of which depends on the reaction temperature and time. In the first series of reactions (Figure 6.3), the amount of $TaBr_5$ in the FPTI precursor mixture was varied from 20 to 90 wt%. Those results showed no significant effect on the TaC/TaO ratio in the final products after carbothermal reaction at 1500 °C, thus the remaining studies were performed using a 50/50 polymer to transition-metal salt weight ratio. A series of reactions were conducted at different temperatures to determine the lowest temperature at which carbide formation significantly diminishes and tantalum oxide becomes the major reaction product. Figure 6.2(b) shows that 41.5 vol% TaC can be produced at 900 °C after 5 hours, while TaC becomes the major phase (68 vol%) after exposure to 1000 °C for only one hour.

Table 6.1. Some physical and chemical properties of transition-metal halide salts, polymer precursors, and final transition-metal products.

Material	Boiling point (°C)	Melting point (°C)	Decomposition temperature (°C)	Solubility in organic solvents
$TaBr_5$	349	280	-	absolute alcohol, ether
$NbBr_5$	360		-	absolute alcohol
WCl_4	300			methanol
WCl_6	347			methanol, ether
FPTI	-	-	530	N-methyl pyrrolidinone
PVAc			280	*N*-methylpyrrolidinone, ethanol, ether
PS			325	*N*-methylpyrrolidinone, ethanol, acetone, ether
TaC	5500	3883	-	hydrofluoric/nitric acid mixture
Ta_2O_5		1880	-	hydrofluoric/nitric acid mixture

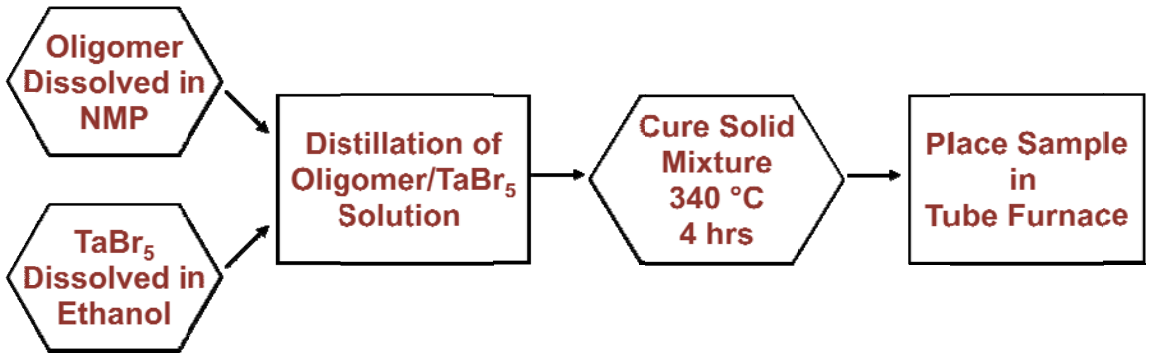

Figure 6.1. Synthesis route for low temperature tantalum carbide formation.

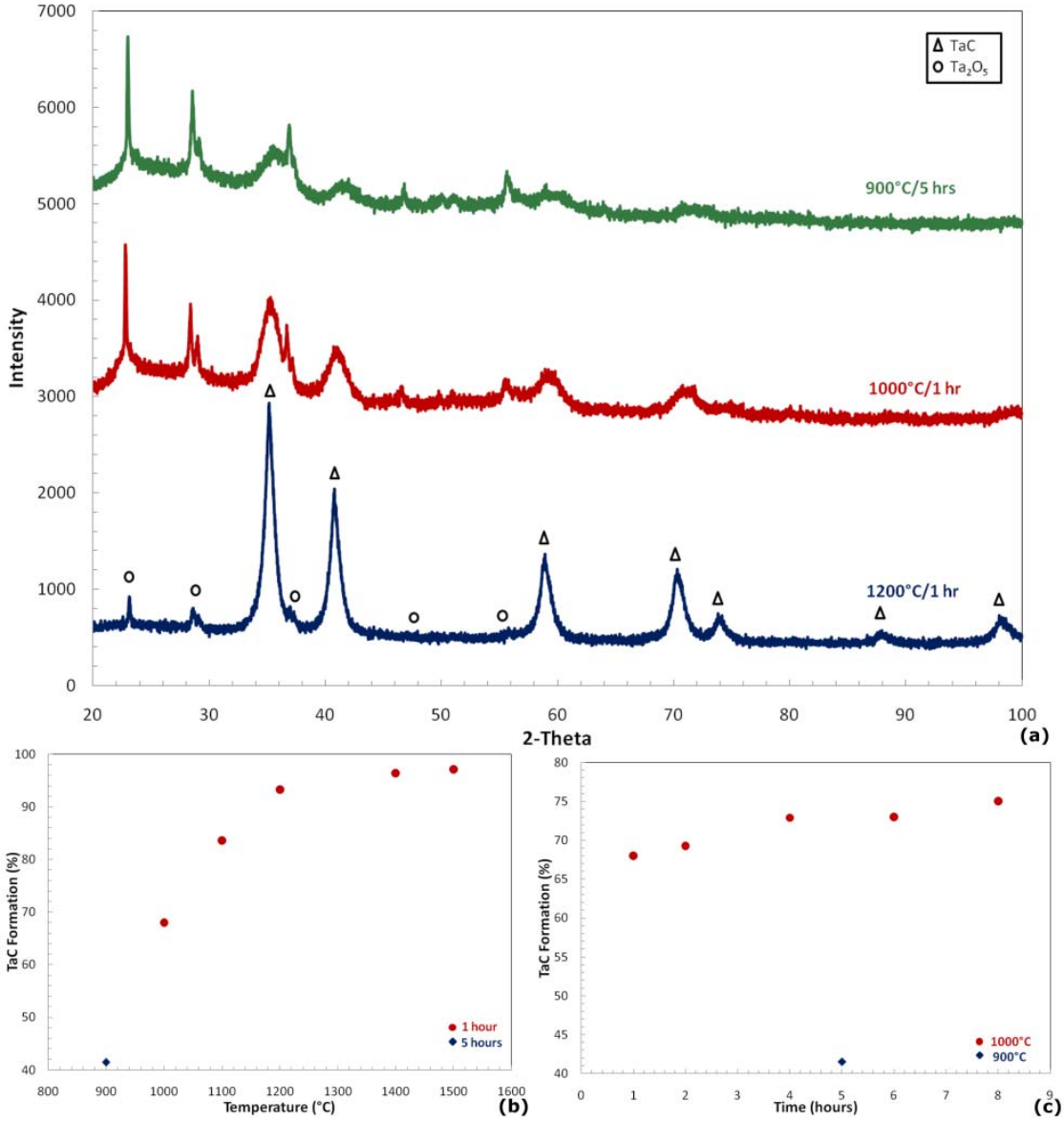

Figure 6.2. (a) XRD spectra of powder after reaction of 50/50 weight ratio of FPTI/$TaBr_5$ precursor mixture at 1200 °C for 1 h (blue), 1000 °C for 1h (red) and at 900 °C for 5 hours (green) indicating presence of two major phases: TaC (peaks labeled with triangles) and Ta_2O_5 (peaks labeled with circles). The card numbers used in the identification of compounds were Ta-C 01-077-0205 and Ta-O 01-079-1375. (b) Amount of TaC formed after reaction at different temperatures for 5 hours at 900 °C and 1 hour at all other temperatures. The trend is semi-logarithmic with more than 90% of TaC formation at a temperature of 1200 °C. (c) Amount of TaC formed at 1000 °C using 50/50 weight ratio of polyimide/$TaBr_5$ salt as a function of time (hours) and 900 °C for 5 hours.

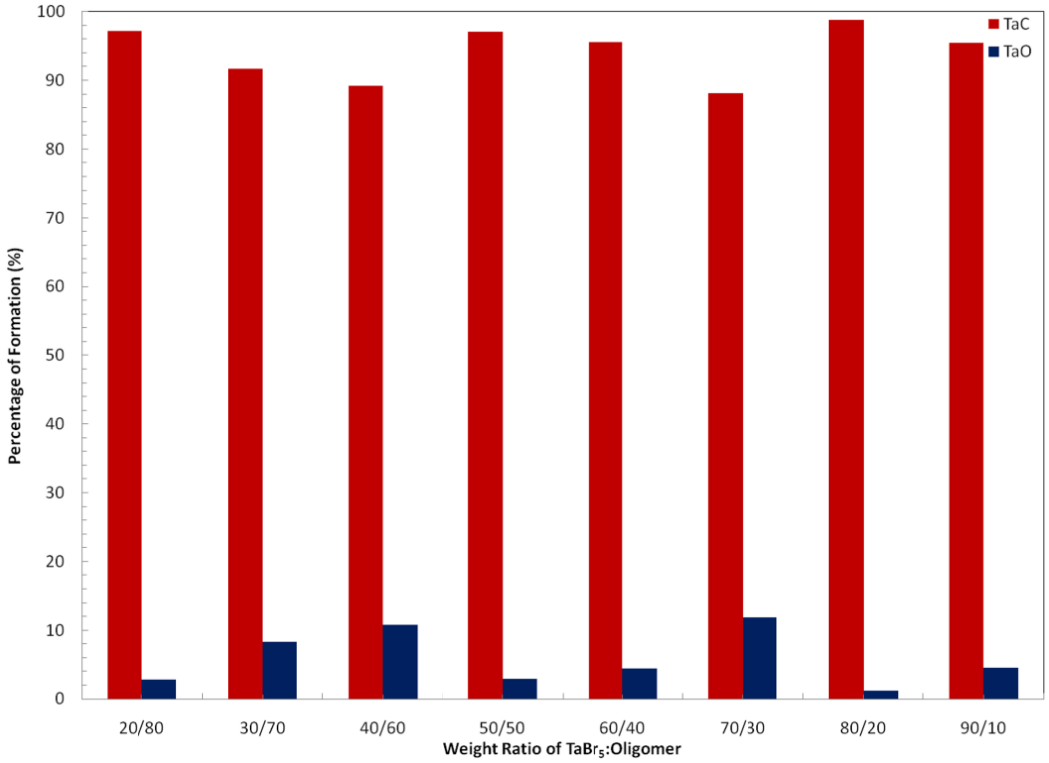

Figure 6.3. Ratio study showing amount of tantalum carbide and oxide formation versus variation of tantalum bromide to FPTI oligomer.

Our results also show (Figure 6.2(c)) a linear increase in amount of TaC in the final product with reaction time at 1000 °C, with a maximum of 75.1 vol% after 8 hours. The formation of tantalum carbide was also confirmed using SEM, equipped with EDS, for the sample made at 1200 °C with less than 6% oxide phase (Figure 6.4(a)). The EDS scan was taken as a field image that is representative of the entire image. The dispersion of tantalum throughout the matrix was confirmed using dot mapping of image (see Figure 6.5). There is an even distribution of all elements throughout the material. Multiple locations were chosen and this confirmed that the TaC particles were uniformly distributed.

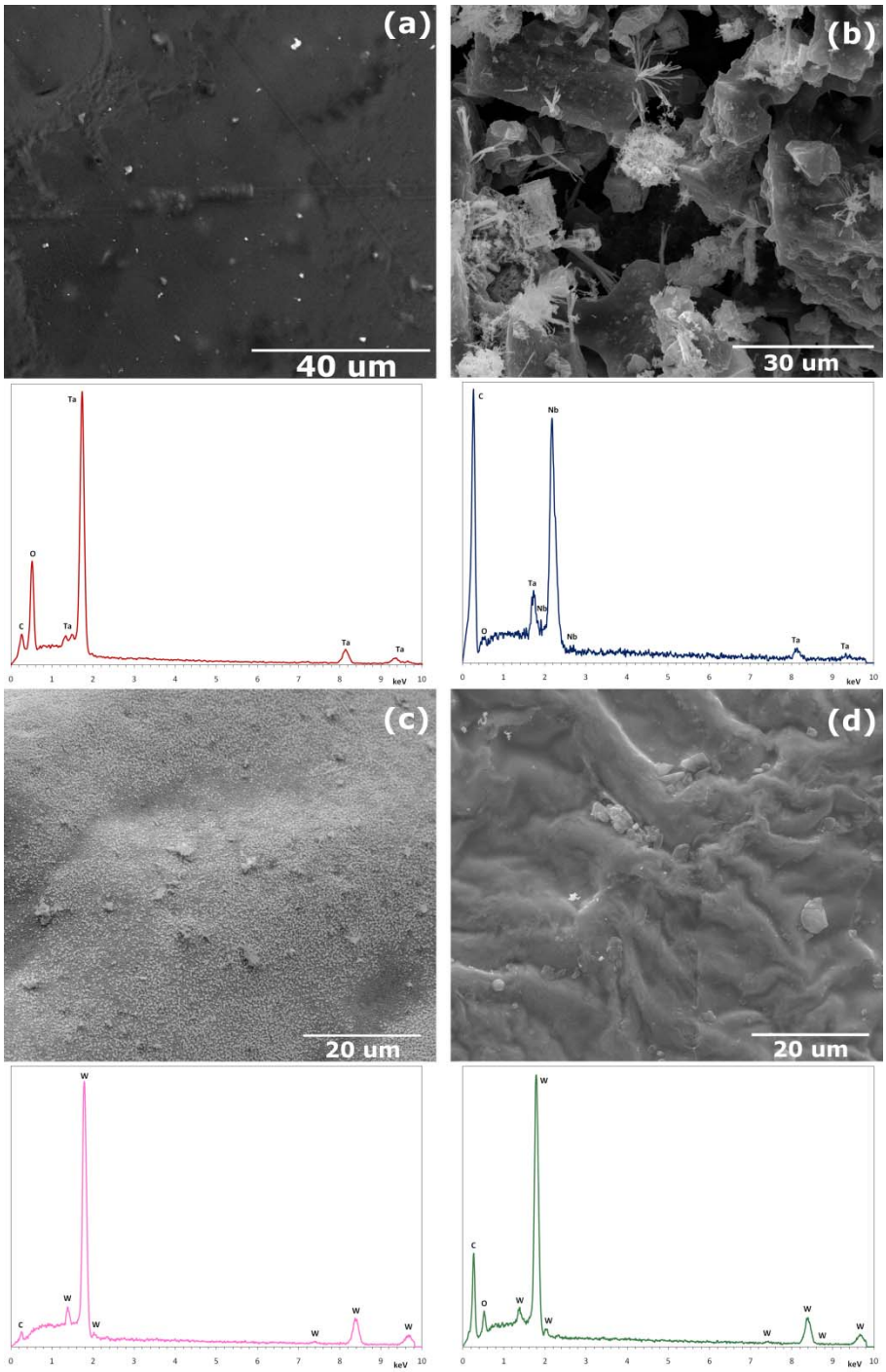

Figure 6.4. SEM images and associated EDS graphs (below the images), following 1200 °C heat treatment of (a) $TaBr_5$ and FPTI polyimide precursor, (b) $NbBr_5$ and FPTI polyimide precursor, (c) WCl_4 and FPTI polyimide precursor, and (d) WCl_6 and FPTI polyimide precursor for 1 hour. The EDS graphs are field scans of the entire image.

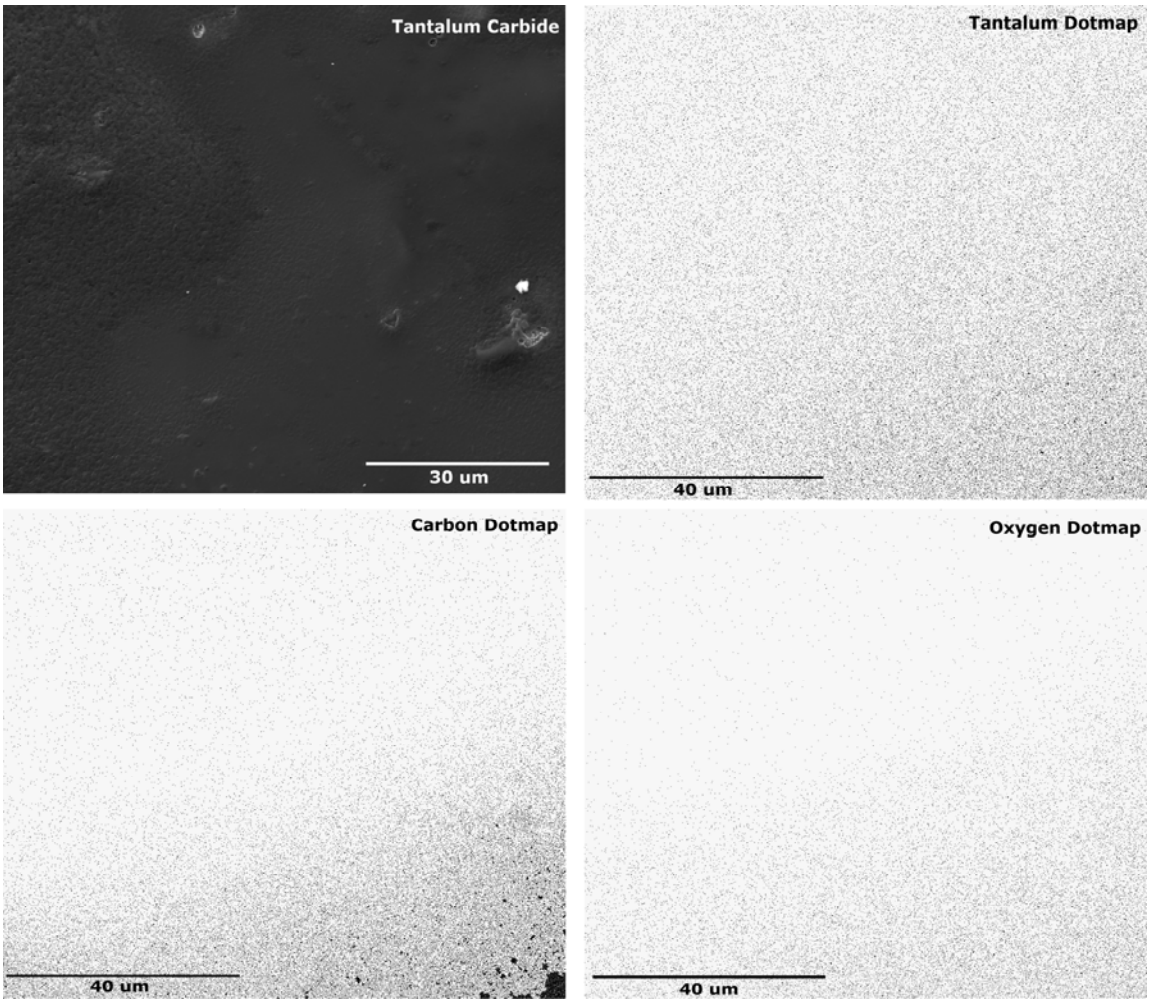

Figure 6.5. SEM dotmaps of a tantalum carbide sample after exposure to 1200 °C for one hour. The top left image is an SEM image of the area represented in each corresponding element dotmap. The tantalum is well dispersed throughout the material, indicating uniform distribution during mixing.

To the best of our knowledge, 900 °C is the lowest temperature, reported in literature, for the synthesis of tantalum carbide with such a high carbide yield (40+ vol%). One possible exception is the work of Ma et al who reported synthesis of TaC by reaction of Mg, Na_2CO_3 and $TaCl_5$ at 600 °C for 8 hours.[83,116] The amount of TaC formed was not reported because they characterized the products after washing in HCl

and distilled water several times. Attempts were made to follow this purification method in the present work, but we observed a loss in TaC with no removal of Ta_2O_5. A similar study[83] reported the formation of pure Ta_2O_5 at 900 °C from a rather complex mixture of $TaCl_5$ solution in HCl and furan resin precursor. The results shown here clearly demonstrate that intimate mixing of transition-metal halides on the molecular level with a polymer precursor, and boiling/evaporation of transition-metal halides at temperatures close to decomposition temperature of polymer precursor, significantly reduce the formation temperature of TaC.

After successfully producing TaC at a relatively low temperature, this process was extended by using commodity polymers with lower decomposition temperatures than that of the polyimide. Polystyrene and polyvinyl acetate were chosen as model polymers because PS is composed of only carbon and hydrogen, while PVAc has an oxygen-containing side group, as shown in Figure 6.6. Carbothermal reduction of PS and $TaBr_5$ at 1200 °C resulted in 93.2 vol% TaC, with the remaining phase being Ta_2O_5. This composition is similar to that obtained from FPTI polyimide/$TaBr_5$, although PS does not contain any oxygen. Following the same procedure with PVAc resulted in greater weight loss after being exposed to a carbide formation temperature of 1200 °C and the lowest amount of carbide phase formed (85 vol%). These results indicate that when the boiling point of the transition-metal halide is lower, or similar to, the polymer decomposition temperature, the presence of the oxygen in polymers does not affect the reaction products. Small amounts of Ta_2O_5 shown here are most likely the result of the reaction with the Al_2O_3 crucible that was used to place the sample in the furnace. In the

case of PVAc, with a decomposition temperature significantly below the boiling point of $TaBr_5$, reaction with oxygen from the polymer precursor leads to a higher amount of oxide in the final product.

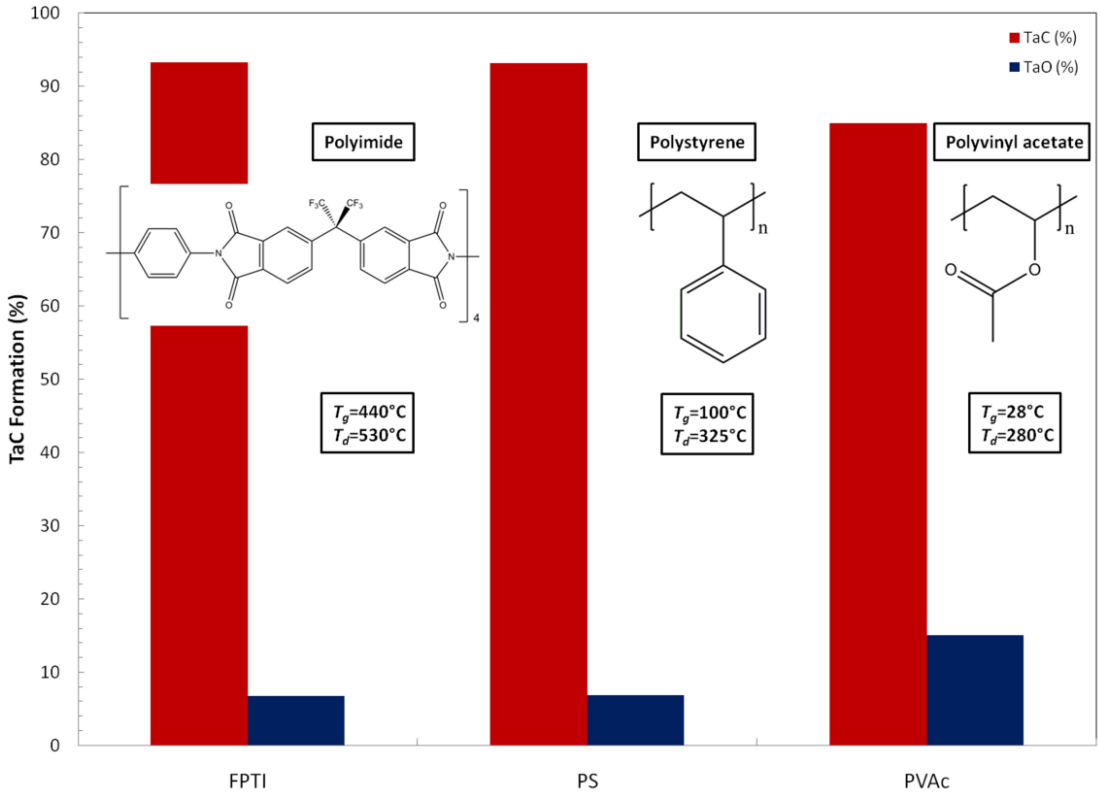

Figure 6.6. Volume fraction of TaC as a function of polymer type for a 50/50 weight ratio of polymer/$TaBr_5$ precursor, with the remaining phase being Ta_2O_5. The reaction conditions for all three types of polymers was 1200 °C for one hour.

The universality of this low temperature synthesis method was further examined by incorporating other transition-metal halides within the polymer precursor. Niobium (V) bromide ($NbBr_5$), tungsten (IV) chloride (WCl_4), and tungsten (VI) chloride (WCl_6) were chosen as model compounds. Here again, $NbBr_5$ and WCl_6 were chosen for their solubility in organic solvents and high boiling point (350 °C), among other similarities to $TaBr_5$ (see Table 6.1). Despite the low sublimation temperature (300 °C) of WCl_4, this salt was chosen due to the lower oxidation state of tungsten. As in the case of FPTI polyimide/$TaBr_5$ precursor, the reaction of $NbBr_5$ with the FPTI polyimide resulted in the formation of 74 vol% transition-metal carbide (NbC) with some minor oxide residue (NbO) at 1200 °C, as shown in Figure 6.7(b). Both WCl_4 and WCl_6 reactions with the FPTI polyimide produced pure transition-metal carbide (100 vol% WC) with no oxide residue (WO), as shown in Figure 6.7(c) and (d). Due to the low sublimation temperature of WCl_4, the mixture of FPTI oligomer and transition-metal salt was cured at a lower temperature (280 °C) before placing in the tube furnace.

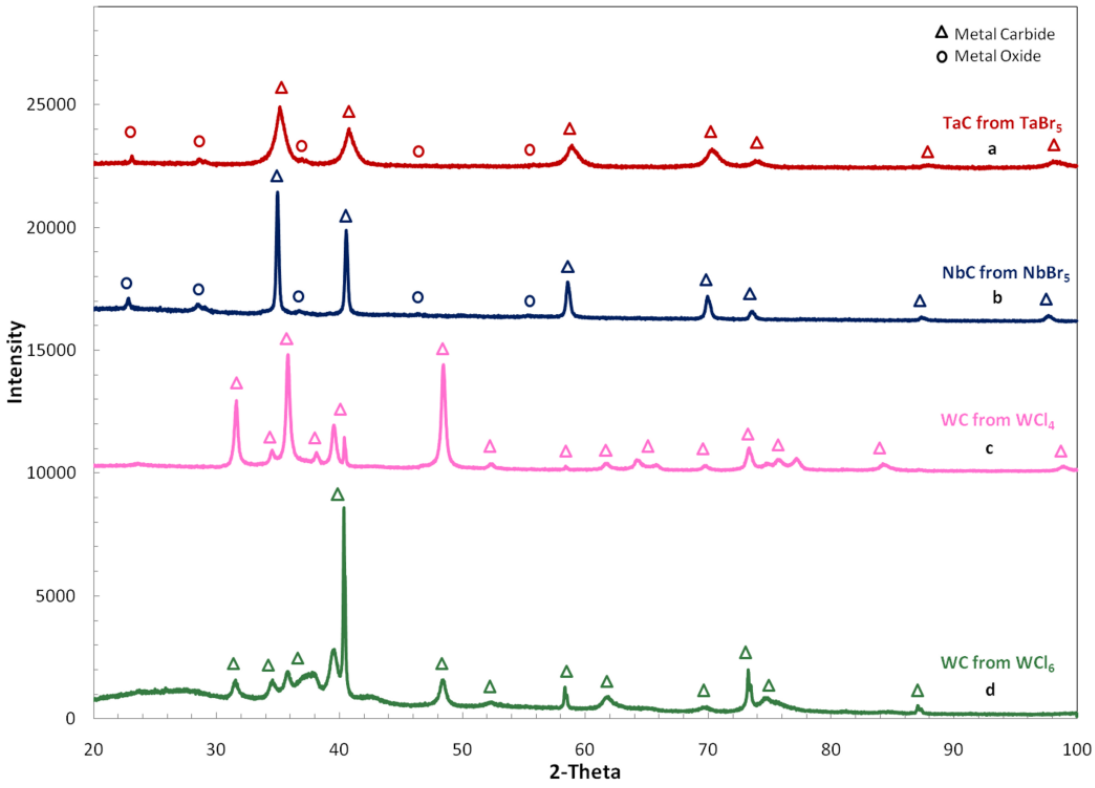

Figure 6.7. XRD spectra of products after reaction at 1200 °C for one hour with mixtures of (a) $TaBr_5$ and FPTI polyimide precursor, (b) $NbBr_5$ and FPTI polyimide precursor, (c) WCl_6 and FPTI polyimide precursor, and (d) WCl_4 and FPTI polyimide precursor. XRD for (a) and (b) show a presence of transition-metal carbides and oxides in the final products and only transition-metal carbides for (c) and (d). The peaks labeled for (a) and (d) are the same labels for (b) and (c), respectively. The card numbers used in the identification of compounds were Nb-C 01-074-1222, Nb-O 01-071-0336, W-C No. 00-035-0776 and W-O No. 00-032-1393.

Scanning electron microscopy and energy-dispersive spectroscopy were performed on these transition-metal carbides to further verify their identity. Niobium carbide (Fig. 6.4(b)) has an interesting microstructure relative to the other carbides. This sample is primarily niobium carbide with a trace of tantalum. The dark colored blocks in the image consist primarily of niobium and tantalum with a small amount of carbon

present, while the white cubes are roughly equal amounts of all three elements. The fibers and flaky material throughout the image contain mostly niobium with trace amounts of carbon and even smaller amounts of tantalum. When the fibers combine to form bundles in the material they consist mostly of carbon with significant quantities of niobium and tantalum. The two tungsten materials, W(IV)C (Fig. 6.4(c)) and W(VI)C (Fig. 6.4(d)), have similar morphologies to tantalum carbide (Fig. 6.4(a)). The white spheres and gray matrix in Figure 6.4(c) contain roughly an equal amount of tungsten and carbon, although the field scan of this image contains mostly tungsten with small amounts of carbon. In Figure 6.4(d), a more uniform tungsten carbide morphology is observed throughout the material. While the field scan shown under the SEM image indicates mostly tungsten present, there are some locations that contain mostly carbon. All of the images shown here suggest that the *in-situ* method utilized to form these transition-metal carbides is successful.

The mechanism for the formation of metal carbides has not been clearly understood to-date, in particular when using polymers as the source of carbon.[83,116,119] A better understanding of the mechanism could lead to the design of a more efficient and lower temperature process. Experiments were performed to determine whether carbide formation must first convert to oxide from the transition-metal halide and polymer. The FPTI/$TaBr_5$ mixture was heated over a range of temperatures from 350 - 600 °C and was expected to show all intermediate compounds that formed upon heating. These temperatures were chosen based on the boiling points, melting points, and decomposition temperatures of the starting materials (as shown in Table 6.1). The XRD

results, shown in Figure 6.8, suggest a mechanism that goes from an amorphous material through tantalum oxide before conversion to tantalum carbide. All peaks from the 500, 600, and 900 °C scans are some form of tantalum oxide, as the much smaller (barely visible) peaks correspond to tantalum oxide (XRD card number 00-035-9222). The lack of appearance of $TaBr_5$ peaks in all spectra, in particular before exposure, confirms that an intimate mixture with the polyimide was obtained (i.e., Ta is dispersed on a molecular level).

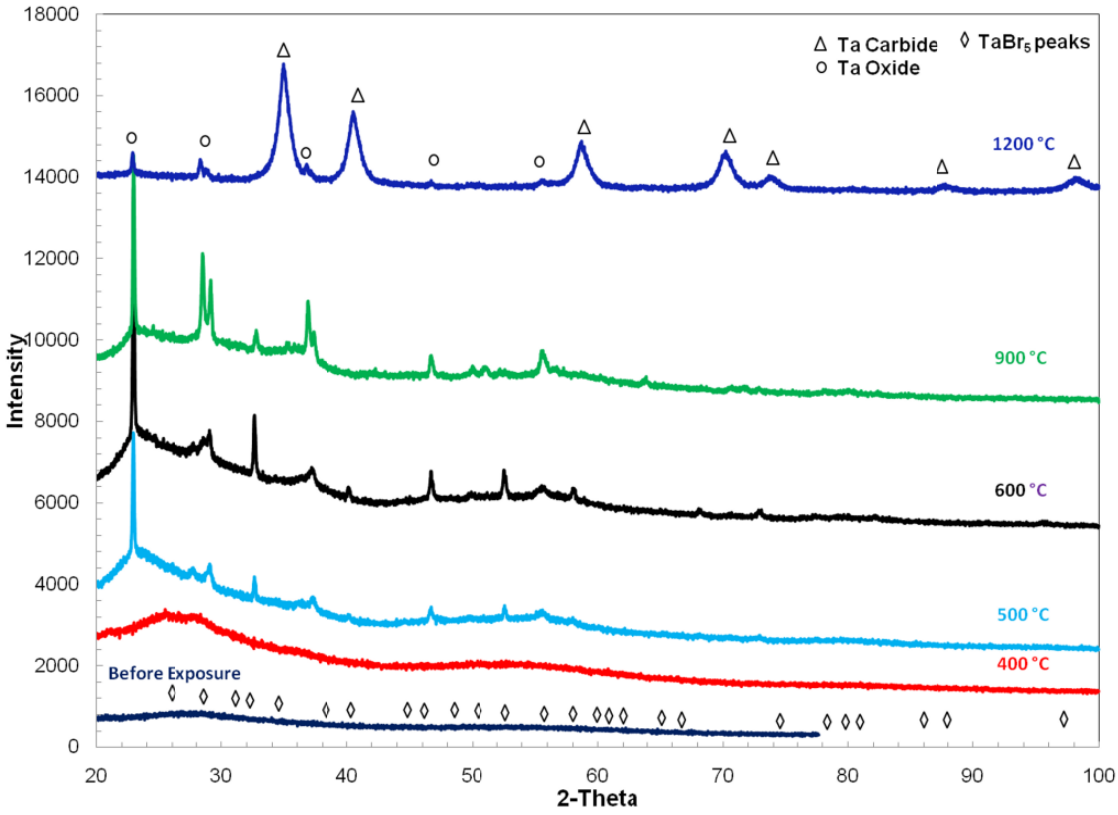

Figure 6.8. Interrupted study performed on 50/50 weight ratio of tantalum bromide to fluorinated phenylethynyl terminated polyimide. Samples were heated to a given temperature and held for one hour followed by flash cooling.

The SEM/EDS images in Figure 6.9 also support the proposed mechanism. Figure 6.9(a) is a representative sample tested at 400 °C for one hour, while Figure 6.9(b) was tested at 600 °C for one hour. The sample at 400 °C contains mostly polyimide with smaller amounts of tantalum, which is expected due to the decomposition temperature of the polyimide (530 °C). At 600 °C, the material changes to containing mostly tantalum with small amounts of carbon and oxygen. EDS was also conducted on different areas within the SEM image, as shown in Figure 6.9(b). The dull white spheres consist mostly of tantalum with small of amounts of carbon and trace amounts of oxygen, and the dark gray areas are equal amounts of tantalum and carbon with small amounts of oxygen. The white fluffy chunk at the bottom of the image in Figure 6.9(b) has a majority of tantalum with carbon and oxygen each making up half of the amount of tantalum, with trace amounts of fluorine and sodium. The white rod-like structures in Figure 6.9(b) contain mostly tantalum with carbon and oxygen present in half and one third the amount of tantalum, respectively. Other measures were taken to confirm whether the proposed mechanism (Equation 6.1) is correctly stated.

$$x\mathrm{TaBr_5} + x\mathrm{O_{source}} \rightarrow x\mathrm{Ta_2O_5} + x\mathrm{HBr} + x\mathrm{Br_2}$$
$$\mathrm{Ta_2O_5} + 7\mathrm{C} \rightarrow 2\mathrm{TaC} + 5\mathrm{CO} \qquad \textbf{Equation 6.1}$$

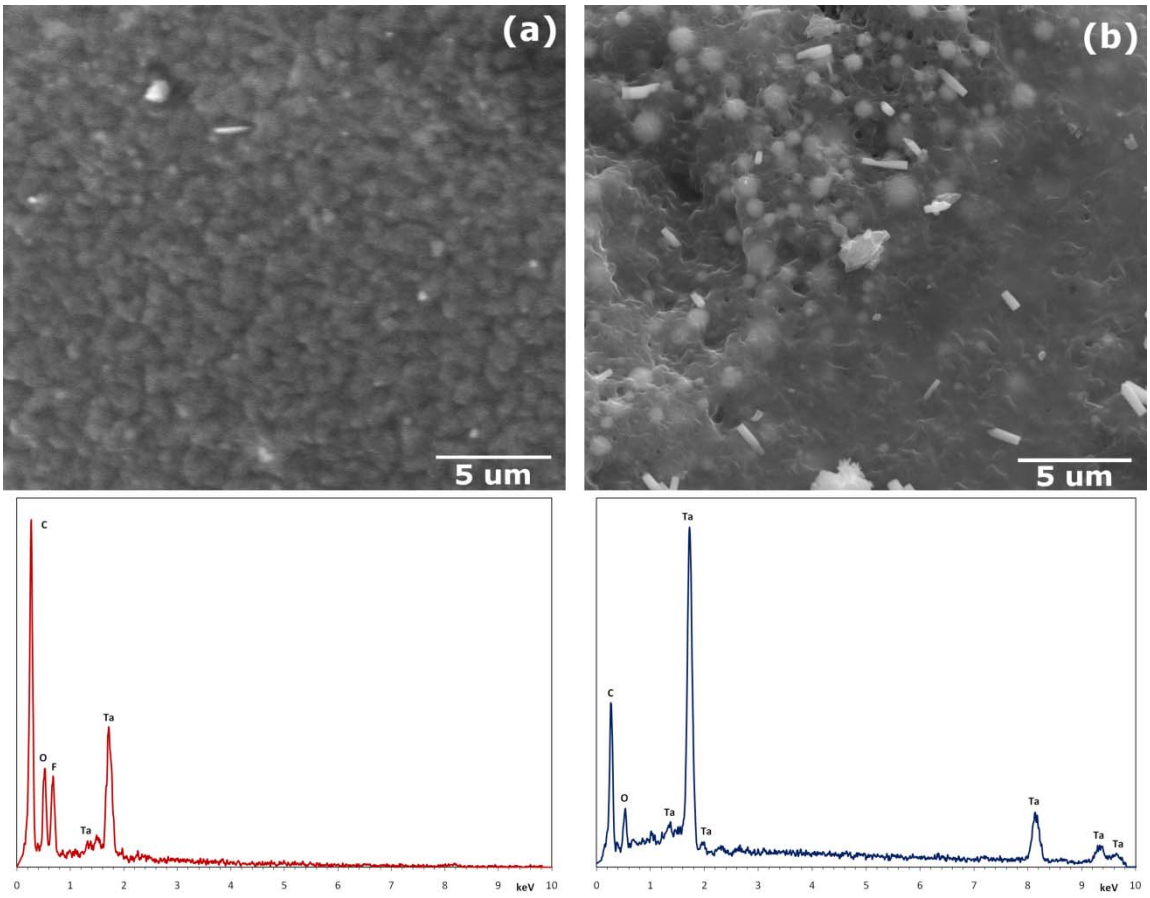

Figure 6.9. SEM image and EDS graph (below the image), following 400 °C (a) and 600 °C (b) heat treatment of $TaBr_5$ and FPTI polyimide precursor, for 1 hour. The EDS graph is a field scan of the entire image.

The first test involved replacing the argon atmosphere with that of a hydrogen/argon environment and heating at 900 °C for 5 hours. This experiment resulted in only tantalum oxide being formed, whereas in the argon atmosphere 43% tantalum carbide was produced. The alumina crucible was replaced with a graphite sheet made into a boat with a lid as another confirmation test. The testing conditions were performed using just an argon atmosphere and a 900 °C/5hrs heating condition, which resulted in 33.2% tantalum carbide formation. These results provide the information needed to validate

that there must be some small or trace amounts of oxygen present in order for the carbide formation to occur. In other words, the partial pressure p_{O2} must be adequate for carbide conversion to take place. According to Chrysanthou et al, the conversion from tantalum oxide to carbide is slow due to the diffusion of CO away from the TaC-Ta_2O_5 reaction interface.[119] However, halides present in the gaseous phases are believed to have catalytic function and contribute to the faster diffusion of tantalum to the carbon particles that form by decomposition of the polymer, as previously postulated by Kim et al,[86] and thus enhancing the overall efficiency of the conversion to the transition-metal carbide. This effect could aid the formation of tantalum carbide at the low temperatures we have observed.

Initial studies involved varying weight ratios between the fluorinated imide oligomer and the transition-metal halide. Weight ratios were varied from 20/80 to 90/10 of the mixture $TaBr_5$/FPTI, while all prior experiments used 50/50 weight ratios (a 30:1 carbon to tantalum atom ratio). Reduced atom ratios of 1:2, 1:3, 1:5, and 1:10 Ta:C were explored to generate carbide materials capable of being shaped or formed because excess carbon likely weakens the final material due to its existence as amorphous carbon. Table 6.2 lists the reaction conditions used with these varying Ta:C atom ratios, as well as the conversion ratios of TaC and Ta_2O_5. At the lower atom ratios (1:2 and 1:3) there was no presence of TaC, as shown by XRD in Figure 6.10. This is likely due to lack of enough carbon atoms present to drive the reaction from Ta_2O_5, or the inability to release the CO byproduct quickly enough from the interface. Figure 6.11 shows that

regardless of the atom ratio a good intimate mixture is obtained after curing of the polyimide Ta:C due to absence of any salt crystal structure.

Table 6.2. Conversion percentages of tantalum carbide and tantalum oxide for various Ta:C atom ratios.

Ta:C Atom Ratio	Temperature (°C)	Time (hr)	TaC % Conversion	Ta_2O_5 % Conversion
1:2	1000	8	0	100
1:2	1200	1	0	100
1:3	1000	8	0	100
1:3	1200	1	0	100
1:5	1000	8	9.2	90.8
1:5	1200	1	57.8	42.2
1:10	1000	8	59.5	40.5
1:10	1200	1	53.5	46.5
1:30	1000	8	81.5	18.5
1:30	1200	1	93.3	6.7

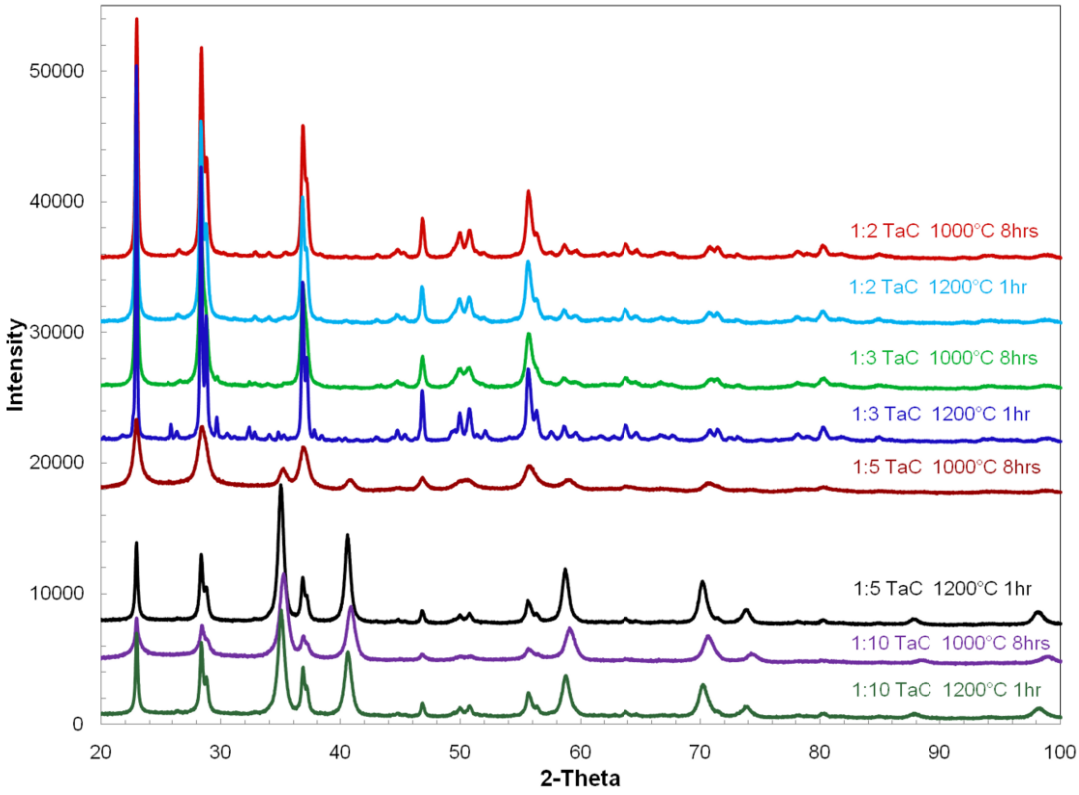

Figure 6.10. Ratio study performed on 50/50 weight ratio of tantalum bromide to fluorinated phenylethynyl terminated polyimide. The ratio of Ta:C was varied from 1:2-1:10 for 1000 °C/8hrs and 1200 °C/1hr heating conditions. The smaller ratios, 1:2 and 1:3, regardless of heating condition, formed only tantalum oxide, whereas the 1:5 and 1:10 ratios formed mostly tantalum carbide.

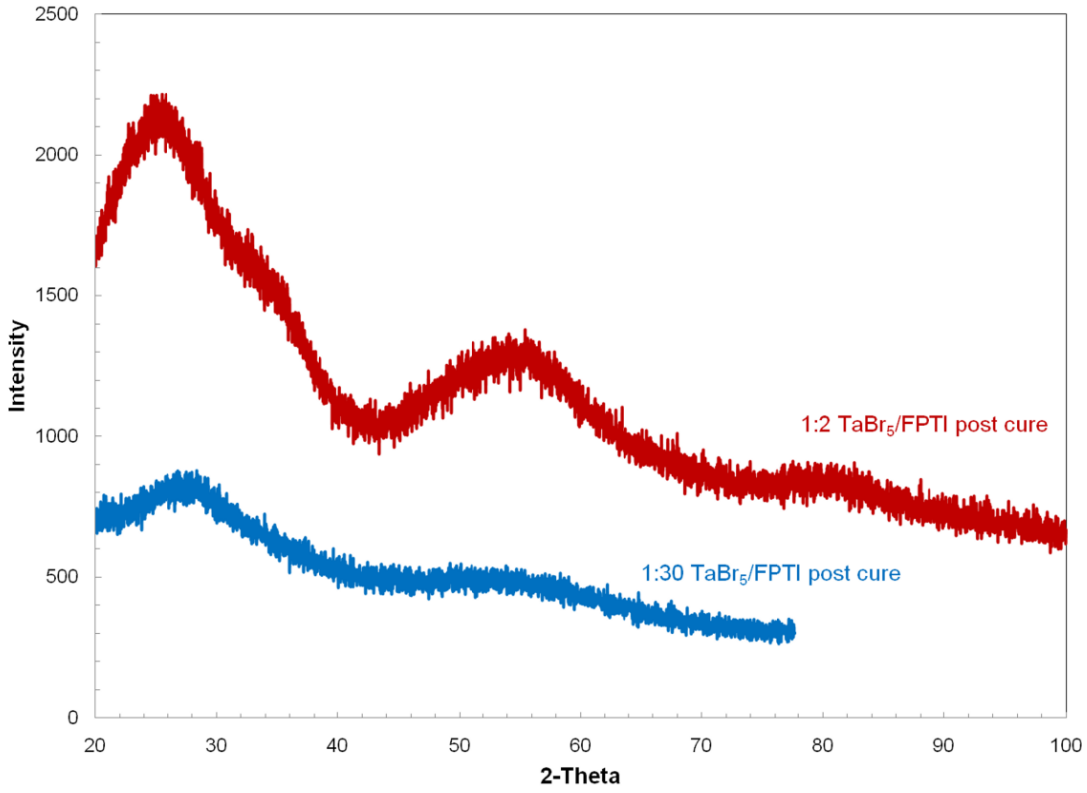

Figure 6.11. Comparison of 1:2 and 1:30 Ta:C atom ratio $TaBr_5$/FPTI systems, post-cured at 340 °C for 4 hours.

6.4 Conclusions

A relatively simple and low temperature method of producing tantalum carbide at low temperatures, from $TaBr_5$ and polyimide via a liquid precursor route, was developed. The significant reduction of tantalum carbide conversion temperature can be attributed to the intimate mixing on the molecular level of transition-metal halides and polymer precursors using two organic solvents. This technique successfully generated a high yield of TaC (>75 vol%) at 1000 °C, beginning with $TaBr_5$ and polyimide. Universality of this technique was demonstrated by using niobium bromide and tungsten

chloride to successfully produce their respective transition-metal carbides. Different types of polymer precursors, such as polystyrene and polyvinyl acetate, were also successfully used to produce TaC. Upon heating, transition-metal halides boil or sublimate at temperatures close to the decomposition temperature of the polymer precursors, allowing the formation of transition-metal carbides by self-propagating gas phase reactions. Additionally, halides present in the gaseous phases are believed to serve a catalytic function and contribute to faster diffusion of tantalum to the carbon particles that form during decomposition of the polymer, as previously postulated by Kim et al,[86] and thereby enhancing the overall efficiency of the conversion to the transition-metal carbide. Mechanistic studies demonstrate the need to form the oxide first from tantalum bromide before conversion to tantalum carbide can take place. In order to lower the processing temperature further, studies are needed to quantify the amount of oxygen needing to be present during the reaction. The influence of catalysts also needs to be evaluated. The formation of thin films or fibers, or processing of carbide matrix composites are now possible by using this low temperature methodology. Using the in-situ, low temperature processing of transition-metal carbides reported here could be advantageous for hypersonic vehicles by forming protective coatings on metallic or polymeric substrates, allowing them to sustain temperatures beyond 1500 °C.

CHAPTER VII

CONCLUSIONS

7.1 Conclusions

7.1.1 Polyimide and Polyimide Carbon Fiber Composite Studies

The goal of this research was to study degradation mechanisms of a fluorinated phenylethynyl terminated polyimide and its carbon fiber composite. A series of studies were performed to investigate the effects of further crosslinking in the polyimide (and associated thermal degradation), heat-related ablation, and blistering due to the combination of moisture and heat. The FPTI polyimide displayed decreasing mechanical properties in regards to increasing time and temperature of further curing conditions. The optimum cure conditions in regards to the glass transition temperature, tensile strength, and elastic modulus was 410 °C for 8 hours. This essentially sets the performance ceiling for these materials, which is important when deciding which materials to use for a given aerospace application.

The presence of moisture was also shown to negatively effect the properties of the FPTI polyimide resin and composite. Regardless of the amount of moisture present, blistering is one way for the trapped moisture to escape. A transverse extensometer with quartz lamps as a heating source measured thickness expansion, and a thermomechanical analyzer (TMA) were both able to measure the onset of blister formation with varying amounts of absorbed moisture (up to 3 wt%) in the samples. The polyimide resin exhibited blister temperatures ranging from 225 – 362 °C, with 1.7 - 3.0 wt% absorbed

moisture, and the polyimide composite had blister temperatures from 246 – 294 °C with 0.5 - 1.5 wt% moisture.

Despite the high T_g (435-455 °C) of the FPTI polyimide, its ability to withstand temperatures >400 °C needed to be investigated for use in the extreme service conditions experienced by military aircraft and reusable space vehicles. A weight loss study was performed on a fluorinated polyimide resin and its carbon fiber composite in an effort to determine its thermal stability and degradation mechanisms. Experiments were conducted using a preheated oven and thermogravimetric analysis to obtain the weight loss. Regardless of the method used or exposure time (2-20 min), the resin and composite exhibited excellent thermal stability (less than 1% weight loss) below 430 °C. After 20 minutes of exposure at 510 °C, the composite remained relatively stable with only 5.3% weight loss using the oven technique, while the neat polyimide sustained 12.6% loss. When degradation occurred, it was found to be the result of thermolysis and oxidation (to a lesser extent). Aircraft requiring extended exposure to temperatures > 430 °C will require alternate materials, such as polymer-ceramic hybrids.

7.1.2 Transition-Metal Carbide Formation

The goal of this research was to develop a processable technique to form tantalum carbide for future high temperature materials from an *in-situ* mixture of tantalum bromide and FPTI polyimide. Intimate mixing on the molecular level was achieved due to the solubility of transition-metal halides and polymers in similar organic solvents, which gives a reduction in the synthesis temperature. The method created is a

relatively simple, low temperature route that generated greater than 90% TaC conversion after exposing a 50:50 weight ratio mixture of $TaBr_5$ and polyimide to 1200 °C for one hour. Even at temperatures as low as 1000 °C, the major product remains TaC. The universality of the technique was explored by using other various transition-metal halides (e.g. niobium bromide, tungsten (IV) and (VI) chloride) and polymers (e.g. polystyrene and polyvinyl acetate). Atom ratios as low as 1:5 Ta:C resulted in formation of TaC, whereas 1:2 and 1:3 Ta:C ratios resulted only in tantalum oxide formation. The mechanism studies performed demonstrate the need to form the oxide first from tantalum bromide before conversion to tantalum carbide can take place. This processing route represents a promising way of lowering synthesis temperature of ultra-high temperature transition-metal carbides that should ultimately allow aircraft to be able to withstand temperatures much greater than polymer-based composites are currently able to.

7.2 Future Work

7.2.1 Polyimide and Polyimide Carbon Fiber Composites

The degradation mechanisms investigated in this work provide an understanding of the limits of the FPTI polyimide and composite under normal conditions. One area that needs more analysis is the crosslinking effects within the composite material. In other words, the polyimide composite may be adversely effected by the further curing conditions set forth in Chapter III. The next step of this work is to incorporate the data

into two parallel complimentary performance models based on the inputs of the fundamental damage mechanism inputs as shown in Figure 7.1.

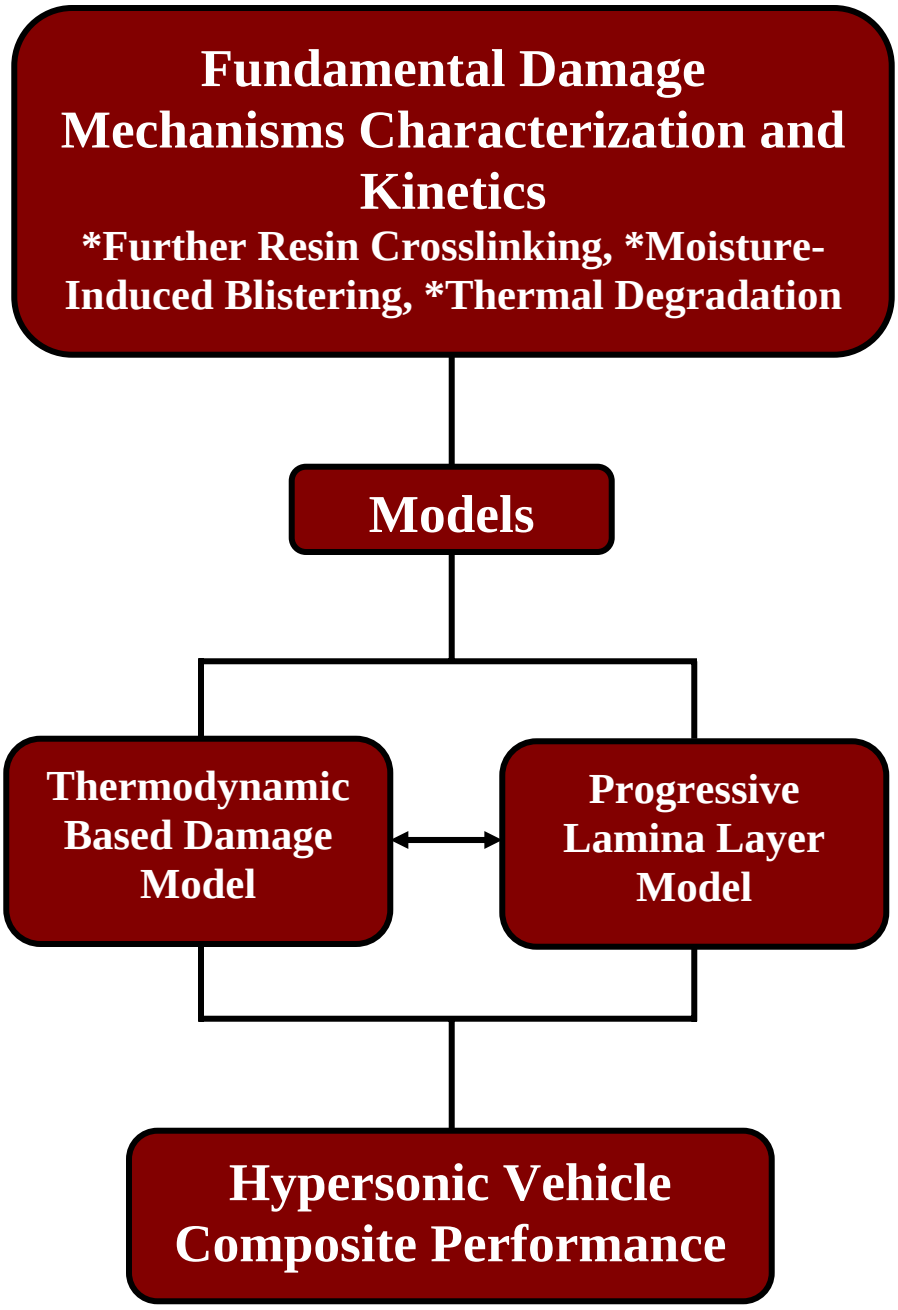

Figure 7.1. Overall technical approach for development of a hypersonic vehicle composite performance model.

One model will to create a lifetime composite model using thermodynamic procedures to incorporate all of the diverse damage mechanisms. The second model involves the progressive lamina failure analysis of the proposed lifetime model development. Both models combined will deal with the thickness and geometric composite designs and will be closely coordinated. They will collect the technical inputs from the damage mechanisms findings to lead to hypersonic vehicle composite performance lifetime predictions and guidance of materials development.

7.2.2 Ultra High Temperature Transition-Metal Carbides

The initial results of our low temperature carbide synthesis, shown in Chapter VI, point toward areas to focus on in future studies, including further reduction of processing temperature and generating robust shapes, coatings and/or fibers of the transition-metal carbide material. Both areas will serve to enhance the work performed thus far, by making this a lower energy technique and providing a means to make useful objects for various applications. The carbide synthesis done thus far has shown that it is not unique to the type of transition-metal halide or polymer used. The results have revealed that the method has worked successfully at relatively low temperatures for four different transition-metal halides and three different types of polymers. Further reducing the formation temperature of these ultra high temperature carbides will lower energy costs and increase the utility of this methodology. We propose two approaches to lower carbide formation temperatures. Changing the inert atmosphere currently used (argon) to an argon/carbon monoxide mixture is the first approach. The effect of changing the

atmosphere during the reaction is to create a reducing atmosphere that should propel the conversion of carbide at lower temperatures. The second approach involves using a catalyst, either in the form of a metal plate (e.g., titanium, platinum, Ni-based super alloy) or by addition of salt to the FPTI/$TaBr_5$ mixture (e.g., NaCl, Mg).[120] The addition of a catalyst is known to speed up the conversion to carbide and also produce better conversion rates.[120-121] Neither of these approaches has been previously reported at temperatures as low as the ones reported in this work.

Initial weight ratios of the mixture $TaBr_5$/FPTI were varied from 20/80 to 90/10 in an effort to generate monolithic carbide pieces. Most experiments used 50/50 weight ratios with a 30:1 carbon to tantalum atom ratio. A reduced atom ratio, such as 1:3, 1:5, 1:10 Ta:C ratio, but these did not result in robust forms. Excess carbon likely weakens the final material because it exists as amorphous carbon. More study is needed to successfully produce robust objects for future applications. An aid to help form shapes of the transition-metal carbide is to add fiber reinforcements, such as silicon carbide fibers and/or carbon nanotubes. The addition of these reinforcements could add stability and strength to the final transition metal carbide, aid in its formation, and possibly lower the processing temperature. The simplest, and possibly most useful procedure in the near term, would be to generate a carbide coating at the surface of an otherwise polymeric object. Localized surface heating could produce a relatively thin (perhaps millimeters thick) protective coating *in-situ* during aircraft flight. This would actually link back to the first objective of lowering conversion temperature. If carbide would form before the polymer undergoes significant thermal degradation, it would effectively

insulate the underlying substrate as the temperature increased further (beyond the T_d of unprotected polyimide).

REFERENCES

(1) Ghosh, M. K.; Mittal, K. L. *Polyimide: Fundamentals and Applications*, Marcel Dekker, Inc: New York, 1996.

(2) Meador, M. A. *Annual Review of Materials Science* **1998**, *28*, 599.

(3) Bowman, C. L.; Sutter, J. K.; Thesken, J. C.; Rice, B. P. *SAMPE Symposium,* Long Beach, CA, 2001; p 1515.

(4) Li, Y.; Morgan, R. J. *Journal of Applied Polymer Science* **2006**, *101*, 4446.

(5) Morgan, R. J.; Shin, E. E.; Lincoln, J. E. Thermal properies of high temperature polymer matrix fibrous composites. *Handbook of Thermal Analysis and Calorimetry: Applications to Polymers and Plastics*, Cheng, S. Z. D., Ed.; Elsevier Science: Amsterdam, 2002; Vol. 3, p 491.

(6) Ju, J.; Morgan, R. J. *Journal of Composite Materials* **2004**, *38*, 2007.

(7) Li, Y.; Obando, N.; Tschen, F.; Morgan, R. J. *Journal of Thermal Analysis and Calorimetry* **2006**, *85*, 125.

(8) Cella, J. A. *Polymer Degradation and Stability* **1992**, *36*, 99.

(9) Chen, J.; Yang, S.; Tao, Z.; Hu, A.; Fan, L. *High Performance Polymers* **2006**, *18*, 377.

(10) Sevkat, E.; Li, J.; Liaw, B.; Delale, F. *Composites Science and Technology* **2008**, *68*, 2214.

(11) Lincoln, J. E.; Morgan, R. J.; Shin, E. E. *Journal of Polymer Science Part B: Polymer Physics* **2001**, *39*, 2947.

(12) Kung, H.-K. *Journal of Composite Materials* **2005**, *39*, 1677.

(13) Cho, D.; Drzal, L. T. *Journal of Applied Polymer Science* **2000**, *75*, 1278.

(14) Chen, C.; Curliss, D.; Rice, B. P. *ACS Symposium Series* **2005**, *891*, 102.

(15) Li, Y.; Murphy, L. A.; Lincoln, J. E.; Morgan, R. J. *Macromolecular Materials and Engineering* **2007**, *292*, 78.

(16) Ghose, S.; Watson, K. A.; Working, D. C.; Siochi, E. J.; Connell, J. W.; Criss, J. M. *High Performance Polymers* **2006**, *18*, 527.

(17) Murphy, L. A. Masters Thesis, Texas A&M University, College Station, TX, 2003.

(18) Storms, E. K. *Refractory Carbides*, Academic Press: New York; 1967.

(19) Oyama, S. T. *The Chemistry of Transition Metal Carbides and Nitrides*, Blackie Academic and Professional: London; 1996.

(20) Jhi, S. H.; Ihm, J.; Louie, S. G.; Cohen, M. L. *Nature* **1999**, *399*, 132.

(21) Rubinshtein, A.; Shneck, R.; Danon, A.; Hayon, J.; Nathan, S.; Raveh, A. *Materials Science and Engineering* **2001**, *A302*, 128.

(22) Fahrenholtz, W. G.; Hilmas, G. E. *NSF-AFOSR Joint Workshop on Future Ultra-High Temperature Materials*; Workshop Report for NSF Grant DMR-0403004; National Science Foundation: Arlington, VA, 2004.

(23) Chan, J. Y.; Kauzlarich, S. M. *Chemistry of Materials* **1997**, *9*, 531.

(24) Ahlen, N.; Johnsson, M.; Nygren, M. *Thermochimica Acta* **1999**, *336*, 111.

(25) Toth, L. E. *Transition Metal Carbides and Nitrides, Refractory Materials*, Academic Press: New York, 1971.

(26) Zhang, X.; Hilmas, G. E.; Fahrenholtz, W. G. *Journal of the American Ceramic Society* **2008**, *91*, 4129.

(27) Zhang, X.; Hilmas, G. E.; Fahrenholtz, W. G. *Materials Science and Engineering A-Structural Materials Properties Microstructure and Processing* **2009**, *501*, 37.

(28) Labes, M. M.; Chen, J. H.; Lin, C. L.; Myer, G. H.; Ivkovich, D. *Materials Research Bulletin* **1988**, *23*, 255.

(29) Strong, A. B. *Fundamentals of Composites Manufacturing: Materials, Methods, and Applications*, 2nd ed.; Society of Manufacturing Engineers: Dearborn, MI, 2008.

(30) Campbell, F. C. *Manufacturing Processes for Advanced Composites*, Elsevier: New York, 2004.

(31) Haresceugh, R. I. Aircraft and Aerospace Applications of Composites. *Concise Encyclopedia of Composite Materials*, Kelly, A., Ed.; MIT Press: Cambridge, MA, 1989; p 1.

(32) Kelly, A. Introduction. *Concise Encyclopedia of Composite Materials*, Kelly, A., Ed.; MIT Press: Cambridge, MA, 1989; p xvii.

(33) Bowen, D. H. Applications of Composites: An Overview. *Concise Encyclopedia of Composite Materials*, Kelly, A., Ed.; MIT Press: Cambridge, MA, 1989; p 7.

(34) Haupert, F.; Wetzel, B. Reinforcement of Thermosetting Polymers by the Incorporation of Micro- and Nanoparticles. *Polymer Composites: From Nano- to Macro-Scale*, Friedrich, K., Fakirov, S., Zhang, Z., Eds.; Springer: New York, 2005; p 45.

(35) Schoeppner, G. A.; Tandon, G. P.; Pochiraju, K. V. Predicting Thermo-oxidative Degradation and Performance of High-Temperature Polymer Matrix Composites. *Multiscale Modeling and Simulation of Composite Materials and Structures*, Kwon, Y., Allen, D. H., Talreja, R., Eds.; Springer-Verlag: New York, 2007; p 359.

(36) Science, D. D. Providing Simple Answers to Everyday Science Questions. http://drdavescience.com/2007/07/10/. (accessed Nov 2009).

(37) Hancox, N. L. High-Performance Composites with Thermoplastic Matrics. *Concise Encyclopedia of Composite Materials*, Kelly, A., Ed.; MIT Press: Cambridge, MA, 1989; p 134.

(38) Mills, P. J.; Smith, P. A. Carbon-Fiber-Reinforced Plastics. *Concise Encyclopedia of Composite Materials*, Kelly, A., Ed.; MIT Press: Cambridge, MA, 1989; p 39.

(39) Bunsell, A. R. Long-Term Degradation of Polymer-Matrix Composites. *Concise Encyclopedia of Composite Materials*, Kelly, A., Ed.; MIT Press: Cambridge, MA, 1989; p 165.

(40) Chung, D. D. L. *Carbon Fiber Composites*, Butterworth-Heinemann: Boston, 1994.

(41) Astrom, B. T. *Manufacturing of Polymer Composites*, Chapman & Hall: London, 1997.

(42) Baker, A. A.; Dutton, S.; Kelly, D. W. *Composite materials for aircraft structures*, 2nd ed.; American Institute of Aeronautics and Astronautics, Inc.: Reston, VA, 2004.

(43) Goodman, S. H. Introduction. *Handbook of Thermoset Plastics*, Goodman, S. H., Ed.; Noyes Publications: Westwood, NJ, 1998; p 1.

(44) Landis, A. L.; Lau, K. S. Y. High-Performance Polyimides and Related Thermoset Polymers: Past and Present Development, and Future Research Directions. *Handbook of Thermoset Plastics*, 2nd ed.; Goodman, S. H., Ed.; Noyes Publications: Westwood, NJ, 1998; p 302.

(45) Wilson, D. Polyimides as Resin Matrices for Advanced Composites. *Polyimides*, Wilson, D., Stenzenberger, H. D., Hergenrother, P. M., Eds.; Chapman and Hall: New York, 1990; p 187.

(46) Bessonov, M. I.; Koton, M. M.; Kudryavtsev, V. V.; Laius, L. A. *Polyimides: Thermally Stable Polymers*, Consultants Bureau: New York, 1987.

(47) Lubowitz, H. R. U.S. Patent 3528950, **1970**.

(48) Owens, G. A.; Schofield, S. E. *Composites Science and Technology* **1988**, *33*, 177.

(49) Serafini, T. T.; Delvigs, P.; Lightsey, G. R. *Journal of Applied Polymer Science* **1972**, *16*, 905.

(50) Chuang, K. C.; Bowles, K. J.; Scheiman, D. A.; Papadopoulos, D. S.; Hardy-Green, D. *International Symposium on Polyimides and Other High Temperature Polymers*, Mittal, K. L., Ed.; VSP BV: Newark, New Jersey, 1999; Vol. 1, p 113.

(51) Cavano, P. J.; Winters, W. E. *Fiber reinforced PMR polyimide composites*; NASA CR-135377; NASA: Washington, DC, 1978.

(52) Rogers, F. E. U.S. Patent 3959350, **1976**.

(53) Gibbs, H. H.; Myrick, D. E. *33rd International SAMPE Symposium,* Anaheim, CA, 1988; p 1473.

(54) Russell, J. D.; Kardos, J. L. *Polymer Composites* **1997**, *18*, 595.

(55) Vanucci, R. D.; Cifani, D. *700°F properties of autoclave cured PMR-II composites;* NASA CR-100923; NASA: Washington, DC, 1988.

(56) Shin, E. E.; Sutter, J. K.; Eakin, H.; Inghram, L.; McCorkle, L.; Scheiman, D. A.; Papadopoulos, D. S.; Kerze, F. *Proceedings of 47th International SAMPE Symposium,* Long Beach, CA, 2002; p 314.

(57) Murray, G. T. *Introduction to Engineering Materials: Behavior, Properties, and Selection*, Marcel Dekker, Inc.: New York, 1993.

(58) Li, Y. PhD Dissertation, Texas A&M University, College Station, TX, 2004.

(59) Hay, J. N.; Boyle, J. D.; Parker, S. F. *Polymer* **1989**, *30*, 1032.

(60) Bilow, N.; Landis, A. L.; Miller, R. J. U.S. Patent 3845018, **1974**.

(61) Landis, A. L.; Bilow, N.; Boshan, R. H.; Lawrence, R. E.; Aponyi, T. J. *ACP Polymer Preprints* **1974**, *15*, 537.

(62) Hergenrother, P. M.; Johnston, N. J. Status of High-Temperature Laminating Resins and Adhesives. *Resins for Aerospace*, May, C. A., Ed.; American Chemical Society: Washington, D. C., 1980; p 3.

(63) Bilow, N.; Landis, A. L.; Boschan, R. H.; Fasold, J. G. *SAMPE Journal* **1982**, *18*, 8.

(64) Hergenrother, P. M. *Encyclopedia of Polymer Science and Engineering*, 2nd ed.; John Wiley & Sons: New York, NY, 1985; Vol. 1, p 61.

(65) Hou, T. H.; Belvin, H. L.; Johnston, N. J. *SAMPE Symposium and Exhibition: A Materials and Processes Odyssey*, Long Beach, CA, 2001.

(66) Connell, J. W.; Smith, J. G., Jr.; Hergenrother, P. M. *Journal of Macromolecular Science-Reviews in Macromolecular Chemistry and Physics* **2000**, *C40*, 207.

(67) Connell, J. W.; Smith, J. G., Jr.; Hergenrother, P. M.; Rommel, M. L. *High Performance Polymers* **2000**, *12*, 323.

(68) Hou, T. H.; Belvin, H. L.; Johnston, N. J. *High Performance Polymers* **2001**, *13*, 323.

(69) Chen, J.; Zuo, H.; Fan, L.; Yang, S. *High Performance Polymers* **2009**, *21*, 187.

(70) Morgan, R. J.; Grunlan, J. C.; Rajagopal, K.; Reddy, J. N. *Performance Characterization of Polyimide-Carbon Fiber Composites for Future Hypersonic Vehicles*; Research Proposal to AFOSR on FA 9550-04-1-0137; Texas A&M University, College Station, TX, 2006.

(71) Johnston, J. A.; Li, F. M.; Harris, F. W.; Takekoshi, T. *Polymer* **1994**, *35*, 4865.

(72) Smith, J. G., Jr.; Hergenrother, P. M. *Polymer Preprints (Am. Chem. Soc., Div. Polym. Chem.)* **1994**, *35*, 353.

(73) Meyer, G. W.; Glass, T. E.; Grubbs, H. J.; McGrath, J. E. *Polymer Preprints (Am. Chem. Soc., Div. Polym. Chem.)* **1994**, *35*, 549.

(74) Lincoln, J. E. PhD Dissertation, Michigan State University, East Lansing, MI, 2001.

(75) helios.augustana.edu/astronomy/space-shuttle-tiles.html. (accessed Jun 2009).

(76) Columbia Sacrafice. columbiassacrafice.com/$D_temperature.htm. (accessed Jun 2009).

(77) Dunbar, D. R.; Robertson, A. R.; Kerrison, R. *Proceedings 2nd International Conference on Composite Materials*, TMS-AIME: Warrendale, PA, 1978; p 1360.

(78) Meetham, G. W. *Journal of Materials Science* **1991**, *26*, 853.

(79) Opeka, M. M.; Talmy, I. G.; Zaykoski, J. A. *Journal of Materials Science* **2004**, *39*, 5887.

(80) Tang, S.; Deng, J.; Wang, S.; Liu, W.; Yang, K. *Materials Science and Engineering A-Structural Materials Properties Microstructure and Processing* **2007**, *465*, 1.

(81) Scatteia, L.; Borrelli, R.; Marino, G.; Bellosi, A.; Monteverde, F. *AIAA/CIRA 13th International Space Planes and Hypersonic Systems and Technologies*, Capua, Italy, 2005; Vol. AIAA 2005-3267.

(82) Ahlen, N.; Johnsson, M.; Nygren, M. *Thermochimica Acta* **1999**, *336*, 111.

(83) Xiang, H.; Xu, Y.; Zhang, L.; Cheng, L. *Scripta Materialia* **2006**, *55*, 339.

(84) Hassine, N. A.; Binner, J. G. P.; Cross, T. E. *International Journal of Refractory Metals and Hard Materials* **1995**, *13*, 353.

(85) Amaral, P. M.; Fernandes, J. C.; Rosa, L. G.; Martinez, D.; Rodriguez, J.; Shohoji, N. *International Journal of Refractory Metals and Hard Materials* **2000**, *18*, 47.

(86) Kim, T.; Wooldridge, M. S. *Journal of the American Ceramic Society* **2001**, *84*, 976.

(87) Gurin, V. N.; Derkachenko, L. I. *Progress in Crystal Growth and Characterization of Materials* **1993**, *27*, 163.

(88) Gurin, V. N.; Korsukova, M. M. *Progress in Crystal Growth and Characterization of Materials* **1983**, *6*, 59.

(89) Nartowski, A. M.; Parkin, I. P.; Mackenzie, M.; Craven, A. J. *Journal of Materials Chemistry* **2001**, *11*, 3116.

(90) Gillan, E. G.; Kaner, R. B. *Chemistry of Materials* **1996**, *8*, 333.

(91) Li, P. G.; Lei, M.; Sun, Z. B.; Cao, L. Z.; Guo, Y. F.; Guo, X.; Tang, W. H. *Journal of Alloys and Compounds* **2007**, *430*, 237.

(92) Claridge, J. B.; York, A. P. E.; Brungs, A. J.; Green, M. L. H. *Chemistry of Materials* **2000**, *12*, 132.

(93) Xiao, T. C.; York, A. P. E.; Williams, V. C.; Al-Megren, H.; Hanif, A.; Zhou, X. Y.; Green, M. L. H. *Chemistry of Materials* **2000**, *12*, 3896.

(94) Volpe, L.; Boudart, M. *Journal of Solid State Chemistry* **1985**, *59*, 332.

(95) Volpe, L.; Boudart, M. *Journal of Solid State Chemistry* **1985**, *59*, 348.

(96) Lu, J.; Hugosson, H.; Eriksson, O.; Nordstrom, L.; Jansson, U. *Thin Solid Films* **2000**, *370*, 203.

(97) O'Brein, R.; Xu, L.; Bi, X.; Eklund, P.; Davis, B. Fischer-Tropsch Synthesis and XRD Characterization of an Iron Carbide Catalyst Synthesized by Laser Pyrolysis. *The Chemistry of Transition Metal Carbides and Nitrides*, Oyama, S. E., Ed.; Blackie Academic and Professional: Glasgow, 1996; p 362.

(98) Zeng, D.; Hampden-Smith, M. J. *Chemistry of Materials* **1993**, *5*, 681.

(99) Hudson, M. J.; Peckett, J. W.; Harris, P. J. F. *Industrial and Engineering Chemistry Research* **2005**, *44*, 5575.

(100) Ishigaki, T.; Oh, S.-M.; Li, J.-G.; Park, D.-W. *Science and Technology of Advanced Materials* **2005**, *6*, 111.

(101) Xiang, H.; Xu, Y.; Zhang, L.; Cheng, L. *Scripta Materialia* **2006**, *55*, 339.

(102) Lei, M.; Zhao, H. Z.; Yang, H.; Song, B.; Tang, W. H. *Journal of the European Ceramic Society* **2008**, *28*, 1671.

(103) Preiss, H.; Schudtze, D.; Klobe, P. *Journal of the European Ceramic Society* **1997**, *17*, 1423.

(104) Dutremez, S.; Gerbier, P.; Guerin, C.; Henner, B.; Merle, P. *Advanced Materials* **1998**, *10*, 465.

(105) Preiss, H.; Schultze, D.; Schierhorn, E. *Journal of Materials Science* **1998**, *33*, 4687.

(106) Rice, B. P. *28th International SAMPE Technical Conference*, Seattle, WA, 1996; Vol. 28, p 778.

(107) Rice, B. P.; Lee, C. W. *29th International SAMPE Technical Conference*, Orlando, FL, 1997; Vol. 29, p 675.

(108) Shin, E. E.; Morgan, D. R. J.; Zhou, J. *45th International SAMPE Symposium*, Long Beach, CA, 2000; Vol. 45, p 389.

(109) Czabaj, M. W.; Zehnder, A. T.; Chuang, K. C. *Journal of Composite Materials* **2009**, *43*, 153.

(110) Shin, E. E.; Morgan, R. J.; Zhou, J.; Lincoln, J.; Jurek, R. *Journal of Thermoplastic Composite Materials* **2000**, *13*, 40.

(111) Bowles, K. J.; Nowak, G. *Journal of Composite Materials* **1988**, *22*, 966.

(112) Adamson, M. J. *Journal of Materials Science* **1980**, *15*, 1736.

(113) Turk, M. J.; Ansari, A. S.; Alston, W. B.; Gahn, G. S.; Frimer, A. A.; Scheiman, D. A. *Journal of Polymer Science Part A: Polymer Chemistry* **1999**, *37*, 3943.

(114) Burns, E. A.; Jones, R. J.; Vaughan, R. W.; Kendrick, W. P. *Thermally stable laminating resins*; NASA CR-72633; NASA: Redondo Beach, CA,1970.

(115) Gajiwala, H. M.; Vaidya, U. K.; Sodah, S. A.; Jeelani, S. *Carbon* **1998**, *36*, 903.

(116) Ma, J.; Du, Y.; Wu, M.; Pan, M. *Materials Letters* **2007**, *61*, 3658.

(117) Ghosh, M. K.; Mittal, K. L. *Polyimide: Fundamentals and Applications*, Marcel Dekker, Inc: New York, 1966.

(118) Meador, M. A. *Annual Review of Materials Science* **1998**, *28*, 599.

(119) Chrysanthou, A.; Grieveson, P. *Materials Science and Engineering* **1995**, *A194*, L11.

(120) Chen, Y.-J.; Li, J.-B.; Wei, Q.-M.; Zhai, H.-Z. *Journal of Crystal Growth* **2001**, *224*, 244.

(121) Jinjiang, Y.; Jun, Z.; Jinguo, L.; Zhi, F. H.; Zhuangqi, H. *Materials Letters* **2004**, *58*, 1130.

VITA

Name: Andrea Diane Adamczak

Address: Dept. Mechanical Eng., TAMU MS 3123, College Station, TX 77843

Email Address: adadamczak@gmail.com

Education: B.S., Chemistry, Austin Peay State University, 2002
M.S., Chemistry, Texas A&M University, 2007
Ph.D., Materials Science and Engineering, 2010

Experience: Department of Mechanical Engineering, Texas A&M University
Research Assistant 2007-2010
NASA Glenn Research Center, Cleveland, OH
Intern 2008
Department of Chemistry, Texas A&M University
Research Assistant 2003-2007; Teaching Assistant 2003-2007
US Zinc, Clarksville, TN
Quality Control Lab Technician 2002-2003
US Army, Ft. Wainwright, AK
Petroleum, Oil, and Lubricant Specialist (E-4) 1994-1998

Awards: NASA Texas Space Grant Consortium Graduate Fellowship Recipient

Selected Presentations:

2010 – 30th High Temple Workshop Destin, FL "Low Temperature Formation of Tantalum Carbide"

2009 – Materials Science and Technology 2009, Pittsburgh, PA "Low Temperature Formation of Ultra High Temperature Metal Carbides"

2009 – 29th High Temple Workshop Napa, CA "Analysis of Blister Formation in Fluorinated Polyimide Resin and Carbon Fiber Composites"

2007 – 233rd National ACS Symposium, Chicago, IL "The Effect of Branch Density on Polyoxymethylene Copolymers"

Publications:

Adamczak, A. D.; Spriggs, A. A.; Fitch, D. M.; Radovic, M.; Grunlan, J. C. *Chemistry of Materials* **2010**.

Adamczak, A. D.; Spriggs, A. A.; Fitch, D. M.; Burke, C.; Shin, E. E.; Grunlan, J.C. *Polymer Composites* **2010**.

Adamczak, A. D.; Spriggs, A. A.; Fitch, D. M.; Radovic, M.; Grunlan, J. C. *Journal of the American Ceramic Society* **2010**.

Adamczak, A. D.; Spriggs, A. A.; Fitch, D. M.; Awad, W.; Wilkie, C. A.; Grunlan, J. C. *Journal of Applied Polymer Science* **2010**, *115*, 2254-2261.

Ilg, A. D.; Price, C. J.; Miller, S. A. *Macromolecules* **2007**, *40*, 7739-7741.